

**Functional analysis of *Drosophila melanogaster* histone
H4 specific acetylase complex and its role in regulating
chromatin structure**

PhD thesis

Anita Oriana Ciurciu
Supervisor: Prof. Dr. Imre M. Boros

Biological Research Center of the Hungarian Academy of Sciences
Institute of Biochemistry

Szeged, 2009

Table of contents

Aknowledgments

1. Introduction.....	5
1.1. Chromatin organization and modifications.....	5
1.2. Histone acetylation.....	7
1.2.1. Histone acetyltransferase families.....	8
1.2.1.1. GNAT superfamily.....	9
1.2.1.2. MYST family.....	12
1.2.2. ADA2 transcriptional adaptors.....	14
1.3. Histone phosphorylation.....	16
1.3.1. The JIL-1 histone H3S10 kinase.....	18
1.4. Histone methylation.....	20
1.4.1. SET domain family of HMT.....	22
1.4.2. Drosophila <i>Su(var)</i> genes.....	22
1.5. ATP-dependent chromatin remodeling.....	23
2. Aims of study.....	26
3. Materials and Methods.....	27
3.1. Drosophila stocks.....	27
3.2. Genetic crosses and phenotype analysis.....	27
3.3. Immunohistochemistry.....	29
3.3.1. Immunostaining of polytene chromosomes.....	29
3.3.2. Immunostaining of polytene nuclei.....	30
3.3.3. Immunostaining of larval tissue.....	30
3.4. Western Blot.....	31
3.5. Recombinant DNA.....	32
3.6. RT-PCR and Q-PCR.....	32
3.7. <i>In vitro</i> and <i>in vivo</i> ecdysone treatment.....	33
4. Results.....	34
4.1. dADA2a in H4 acetylation.....	34
4.1.1. Characterization of <i>dAda2a</i> mutants.....	34
4.1.2. Genetic interaction between <i>dAda2a</i> and <i>dGcn5</i>	39
4.1.3. Failure in ecdysone response in <i>dAda2a</i> mutants.....	40
4.1.4. Lack of dADA2a function results in decreased H4 acetylation.....	44
4.2. H4 acetylation is linked to JIL-1 kinase function.....	50
4.2.1. Decreased H3S10ph level in mutants deficient in ATAC function.....	50
4.2.2. JIL-1 overexpression restores H3S10ph and suppresses phenotypic features of ATAC mutants.....	52
4.2.3. Mutations of ATAC subunits enhance the spreading of histone H3K9me2 by SU(VAR)3-9.....	55
4.2.4. Loss of H4K12ac decreases JIL-1 localization to chromatin.....	58
5. Discussions.....	62
6. Summary.....	73

7. Abbreviations.....	76
8. Bibliography.....	78

ACKNOWLEDGMENTS

First of all I would like to thank my supervisor, Prof. Dr. Imre M. Boros for giving me the possibility to join his group, for guiding me in the scientific field, and his kind support throughout my studies.

I am very grateful to Dr. Orbán Komonyi for introducing me in the genetics of *Drosophila melanogaster* as well as for his support and advice in the progress of this study. Special thanks to our technician Katalin Ökrös Gyuláné for her technical assistance.

I gratefully thank the Biological Research Center, the Institute of Biochemistry and the Marie Curie Actions for offering me the possibility and the fellowship to carry on this study.

Many thanks to all my colleagues from Biological Research Center, Eukaryotic Transcription Regulation Group and from The University of Szeged, Department of Biochemistry and Molecular Biology for their strong support and help. Special thank to my colleagues, Cristina Popescu, Edith Vamos and Manuela Jurca and to my family, for their continuous help and moral support.

I am also grateful to Dr. Laszlo Tora for helping with reagents and critical advices and to Dr. Kristen Johansen for JIL-1 mutants and antibody.

This work was carried out in the Institute of Biochemistry, Biological Research Center of the HAS and in the Department of Biochemistry and Molecular Biology, Faculty of Biology, University of Szeged, Hungary.

1. INTRODUCTION

1.1. Chromatin organization and modifications

The compartmentalization of DNA within the nucleus of eukaryotic cells requires an extreme compaction of this highly charged polymer. Compaction is achieved through association of the DNA with a set of extremely basic histone proteins to form a structure known as chromatin. The fundamental repeat unit of chromatin is the nucleosome, which is composed of an octamer of the four core histones, H2A, H2B, H3, and H4, and 147 base pairs of DNA wound in two turns around the exterior of the octamer (Fig 1.1.). Based on amino acid sequence, histone proteins are highly conserved from yeast to human. Nucleosomes are composed of a globular domain and flexible „histone tails” that protrude outside from the surface and fold into progressively higher-order structures. Although the structure of the nucleosome is well characterized (107), less is known about the molecular nature of more highly folded structures. Chromatin folding is quite dynamic, and the degree of folding directly influences the activity of DNA in transcription, replication, and recombination. How individual, differentially folded chromatin domains are created or maintained is a question of considerable importance to biological regulation.

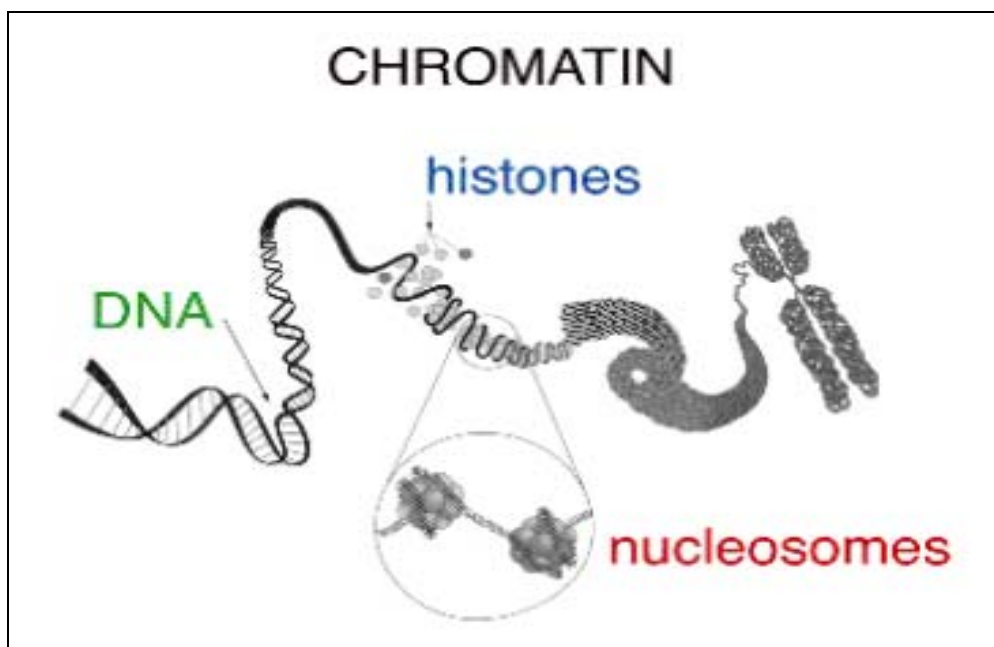


Fig. 1.1. Schematic view of various levels of eukaryotic chromatin compaction, from DNA packaging by histone into nucleosomes till folding into higher-order structures of chromosomes (Makeba D.L., 2003)

Nature has evolved elaborate mechanisms to dynamically modulate chromatin structure, including chromatin remodeling by ATP-dependent complexes, covalent histone modifications (Fig. 1.2.) and utilization of histone variants (161). A wealth of mostly correlative studies published over the past three decades suggests that posttranslational modification of the histones modulates chromatin folding and thereby gene activity. The ATP-dependent remodeling complexes use the energy of ATP hydrolysis in conjunction with the Swi2 superfamily of proteins to remodel the nucleosome patterning along chromatin fiber. Other mechanisms involve the recognition of covalent modifications in the histone N-terminus by chromatin-dependent factors.

The identification of the enzymes that direct modifications has been the focus of intense activity over the last 10 years. Enzymes have been identified for acetylation (144), methylation (179), phosphorylation (118), ubiquitination (138), sumoylation (114), ADP-ribosylation (71), deimination (40, 165) and proline isomerization (115).

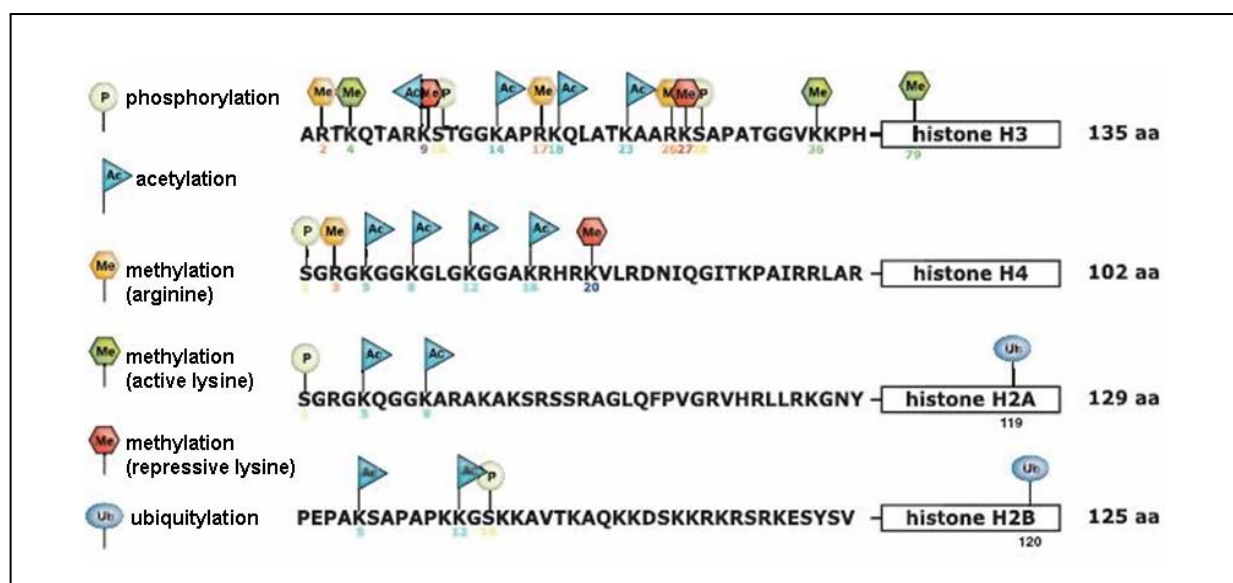


Fig. 1.2. Covalent modifications of the N-terminal tails of the canonical core histones. (Allis et al., Epigenetics, 2006)

Molecular mechanisms underlying the use of each individual histone modification can be generalized into two categories, *cis* and *trans* mechanisms (161). *Cis* mechanisms achieve alteration of intra-and internucleosomal contacts via changes of steric or charge interactions, for this prominent example include histone acetylation and deacetylation. It has been proposed

that histone acetylation, a modification associated with transcriptional activation, unfolds chromatin via neutralization of the basic charges of lysines (93). Indeed recent studies with recombinant nucleosomal arrays have demonstrated that the acetylation of H4K16 inhibits the formation of compact 30 nm fibers and higher-order chromatin structures (139). *Trans* mechanisms involve utilization of non-histone 'readers' that bind specific histone modifications and lead to the corresponding functional consequences. Prominent examples include H3K4 methylation, H3K9 methylation and H3K27 methylation, which are recognized by inhibitor of growth (ING) proteins, heterochromatin protein 1 (HP1) and polycomb protein, respectively.

It is hypothesized that the combination of specific histone modifications signifies a „histone or epigenetic code” that is written by some enzymes (writers) and removed by others (erasers) and is readily recognized by proteins (readers) that are recruited to modifications and bind via specific domains. These writing, reading and erasing activities, in turn establish the optimal local environment for chromatin-template biological processes, such as transcriptional regulation and DNA damage repair (161).

1.2. Histone acetylation

The phenomenon of histone acetylation in the eukaryotic cell has been known for many years, and since 1996 various histone acetyltransferase (HAT) activities have been isolated and partially characterized. Numerous groups sought to identify enzyme activities capable of transferring acetyl groups from acetyl coenzyme A (acetyl-CoA) onto histone acceptors (i.e. the ϵ -amino groups of conserved lysine residues within the core histones). Typically, cell extracts or partially purified fractions were used in conventional, insolution enzymatic assays (1). Identifying which polypeptides were responsible for these HAT activities, however, proved to be challenging and elusive for many years. HAT activities were grouped into two general classes based on their suspected cellular origin and functions. Cytoplasmic, B-type HATs likely catalyze acetylation events linked to the transport of newly synthesized histones from the cytoplasm to the nucleus for deposition onto newly replicated DNA, they are believed to have housekeeping role in the cell. Conversely, nuclear, A-type HATs likely catalyze transcription-related acetylation events (131). Recent evidence indicates that some HAT proteins may function in multiple complexes or locations and thus not precisely fit these historical classification (132).

There are currently two theories as to how histone acetylation might facilitate transcription. One predicts that acetylation affects transcription by neutralizing histone charge, which weakens histone-DNA and internucleosome contacts, reducing chromatin compaction (171). The other hypothesis, which does not exclude the first, is commonly known as the „histone code” and proposes that covalent modification of histones provides an epigenetic marker for gene expression (147). In this case the acetylation constitutes a marker on histone tail recognized by factors involved in either activation or gene repression.

In particular, an enrichment of acetylated histone isoforms is often observed on transcribed DNA sequences. This was first directly demonstrated by pioneering chromatin immunoprecipitation assays using antibodies that preferentially recognize hyperacetylated histones. These studies demonstrated that acetylated histones localize more globally to regions of general DNase I sensitivity, correlating with transcriptional competence. Histone acetylation and general sensitivity to nuclease digestion are now often recognized as hallmark properties of transcriptionally active, or competent/poised, chromatin (reviewed in (131)).

1.2.1. Histone Acetyltransferase Families

The histone acetyltransferases are divided into five families including: GCN5-related N-acetyltransferases (GNATs), the MYST (for „MOZ, Ybf2/Sas3, Sas2 and Tip60”)-related HATs, p300/CBP HATs, the general transcription factor HATs including TFIID subunit TAF1, and the nuclear hormone-related HATs SRC1 and ACTR (SRC3) (33).

Four sequence motifs whose functions are not fully understood – C, D, A, B in the N-terminal to the C-terminal order - define this superfamily (Fig. 1.3.). The C motif is found in most of the GNAT acetyltransferases but not in the majority of known HATs. Motif A is the most highly conserved region, and it is shared with another HAT family, the MYST proteins. Furthermore, it contains an Arg/Gln-X-X-Gly-X-Gly/Ala segment that has been specifically implicated in acetyl-CoA substrate recognition and binding (48, 170).

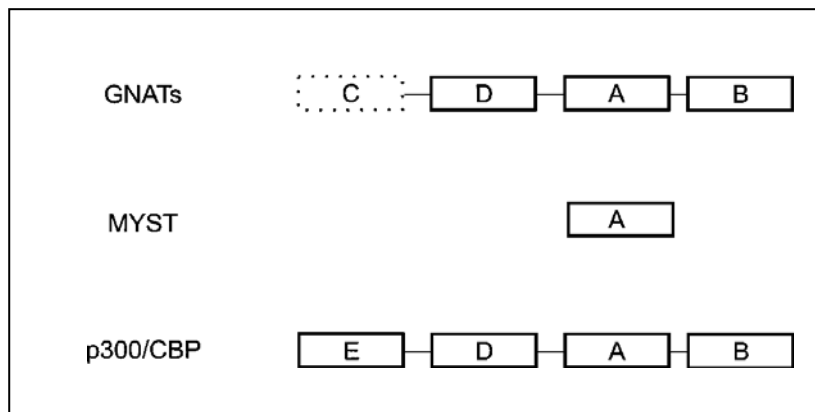


Fig. 1.3. HAT domain motifs. The relative positions of conserved sequence motifs in the three HAT families GNAT, MYST, and p300/CBP are indicated. Motif A contains the highly conserved acetyl-CoA binding site (Roth S., et al, 2001, Annu. Rev. Biochem)

1.2.1.1. GNAT Superfamily

The best understood set of acetyltransferases is the GNAT superfamily (116) which have been grouped together on the basis of their similarity in several homology regions and acetylation-related motifs. This group includes the HAT GCN5, its close relatives, and at least three more distantly related HATs, Hat1, Elp3 and Hpa2. It also contains a variety of other eukaryotic and prokaryotic acetyltransferases with different substrates, indicating the conservation and wide application of this type of acetylation mechanisms throughout evolution.

GCN5 (KAT2)

The first protein identified as an A-type, transcription-related HAT was discovered in the ciliate *Tetrahymena thermophila* (23). By way of an in-gel assay of nuclear extract chromatographic fractions run on sodium dodecyl sulfate-polyacrylamide gel electrophoresis (SDS-PAGE), a 55-kDa polypeptide (p55) was found to have acetylation activity on free histones (22). Subsequent protein sequencing revealed that it was a homolog of *Saccharomyces cerevisiae* yGCN5 (general control nonderepressible-5) (KAT2) (18, 62), previously identified as a transcriptional adaptor (or coactivator) involved in the interaction between certain activators and the transcription complex (18,108,140). Homologues of GCN5 have more recently been cloned and sequenced from numerous divergent organisms - such as human (28),

mouse (173), *Drosophila melanogaster* (141), *Arabidopsis thaliana*, and *Toxoplasma gondii* (73) - suggesting that its function is highly conserved throughout the eukaryotes.

To date, yeast GCN5 (yGCN5) is the best characterized of the HATs, both structurally and functionally and both *in vivo* and *in vitro*. Various studies have mapped and characterized the functional domains of yeast GCN5, shown in Fig. 1.4 (27, 29). These include a C-terminal bromodomain, an ADA2 interaction domain, and the HAT domain, which by use of truncation mutants was found to be required for adaptor-mediated transcriptional activation *in vivo* (29). The yGCN5 HAT domain was also functionally analyzed by alanine scan mutagenesis. These analyses identified conserved residues critical to HAT activity and demonstrated the direct correlation of yGCN5 HAT function with cell growth, *in vivo* transcription, and histone acetylation at the yGCN5-dependent *HIS3* promoter *in vivo* (95, 163). A further study with some of these mutants showed that yGCN5's HAT activity has an effect on chromatin remodeling at the *PHO5* promoter *in vivo* (67). The substrate specificity of yGCN5 has also been investigated. *In vitro*, recombinant yGCN5 was found to acetylate both histone H3 and H4. Yeast protein sequence analysis of these reaction products revealed that the primary sites of acetylation were lysine 14 on histone H3, and lysines 8 and 16 on histone H4 (94). Although recombinant yGCN5 can acetylate free histones efficiently, it is unable to acetylate nucleosomal histones (64, 94, 133), the more physiological substrate, except under special conditions and at high enzyme concentrations (156). Only in the context of multisubunit native complexes such as SAGA (Spt-Ada-Gcn5-Acetyltransferase) and ADA (Alteration Deficiency in Activation) is yGCN5 able to acetylate nucleosomes effectively, indicating that the influence of other proteins is required to confer this activity. Yeast GCN5 bromodomain is required for full activity within SAGA complex, but is not required when GCN5 is within the ADA complex (145). While ADA complex remains poorly understood, yeast SAGA complex function mostly as coactivators that acetylates nucleosomal H3 and H2B and facilitate chromatin remodeling, transcription, nuclear export of mRNA, and nucleotide excision repair (8).

In mammals (humans and mice), the GCN5 subclass of acetyltransferases is represented by two closely related proteins, GCN5 and p300/CREB-binding protein-associated factor (PCAF). These proteins share a remarkable degree of homology (about 70% identity and 80% similarity) throughout their sequences, and a distinguishing feature is an approximately 400-residue amino-terminal region not present in yeast GCN5 (Fig. 1.4) (173); such an extension is seen, however, in *Drosophila* GCN5 (dGCN5) (141). GCN5 appears more widely expressed

than PCAF and at higher levels in mouse embryos. Consistent with this, GCN5 is required for early development, while PCAF is dispensable for mouse viability (112).

The function of human GCN5 (hGCN5) has also been investigated *in vitro* and *in vivo*, and it was found to carry out transcriptional adaptor roles analogous to those of yeast GCN5 (28). Further studies showed that hGCN5 had HAT activity *in vitro* (175) and that its HAT domain could successfully substitute for that of yGCN5 *in vivo*, indicating the evolutionary conservation of this HAT function (164). The HAT domain of human GCN5 is of course indispensable to its acetylation function, but interestingly, two other domains appear to have an influence on its HAT activity and substrate use. Because of the apparent existence of multiple alternatively spliced versions of human GCN5, the original cDNA clones lacked its N-terminal region. While recombinant short-form human GCN5 could acetylate histone H3 (and to a lesser extent H4) only as free histones (164, 175), the full length forms of human and mouse GCN5 were recently shown to be competent for the acetylation of nucleosomal histones, implicating the N-terminal region in chromatin substrate recognition (173). The C-terminal bromodomain is another region that apparently has an effect on human GCN5 HAT function, interacting with the DNA-dependent protein kinase holoenzyme, which inhibits GCN5's HAT activity by way of phosphorylation (14).

Differently from mammals, only one *Gcn5* homologue was identified in *Drosophila* (141). Smith et al. cloned the 98 kDa *Drosophila Gcn5* and showed that in addition to HAT- and bromodomain it contains the PCAF homology region, as well. dGCN5 has been isolated in at least two GNAT complexes that contain distinct ADA2 transcriptional adaptors (97, 110). A 1.8 MDa SAGA like complex include the ADA2b variant, the dADA3 and Spt homologues, and several TAFs. In addition, dGCN5 associates with the dADA2a variant and dADA3 in a 0,7 MDa ATAC complex (66, 110, 151). Carre and colab. showed that *Drosophila* GCN5 is the major HAT for the lysine residues K9 and K14 of histone H3, is required for larva-to-adult metamorphosis and has an essential function in the control of cell cycle in imaginal tissues (31).

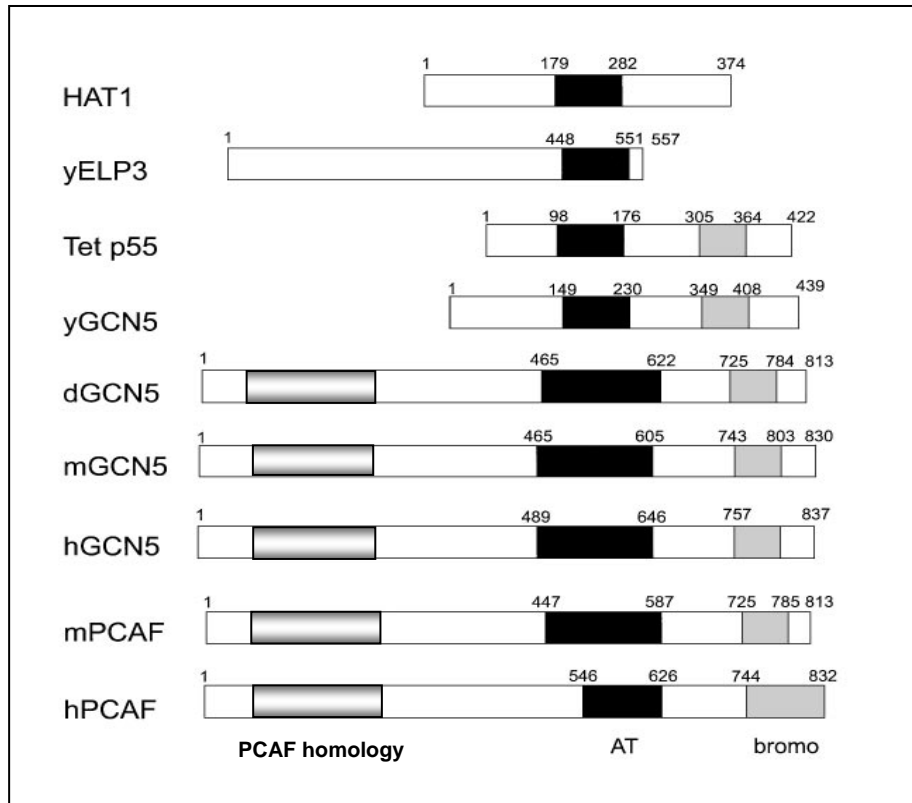


Fig. 1.4. The relative sizes and locations of conserved motifs for the GNAT superfamily of HATs. AT, acetyltransferase domain; bromo, bromodomains; PCAF homology domain (Roth S., et al, 2001, *Annu. Rev. Biochem*)

1.2.1.2. MYST Family

Another group of related proteins predicted to be either HATs or ATs, is the MYST family that contains the GNAT motif A described above. It is named for its founding members: MOZ, Ybf2/Sas3, Sas2, and Tip60; (62, 64) (Fig. 1.5). In addition the MYST family includes the recently identified, yeast Esa1, *Drosophila* MOF and human HBO1 and MORF (144). Multiple MYST family members contain zinc fingers as well as chromodomains, which are protein - protein interaction domains often found in heterochromatin-associated protein (55). Although the relationship of these domains to HAT function remains unclear, one intriguing possibility is that chromodomains serve as chromatin-targeting modules for the MYST family, similar to the function of bromodomains found in other HATs (169).

Tip60, for TAT-interactive protein with a mass of 60 kDa (87) was the first human MYST member with demonstrated HAT activity (174).

Sas3 is the yeast homolog of the human oncogene MOZ (for monocytic leukemia zinc finger protein). An in-frame chromosomal translocation between CBP and MOZ creates a novel fusion protein associated with oncogenic transformation leading to human disease. Sas3 is the catalytic subunit of a yeast HAT complex that exhibits specificity for nucleosomal H3, NuA3 (85). The HAT activity of MOZ has not yet been demonstrated, but sequence similarities between Sas3 and MOZ make it likely that MOZ is a HAT. Interestingly, both the acetyl-CoA binding motif and the adjacent zinc finger of the Sas3 MYST catalytic domain are required for HAT activity (153).

The human protein **HBO1** (HAT bound to ORC 1) was the first HAT identified in association with components of the origin of replication complex (77).

The yeast protein **Esa1** (Essential Sas family Acetyltransferase 1) was the first essential HAT to be identified in yeast (37), and Esa1 is now known to be the catalytic subunit of the NuA4 HAT complex (Nucleosomal Acetyltransferase for H4) (5).

Drosophila **MOF** (male absent on the first) is homologous to Esa1 and is involved in dosage compensation in flies (3, 74). Since male fruit flies have only one copy of the X chromosome compared to females' two, dosage compensation occurs in males to cause a twofold increase in the expression of X-linked genes. Association of a dosage compensation complex with the chromosomes is correlated with increased acetylation of histone H4 at K16 residue (19). Indeed, mutation of the single glycine (Gly) to glutamic acid in motif A (Arg/Gln-X-X-Gly-X-Gly/Ala) led to the original discovery of MOF, supporting a critical role for HAT (74). *mof* mutant males lack the acetylation of histone 4 at lysine 16, normally associated with male X chromosome (74).

The human ortholog of the MOF (hMOF) has the same substrate specificity and recent purification of the human and *Drosophila* MOF complexes showed that these complexes are highly conserved through evolution. Several studies have shown that loss of hMOF in mammalian cells lead to a complex phenotype: a G2/M cell cycle arrest, nuclear morphological defects, spontaneous chromosomal aberrations, reduced transcription of specific genes and impaired DNA repair response upon ionizing irradiation. Moreover, hMOF is involved in ATM activation in response to DNA damage and acetylation of p53 by hMOF influences the cell's decision to undergo apoptosis instead of a cell cycle arrest (129).

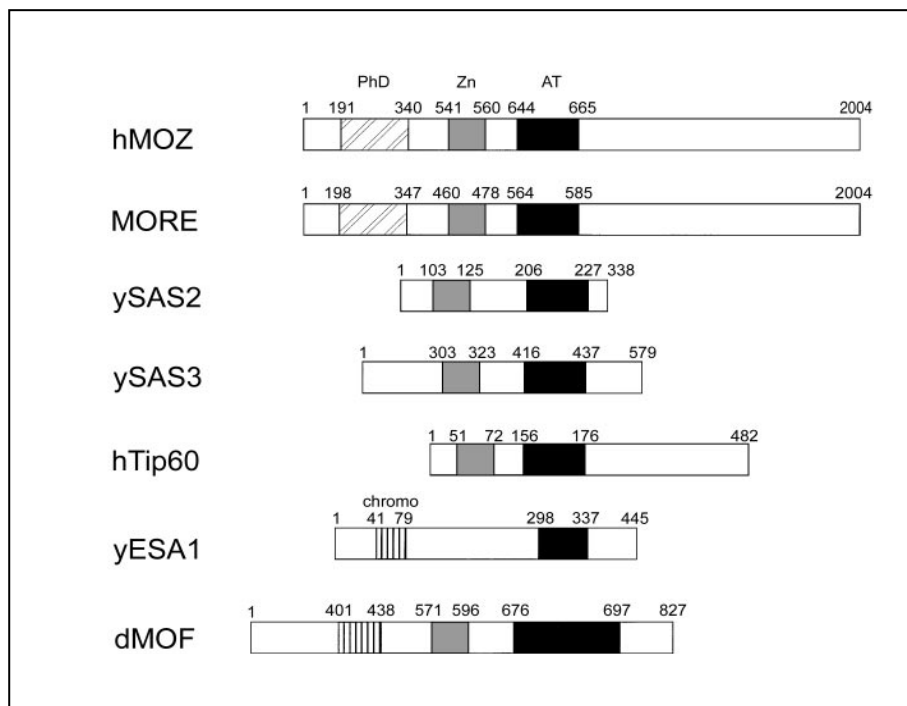


Fig. 1.5. The relative sizes and locations of conserved motifs for the MYST superfamily of HATs. AT, acetyltransferase domain; PhD, plant homeo domains; Zn, zinc finger domains; chromo, chromodomains are indicated (Roth S., et al, 2001, Annu. Rev. Biochem).

1.2.2. ADA2 transcriptional adaptors

After the discovery of the GCN5 HAT and GCN5 homologues in virtually all eukaryotes, different studies revealed that recombinant GCN5 mainly acetylates free histone H3, but exhibits lower HAT activity on nucleosomal histones substrates (94). This suggested that GCN5 requires other factors to acetylate nucleosomes and eventually led to the biochemical characterization of SAGA and ADA acetyltransferase complexes from yeast (64). The yeast ADA2-type adaptor proteins (yAda1, yAda2, yAda3, yAda4) have been isolated in a genetic screen (18). The structure of the ADA2 adaptor protein is highly conserved. It contains a Zn finger domain, a SANT domain and three so called ADA boxes (110) (Fig 1.6.). The ADA2 SANT-a region is needed for full HAT activity of SAGA, particularly on nucleosomal substrates. Yeast ADA2 SANT domain was show to be particularly important in potentiating the function of the ySAGA complex (146).

In contrast to the single *Ada2* gene present in *Saccharomices cerevisiae*, the *Drosophila melanogaster* genome contains two genes referred to as *dAda2a* and *dAda2b*, encoding related *Ada2* gene (97, 110). The analysis of the gene encoding the *Drosophila* ADA2a (dADA2a) protein revealed that in addition to dADA2a this gene encodes the Pol II subunit RPB4 by

alternative splicing. The N-terminal of the two proteins is encoded by the same exon (Fig. 4.1). Two genes that encode ADA2 homologues were also found in several other metazoan organisms like *Arabidopsis thaliana*, mice and human, but not in *C. elegans*.

Both *dAda2a* and *dAda2b* genes are localized on the 3rd chromosome at the 90F10 and 84F5 cytological region, respectively. Significant homology exists between dADA2a and dADA2b proteins only in their N-terminal regions, where the ZZ and SANT domains are present (Fig. 1.6.).

Biochemical separation of ADA2-containing *Drosophila* complexes indicated that dADA2a is present in a smaller (0.7MDa) complex, while dADA2b is present in a larger (2MDa) complex. The latter, most probably corresponding to dSAGA (97, 110). More recently, Guelman et. al reported the biochemical separation of a further dADA2a-dGCN5-containing complex, ATAC (Ada Two A Containing complex) (68). In both dSAGA and ATAC complex, dGCN5, dADA2 and dADA3 are common constituents, which raise the question of how the functional divergence of these complexes is determined.

Very recently the identification of the SWIRM domain in the C-terminal part of the hADA2 α was reported (125). SWIRM is a conserved domain found in several chromatin-associated proteins. The SWIRM domain was shown to be important for many mammalian nuclear function such as histone demethylation, chromatin remodeling and transcription activation through the ADA2 coactivator (13, 125). The SWIRM domain of the human transcriptional activator hADA2 α has a possible function in potentiating the activity of the ACF (ATP-utilizing Chromatin assembly and remodeling Factor) complex in chromatin remodeling (125). In addition to the hADA2 α , regions homologues to the SWIRM domain were identified for yADA2, dADA2a, and mADA2a, but were not reported for hADA2 β or dADA2b.

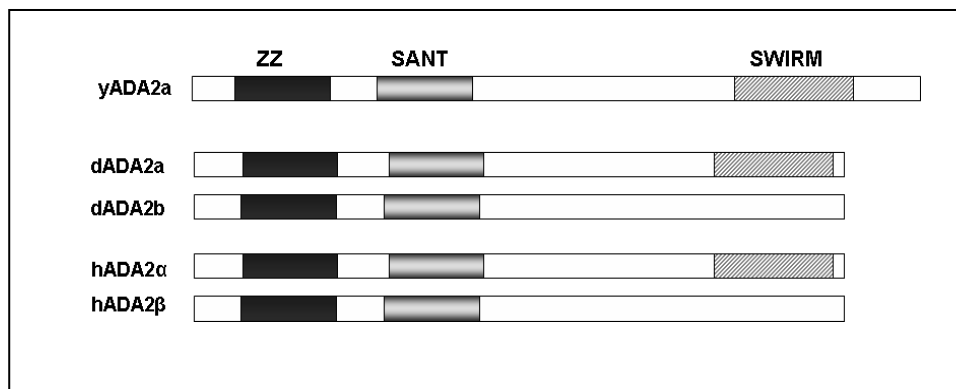


Fig. 1.6. ADA2-type adaptor protein is conserved between organisms from yeast to human. The conserved motifs are indicated. ZZ, Zn finger domain, SANT domain, SWIRM domain

Independent studies of Pankotai et al. and Qi et al demonstrated that *Drosophila* ADA2b is required for viability and is involved in histone H3 acetylation at the lysine 9 and 14, but does not affect the H4K8 acetylation (120, 124). In addition, dADA2b has a role in specific gene activation, p53-mediated processes and TAF10 localization (TBP-Associated Factor 10) (120). Recent results showed that dADA2b, as part of *Drosophila* SAGA complex, is implicated in the export of newly formed mRNA through the NPC (Nuclear Pore Complex) (96). In general, dADA2b is part of multiprotein complexes with important roles in the regulation of transcription.

1.3. Histone phosphorylation

Phosphorylation is the most well known posttranslational modification because it has long been understood that kinases regulate signal transduction from the cell surface, through the cytoplasm, and into the nucleus, leading to changes in the gene expression. *In vivo*, proteins can be phosphorylated at serine, threonine and tyrosine; these residues can be modified by substituting a phosphate for a hydroxyl group to give an o-phosphate linkage.

The histone H3 serine 10 residue (H3S10) is an important phosphorylation site for chromatin formation from yeast to humans, and appears to be especially important in *Drosophila* (118). H3 is phosphorylated at S10 in two circumstances: first, there is a highly conserved and wide spread phosphorylation of H3S10 as cells enter mitosis; second, the same phosphorylation at the S10 residue is highly associated with gene activation and chromatin

loosening. This presents us with a paradox: on one hand, the modification is associated with chromatin condensation and suppression of transcription as cells enter mitosis, and, on the other hand it is associated with the transcriptional activation of selected genes (reviewed in (118)).

Studies in maize indicate that histone H3S10 phosphorylation during mitosis and meiosis begins late in prophase, after chromosome condensation has been initiated, and appears to be associated with chromosome cohesion rather than condensation (88). Members of the aurora AIR2–Ipl1 (Aurora/Ipl1-Related protein) kinase family have been found to govern histone H3 phosphorylation at S10 during mitosis in several organisms (41, 63). The action of these kinases is thought to be required for the proper recruitment of the condensin complex and assembly of the mitotic spindle in a phosphorylated histone H3-dependent manner (63). These kinases are counterbalanced by the activity of type1 phosphatases (protein phosphatase 1 - PP1) (76, 111). Regulation of the level of histone H3 phosphorylation via the interplay between the activities of protein kinase and phosphatase is thought to be the primary means of promoting proper chromosomal condensation and segregation (70).

Evidence from the analysis of gene expression in *Drosophila* has provided additional examples of genes that appear to follow the independent parallel pathway of histone modification during induction of transcription. Nowak et al. took advantage of the heat-shock responsive genes of *Drosophila*, and examined the genome-wide distribution of histone H3K14-acetylation and S10-histone H3 phosphorylation (117). By analyzing polytene chromosomes that were prepared from heat shocked larvae, it was found that acetylated histone H3 and H4 at residues described as essential for transcription (i.e. K14 of H3 and K8 of H4) do not change their distribution. However, the distribution of S10-phosphorylated histone H3 changes dramatically and is only detected at those loci that contain actively transcribing heat-shock genes. In addition, repression of transcription at non-heat-shock genes is accompanied by dephosphorylation of histone H3. These results suggest that the genomic distribution of histone H3 and H4 acetylation remains more or less static, whereas histone phosphorylation changes dynamically in a manner that is reminiscent of the transcriptional profile of the cell (117). It also appears that the structure of the particular promoter itself might affect how histones are modified at a particular locus. Examination of the modification status of histone H3 at the promoters of GAL4-driven transgenes in *Drosophila* reveals that, whereas S10-phosphorylated histone H3 molecules can be detected at active GAL4-regulated transgenes, active transgenes that do not bind TATA binding protein (TBP) are not H3-phosphorylated, raising the possibility that other histone modifications might have a role in their regulation

(98). One interesting result arising from this and previous studies (123) is the observation that antibodies against transcription-specific acetylated histones predominantly stained the non-transcribed 40,6-diamidino-2-phenylindole (DAPI)-staining band regions of *Drosophila* polytene chromosomes. By contrast, histone phosphorylation is confined solely to the actively transcribed interband regions of polytene chromosomes. These results suggest that, in *Drosophila*, histone phosphorylation is intimately linked to transcriptional activation and that the presence of acetylated histones might not necessarily denote regions of actively transcribed genes (98).

1.3.1. The JIL-1 histone H3S10 kinase

In 1999 Jin et al. characterized a novel tandem kinase in *Drosophila*. They designated the protein JIL-1 and showed that localizes specifically to euchromatic interband regions of polytene chromosomes, and it is the predominant kinase regulating histone H3S10 phosphorylation during interphase (84, 166). Histone H3S10 phosphorylation levels are severely reduced in JIL-1 hypomorphic or null mutants; however, the histone H3S10 levels are restored by introduction of transgenic JIL-1 activity. Furthermore, analysis of JIL-1 null and hypomorphic alleles showed that JIL-1 is essential for viability and that reduced levels of JIL-1 protein lead to a misalignment of the interband polytene chromatin fibrils that is further associated with coiling of the chromosomes and an increase of ectopic contacts between non-homologous regions (45, 83, 166, 177, 178, 180). This results in a shortening and folding of the chromosomes with a non-orderly intermixing of euchromatin and the compacted chromatin characteristic of banded regions (45). Based on these findings a model was proposed in which JIL-1 functions to establish or maintain euchromatic chromatin regions by repressing the formation of contacts and intermingling of non-homologous chromatid regions. In order to further study the mechanisms of perturbations to chromatin structure in the absence of JIL-1 activity and histone H3S10 phosphorylation Zhang et al. (177) studied the distribution of the heterochromatin markers H3K9me2 and HP1 in JIL-1 null mutant backgrounds. In *Drosophila* formation of heterochromatin and repression leads to deacetylation of histone H3K9 followed by dimethylation of this residue and recruitment of HP1 (51, 99, 113). Thus, dimethylation of histone H3K9 and the presence of HP1 serve as major chromatin modification marks for the presence of transcriptionally silenced chromatin (59, 152). The studies of Zhang et al. (177) demonstrated that a reduction in the levels of the JIL-1 histone H3S10 kinase resulted in the spreading of the major heterochromatin markers H3K9me2 and HP1 to ectopic locations on the

chromosome arms with the most pronounced increase on the X chromosomes. However, overall levels of the H3K9me2 mark and HP1 were unchanged, suggesting that the spreading is accompanied by a reduction in the levels of pericentromeric heterochromatin in JIL-1 hypomorphic mutant backgrounds.

Genetic interaction assays demonstrated that JIL-1 functioned *in vivo* in a pathway with SU(VAR)3-9 which is a major catalyst for dimethylation of the histone H3K9 residue (135). Zhang et al. (177) provided further evidence that JIL-1 activity and localization were not affected by the absence of SU(VAR)3-9 activity, suggesting that JIL-1 was upstream to SU(VAR)3-9 in this pathway. Taken together these findings suggested that JIL-1 functions in a novel pathway to establish or maintain euchromatic regions by antagonizing SU(VAR)3-9 mediated heterochromatinization (177). According to the histone code (147) and the recently proposed binary switch model (58) phosphorylation of a site adjacent to a methyl mark that engages an effector molecule may regulate its binding. JIL-1 phosphorylates the histone H3S10 residue in euchromatic regions of polytene chromosomes (84, 166), raising the possibility that this phosphorylation at interphase prevents ectopic recruitment and/or spreading of the heterochromatin-promoting factors HP1 and SU(VAR)3-9, thus antagonizing the formation of silenced heterochromatin at interbands.

Interestingly, some of the strongest suppressors of PEV described, *Su(var)3-1* mutations, were recently identified to be alleles of the JIL-1 locus that generate proteins with COOH-terminal deletions (51). Furthermore, Lerach et al. (101) demonstrated that JIL-1 hypomorphic loss of function mutations also act as strong suppressors of PEV at the *wm4* locus. However, an important difference between *Su(var)3-1* and *JIL-1* hypomorphic alleles is that while the amount of heterochromatic factors is constant in both mutant backgrounds (51, 177) there is a marked redistribution of the heterochromatic markers H3K9me2 and HP1 in *JIL-1* hypomorphic mutants (177). Therefore, the underlying molecular mechanism of suppression of PEV in *Su(var)3-1* mutants is likely to be different from that occurring in loss-of-function null and hypomorphic JIL-1 alleles.

The finding that the JIL-1 kinase is associated with the MSL complex and that histone H3S10 phosphorylation is up-regulated on the male X chromosome in a pattern similar to that of the JIL-kinase suggests that regulation of histone H3S10 phosphorylation may also play a role in dosage compensation mechanisms (84, 166). Nonetheless, the wild-type interphase polytene male X chromosome showed a striking enhancement of H3S10ph levels that was absent in JIL-1 mutant animals and this same pattern also was observed using antibodies specific for the double modification of S10ph and K14ac residues of histone H3 (166). It has

been proposed that, whereas phosphorylation of H3S10 may signal mitosis, phosphorylation of H3S10 in the context of acetylation would instead be an indicator for gene activity (147, 159). Thus, the male X is epigenetically modified with chromatin marks that are associated with higher levels of transcriptional activity that includes phosphorylated histone H3S10. Interestingly, the recent demonstration that conditional depletion of HP1 in transgenic flies results in increased male lethality suggests that modulation of transcription in a sex-specific manner may also involve epigenetic regulation of HP1 activity (104) and raises the prospect that the mechanism underlying this regulation might involve a methyl/phos binary switch.

More recently, Cai et al. using different antibodies against H3S10ph showed that there is no redistribution or up regulation of JIL-1 or H3S10 phosphorylation at transcriptionally active puffs in such polytene squash preparations after heat shock treatment. Furthermore, they also provide evidence that heat shock induced puffs in *JIL-1* null mutant backgrounds are strongly labeled by antibody to the elongating form of RNA polymerase II (Pol IIO^{ser2}) indicating that Pol IIO^{ser2} is actively involved in heat shock induced transcription in the absence of H3S10 phosphorylation. This data support a model where transcriptional defects in the absence of histone H3S10 phosphorylation are the result of structural alterations of chromatin (26).

1.4. Histone methylation

In addition to acetylation and phosphorylation, important progress has also been made in the studies of another type of covalent modification: methylation of histone H3 and H4. Like acetylation and phosphorylation, protein methylation is a covalent modification commonly occurring on carboxyl groups of glutamate, leucine, and isoprenylated cysteine, or on the side-chain nitrogen atoms of lysine, arginine and histidine residues (38). Although a number of studies have indicated a role of protein methylation in signal transduction and RNA metabolism (4, 61), the precise function of protein methylation remains largely unknown.

Arginine can be either mono- or dimethylated, with the latter in symmetric or asymmetric configurations. Similar to arginine methylation, lysine methylation on the ϵ -nitrogen can also occur as mono-, di-, or trimethylated forms. Studies in the past years have identified several RNA associated proteins including hnRNP A1, fibrillarin, and nucleolin as substrates of type I protein Arginine methyltransferase (PRMT), whereas the only substrate identified so far for type II PMRT is the myelin basic protein (61).

Early studies using metabolic labeling followed by sequencing of bulk histones have shown that several lysine residues, including lysine 4, 9, 27 and 36 of histone H3 and lysine 20 of H4, are preferred as sites of methylation (149). In addition, members of the protein arginine methyltransferase family can also methylate histones *in vitro* (61). However, direct evidence linking histone methylation to gene activity was not available until recently. One major obstacle in studying the function of histone methylation is the lack of information regarding the responsible enzymes. Recent demonstration that a nuclear receptor coactivator-associated protein, CARM1 (also known as PRMT4), is a H3-specific arginine methyltransferase and that the human homolog of *Drosophila* heterochromatic protein SU(VAR)3-9, is a H3 specific lysine methyltransferase, provided substantial evidence for the involvement of histone methylation on transcriptional regulation (33, 128).

The arginine methyltransferases (PRMTs) family of HMTs protein catalyze the transfer of methyl groups from S-adenosyl-L-methionine (SAM) to the guanidino nitrogens of arginine residues (61). As the founding member of the PRMT family, PRMT1 was initially identified from a yeast two-hybrid screen as a protein interacting with the immediate-early gene product TIS21 and the antiproliferative protein BTG1 (103). In an effort to isolate enzymes that methylate core histones, Wang and colleagues purified one of the most abundant H4-specific HMTs from HeLa cells. The enzymatic activity correlated with a single polypeptide identified as PRMT1 and the methylation site was identified to be Arg 3 (162). Importantly, an antibody that specifically recognized methylated H4-R3 recognized histone H4 purified from HeLa cells (148, 162). Methylation on H4-R3 is not limited to mammalian cells, as the highly specific antibody also recognized H4 purified from chicken and yeast (148).

In addition to PRMT1, four other mammalian proteins belonging to the PRMT family have been reported: CARM1 (coactivator-associated arginine methyltransferase 1), PRMT2, PRMT3 and PRMT5, the newest member of the PRMT protein family. CARM1 preferentially methylates histone H3 *in vitro* (33), and mapping of the residues demonstrated specificity for Arg 2, Arg 17, and Arg 26 (136). CARM1 also methylates the carboxyl terminus of histone H3 at one or more of the four arginine (128/129/131/134) residues (136). The gene encoding PRMT2 was identified by screening the EST (expressed sequence tag) databases (89). Whether PRMT2 possesses protein arginine methyltransferase activity remains to be demonstrated. PRMT3 was identified in a yeast two-hybrid screen using PRMT1 as bait (154). PRMT3 functions as a monomer and is predominantly localized in the cytoplasm (154). PRMT5 is the newest member of the PRMT protein family.

1.4.1. SET domain family of HMT

The SET domain is an evolutionarily conserved sequence motif initially identified in the *Drosophila* position effect variegation (PEV) suppressor SU(VAR)3–9 (Suppressor of position-effect Variegation 3-9) (155), the *Polycomb*-group protein Enhancer of zeste (86), and the *trithorax*-group, protein Trithorax (143). Over 200 proteins of diverse functions, ranging from mammals to bacteria and viruses, have been identified to contain this motif. A major function of the SET domain-containing proteins is to modulate gene activity (82). However, the underlying mechanism is not understood. A clue that the SET domain may be an important signature motif for protein methyltransferases came from studies on several plant SET-domain-containing proteins, where it was found that several of the proteins possessed protein methyltransferase activity (90, 181).

One of the founding members of the SET domain protein family, *Drosophila* SU(VAR)3–9 was identified in genetic screens aimed at isolating suppressors of PEV (155). In addition to the SET domain, the SU(VAR)3–9 protein also contains an evolutionarily conserved chromodomain found in a group of chromatin-related proteins (92). Mutations in the fission yeast homolog *clr4* disrupt the association of Swi6p with heterochromatin and result in chromosome segregation defects (50). Studies with the human (*SUV39H1*), and mouse (*Suv39h1*) homolog's of SU(VAR)3–9 demonstrated that the encoded polypeptide associates with the mammalian heterochromatic protein HP1, a homolog of Swi6p. Therefore, the function of SUV39H1/Clr4 and HP1/Swi6p in heterochromatic gene silencing seems to be conserved from yeast to human. Core histones have long been known to play important roles in heterochromatic gene silencing, but the role of histone methylation in heterochromatin silencing was not known until recently. The demonstration that Suv39H1 and Clr4 possess intrinsic histone methyltransferase activity supports a role of histone methylation in heterochromatin silencing (128).

1.4.2. Su(var) genes (*Drosophila* HMTs)

In *Drosophila*, >50 *Suppressor of position-effect variegation*, *Su(var)*, loci exist, of which ~15 have been molecularly defined. *Su(var)* genes encode structural components of heterochromatin, such as the zinc finger protein SU(VAR)3-7 (42, 80) and the chromodomain protein HP1 encoded by SU(VAR)2-5 (54, 55), but also enzymes that can modify histone N-termini (tails), such as the histone methyltransferase (HMTase) SU(VAR)3-9 (128, 135). SU(VAR)3-9, HP1, and SU(VAR)3-7 are inherent components of heterochromatin. In a

genetic hierarchy, SU(VAR)3-9 is dominant over the other two genes indicating an important role for histone lysine methylation in heterochromatin formation (135).

In *Drosophila*, H3K9 dimethylation was found to be enriched at heterochromatin (135). The development of highly specific antibodies that can discriminate mono-, di-, and trimethylation of H3K9 versus H3K27 (122) now allowed to characterize all H3K9 and H3K27 methylation states in *Drosophila*. The data reveal that *Su(var)3-9* mainly controls H3K9 di- and trimethylation at pericentric heterochromatin, whereas all H3K27 methylation is mediated by *Enhancer of zeste (E(z))*. The identification and characterization of novel point mutants in *Su(var)3-9* that show differential HMTase activities demonstrate that the silencing potential of *Su(var)3-9* is mainly determined by the kinetic properties of the HMTase reaction. Importantly, the PEV modifier *Su(var)3-1* was identified as a key antagonist for *Su(var)3-9*-dependent gene silencing (166).

1.5. ATP-dependent chromatin remodeling

ATP-dependent chromatin remodeling enzymes, highly conserved in organisms from yeast to humans, are similar to the SNF (sucrose non-fermenting) family of DNA translocases and all contain a catalytic ATPase subunit. These ATPase machineries utilize the energy of ATP hydrolysis to mobilize nucleosomes along DNA, evict histones of DNA or promote the exchange of histone variants, which in turn modulate DNA accessibility and alter nucleosomal structures (15). Based on distinct domain structures, there are four well-characterized families of mammalian chromatin-remodeling ATP-ases: the SWI/SNF (switching defective/sucrose non-fermenting) family, the ISWI (imitation SWI) family, the NuRD (nucleosome remodeling and deacetylation)/Mi-2/CHD (chromodomain, helicase, DNA binding) and the Ino80 (inositol requiring 80) family (11, 15). Members of the SWI/SNF family, like BRM (*Drosophila* homologue of the brahma protein) and BRG1 (Brahma-Related Gene 1) contain a C-terminal bromodomain that bind acetylated histones tails (72). Involvement of the SWI/SNF members in DNA replication, development, differentiation, signaling, splicing, DNA damage repair and replication was also demonstrated (11, 60, 109).

The ISWI (imitation switch) chromatin remodeling ATPase was first identified in *Drosophila* due to its sequence homology to the yeast SWI2/SNF2 enzyme (56). ISWI remodelers exist in all eukaryotes and constitute a prominent subgroup of the SNF2 ATPase superfamily (49). In *Drosophila*, ISWI is a component of three known chromatin remodeling complexes: NURF (nucleosome remodeling factor), ACF (ATP-utilizing chromatin assembly

and remodeling factor) and CHRAC (chromatin accessibility complex) (79, 157, 158, 160). In all three complexes, ISWI serves as the ATP-dependent motor that drives nucleosome assembly or changes in nucleosome structure.

Analysis of flies with mutations in the *Iswi* gene has shown that ISWI function is required for the maintenance of functional chromosome structure. In particular, in *Iswi* null mutants, which develop until late larval stages and then die, the structure of the male X chromosome is grossly disturbed and the chromosome appears decondensed (46). In flies the male X chromosome is dosage compensated (150) and marked by chromosome-wide histone H4K16 acetylation and its double transcribed genes. Blocking H4K16 acetylation rescues the structure of the male X in ISWI mutants (39). These and other findings suggest that ISWI and H4K16 acetylation play opposing roles in establishing male X chromosome structure or the H4K16ac makes the X male sensitive to the loss of ISWI function.

Recent work has uncovered the potential for an additional mode of ISWI regulation: experiments with *Drosophila* cell lines showed that ISWI is posttranslationally modified by acetylation *in vivo* (57). The amino acid sequence surrounding the acetylated lysine shares similarity with the sequence surrounding K14 of histone H3. Indeed, the histone acetyltransferase dGCN5 efficiently acetylates ISWI at the lysine 753 site *in vitro* and depletion of dGCN5 in cultured cells reduces the amount of acetylated ISWI. The acetylation levels of ISWI are modulated during embryogenesis, suggesting that ISWI acetylation is under developmental control (57).

More recently, Burgio et al. using genetic assays identified new factors that interact with ISWI *in vivo*. Among these factors members of the deacetylase complex, the Sin3A and Rpd3 were found to physically interact with ISWI and co-localize on polytene chromosomes. Chromatographic separation showed that ISWI is associated with histone H3/H4 deacetylase activity. In the absence of functional ISWI both the Sin3A and Rpd3 levels are reduced. According to this data the Sin3A/Rpd3 complex cooperates with ISWI to deacetylates histone and facilitate ISWI chromatin remodeling *in vivo* (24).

The nucleosome remodeling factor (NURF) is the founding member of the ISWI family of ATP-dependent chromatin remodeling factors. Like other ATP-dependent chromatin remodeling enzymes, NURF is a large multi-subunit protein complex that uses the energy of ATP hydrolysis to change the dynamic properties of nucleosomes (158, 172). Although NURF is composed of four subunits, only the largest subunit (in *Drosophila* NURF301; in humans BPTF) is specific to NURF (12, 172). In *Drosophila*, mutation of *nurf301* blocks activation of the homeotic selector genes *Ultrabithorax* and *engrailed* (6). siRNA-mediated knock-down of

BPTF in human cells also prevents the activation of the human homologs, *engrailed-1* and *engrailed-2* (12). However, the larval lethal phenotypes of *nurf301* and *Iswi* mutants (6, 46) suggest that NURF has additional transcriptional targets. More recently, microarray analysis was used to compare genome-wide expression profiles between wild-type and *nurf301* flies (7). This work has identified a large set of genes regulated by ecdysone receptors, as ecdysone-regulated genes are activated during larval-pupal metamorphosis in wild-type flies but fail to be expressed in the mutant. Moreover, the ecdysone receptor interacts with NURF both physically and genetically. These results provide an elegant molecular explanation for the observed phenotype of *nurf301* mutants and establish NURF as a chromatin remodeling complex that is required for the timely activation of a defined transcriptional program during development.

Interestingly, the histone H4 tail is important for NURF-ISWI-driven nucleosome remodeling (50, 69, 126). Deletion of the H4 tail or grafting the tail onto another histone abolishes ISWI ATPase stimulation and nucleosome sliding. A hydrophilic patch of three amino acids that contacts nucleosomal DNA is critical for ISWI stimulation, suggesting that the epitope recognized by ISWI is composed of both DNA and H4 residues (36, 69).

Taken together, ISWI-containing chromatin remodeling complexes play both general and specific roles during *Drosophila* development. Their tasks identified so far range from maintaining the overall structure of entire chromosomes to ensuring the activation of individual genes (20).

2. AIMS OF STUDY

1. In *Drosophila* and several other metazoan organisms, there are two genes that encode related but distinct homologues of ADA2-type transcriptional adaptors. By using mutant *Drosophila* lines, it was shown that *Drosophila* ADA2b protein is present in the dSAGA complex and has a role in H3 acetylation. Since in *Drosophila* the existence of another ADA2-type adaptor was reported, but its role was unknown, our aims were to characterize the *Drosophila* *Ada2a* mutants and to investigate the *in vivo* functional role of ADA2a protein.
2. During this work it was found that dADA2a is a component of ATAC complex and we showed that it plays a role in H4 acetylation. In mutants of *dAda2a* and several ATAC subunits, (*dGcn5* and *dAda3*), there is an alteration of chromosome structure similar to structural changes observed in the absence of JIL-1 kinase. Since chromosome structural defects are not seen in dADA2b containing-complex, we investigated the role of ATAC in maintaining chromatin structure and if the similar phenotypes of ATAC mutants and the *Drosophila* JIL-1 kinase reflect a functional interaction.

3. MATERIALS AND METHODS

3.1. *Drosophila* stocks

Fly stocks were raised at 25°C on standard cornmeal medium containing nipagin. The *dAda2a*^{d189} and *dAda2a*^{hyp} alleles have been described (91, 120, 121). *dGcn5* null and hypomorph alleles *dGcn5*^{E333st}, *dGcn5*^{sex204} and *dGcn5*^{C137T} and the strains carrying the transgenes that lack the HAT or the ADA interacting domain, *dGcn5*ΔHAT and *dGcn5*ΔADA were kindly provided by C. Antoniewsky (31). The *JIL-1*^{Z2} allele and the JIL-1-GFP wild-type transgene P(hs83-GFP-JIL-1,w+) were kindly provided by dr. K. Johansen (84, 166, 178). *dAda3*² allele described in Grau et al. was kindly provided by dr. Alberto Ferrus. All alleles were kept as heterozygotes with TM6C, Tb Sb, TM6B, TbHu or T(2;3)TSTL, Cy; Tb Hu balancer chromosomes and mutants were selected on the basis of the Tb⁺ phenotype. *dAda3*² stock was maintained using FM7, B GFP⁺ balancer and the mutants were selected on the basis on GFP⁻ phenotype. The *dSu(var)3-9*¹ and *dSu(var)3-9*² stocks were obtained from the Bloomington stock center and were maintained on TM3, Sb Ser balancer (155), (130). As control the *w*¹¹¹⁸ strain was used (134). Other stocks used in this study were obtained from Szeged and Bloomington Stock Centers, unless otherwise indicated.

3.2. Genetic crosses and phenotype analysis

All crosses were performed at 25°C. To produce *dAda2a dGcn5* double mutants, *dGcn5*^{E333st} and *d189* or, alternatively, *dGcn5*^{C137T} and *d189* alleles were recombined into the same chromosome. *dAda2a*-null *dGcn5* hypomorph mutants (*P[DtlRpb4]/+;dGcn5*^{E333st}*d189/dGcn5*^{C137T}*d189*) were obtained from crosses *P[DtlRpb4];dGcn5*^{E333st}*d189/TM6C* X *dGcn5*^{C137T}*d189/TM6C*. The overexpression of dGCN5 in the *dAda2a* mutant background was achieved by crossing *P[act-GAL4];P[DtlRpb4]d189/T(2;3)TSTL* to *P[UAS-Gcn5];d189/TM6C*. The genotypes *P[DtlRpb4]/+;P[DtlAda2a]*^{79/1}*d189/d189* and *+/+;P[DtlAda2a]*^{79/1}*d189/P[DtlRpb4]d189* represent *dAda2a* hypomorphs and for simplicity are labeled *dAda2a*^{hyp1} and *dAda2a*^{hyp2}, respectively. *dAda2a*^{hyp1} in a wild-type or heterozygous *dGcn5* background was obtained from the crosses *P[DtlRpb4];P[DtlAda2a]*^{79/1}*d189/TM6C* X *d189/TM6C* and *P[DtlRpb4];P[DtlAda2a]*^{79/1}*d189/TM6C* X *dGcn5*^{E333st}*d189/TM6C*, respectively. In order to obtain *dAda2a*^{hyp2} in combination with normal or overexpressed dGCN5 levels, the following crosses

were performed: $P[DtlAda2a]^{79/1}d189/TM6C$ X $P[act-GAL4];P[DtlRpb4]d189/T(2;3)TSTL$ and $P[UAS-Gcn5];P[DtlAda2a]^{79/1}d189/TM6C$ X $P[actGAL4];P[DtlRpb4]d189/T(2;3)TSTL$, respectively.

The overexpression of JIL-1 in *dAda2a* and *dGcn5* mutant backgrounds was achieved by crossing $P[hs83-GFP-JIL-1]/P[hs83-GFP-JIL-1];d189/TM6B$ to $P[DtlRpb4]d189/TM6C$. The analyzed genotype was $P[hs83-GFP-JIL-1]/+;d189/P[DtlRpb4]d189$. The animals with the genotype $P[hs83-GFP-JIL-1]/+;dGcn5^{E333st}/dGcn5^{sex204}$ were obtained by crossing $P[hs83-GFP-JIL-1]/P[hs83-GFP-JIL-1];dGcn5^{sex204}/TM6B$ were crossed to $dGcn5^{E333st}/TM6C$. For the ectopic expression of the *hs83-GFP-JIL-1* transgene the animals were heat shocked 3-4 times before analyzing at 37°C for 30 min starting with L1 stage.

In order to obtain *dAda2a* or *dGcn5* hypomorph in combination with overexpressed JIL-1, the following crosses were performed: $P[hs83-GFP-JIL-1]/P[hs83-GFP-JIL-1];d189/TM6B$ to $P[DtlRpb4];P[DtlAda2a]^{79/1}d189/TM6C$ and $P[hs83-GFP-JIL-1]/P[hs83-GFP-JIL-1];dGcn5^{sex204}/TM6B$ to $dGcn5^{C137T}/TM6B$. The analyzed genotypes were $P[hs83-GFP-JIL-1]/P[DtlRpb4];P[DtlAda2a]^{79/1}d189/d189$ and $P[hs83-GFP-JIL-1]/+;dGcn5^{sex204}/dGcn5^{C137T}$. The control crossings were: $dAda2a^{d189}/TM6C$ to $P[DtlRpb4];P[DtlAda2a]^{79/1}d189/TM6C$ and $dGcn5^{sex204}/TM6B$ to $dGcn5^{C137T}/TM6C$.

To produce *dAda2a/dSu(var)3-9* and *dGcn5/dSu(var)3-9* double mutants, *d189* or *dGcn5^{sex204}* and *dSu(var)3-9* alleles were recombined into the same chromosome and the recombinant strains were crossed to $P[DtlRpb4]d189/TM6C$ and $dGcn5^{E333st}/TM6C$, respectively. The analyzed genotypes were $dSu(var)3-9d189/P[DtlRpb4]d189$ and $dSu(var)3-9dGcn5^{sex204}/dGcn5^{E333st}$.

For the overexpression of the *dGcn5* variant constructs with PCAF, HAT or ADA-interacting domains deleted following crossing were done: $dGcn5^{E333st}/TM6C$ X $P[UAS-dGcn5 \Delta Pcaf]/P[UAS-dGcn5 \Delta Pcaf]$; $daGal4-dGcn5^{sex204}/TM6B$, $dGcn5^{E333st}/TM6C$ X $P[UAS-dGcn5 \Delta HAT/UAS-dGcn5 \Delta HAT]$; $daGal4-dGcn5^{sex204}/TM6B$, $dGcn5^{E333st}/TM6C$ X $P[UAS-dGcn5 \Delta ADA/UAS-dGcn5 \Delta ADA]$; $daGal4-dGcn5^{sex204}/TM6B$.

For the rescue experiments, the L3 animals identified as non-*Tubby* were gently transferred to new vials, allowed to develop at 25°C, analyzed and scored for pupa formation or hatching rate. For determination of the sex ratio homozygous L3 animals carrying the JIL-1 transgene were gently transferred to new vials after differentiating the sexes based on the presence of testes under a dissecting microscope. The number of counted animals was as follows:

Genotype	No. of analyzed animals
<i>P[DtlRpb4];d189/d189</i> (control)	485
<i>dGcn5^{sex204}/dGcn5^{E333st}</i> (control)	330
<i>P[hs83-GFP-JIL-1]/+;d189/ P[DtlRpb4]d189</i>	357
<i>P[hs83-GFP-JIL-1]/+; dGcn5^{E333st}/dGcn5^{sex204}</i>	343
<i>Su(var)3-9 d189/ P[DtlRpb4] d189</i>	361
<i>dSu(var)3-9 dGcn5^{sex204} /dGcn5^{E333st}</i>	283
<i>P[DtlRpb4]; P[DtlAda2a]^{79/1} d189/d189</i>	625
<i>dGcn5^{sex204}/dGcn5^{C137T}</i>	456
<i>P[hs83-GFP-JIL-1]/P[DtlRpb4]; P[DtlAda2a]^{79/1} d189/d189</i>	781
<i>P[hs83-GFP-JIL-1]/+; dGcn5^{sex204}/dGcn5^{C137T}</i>	488

3.3. Immunohistochemistry

3.3.1. Immunostaining of polytene chromosomes

Polytene chromosome spreads were obtained from the salivary glands of wandering larvae of the genotype indicated. The L3 larvae were dissected in 30 μ l Sol.1, transferred to 30 μ l Sol.2 for 40sec, fixed in Sol.3 (3.7% formaldehyde) for 40sec followed by incubation in 45% acetic acid for 1min. The chromosome spreads were checked under an optical microscope and kept in 1X PBST. Slides were blocked in PBST (PBS + 0.1% Tween-20) + 5% BSA or fetal calf serum for 1 h at 25°C and incubated overnight at 4°C in a mixture of primary antibodies. Samples were washed 3X 5min in PBST and incubated with a mixture of secondary antibodies 1h at 25°C followed by 3X 5min wash in PBST. The slides were incubated with DAPI in PBST for 2 min at 25°C, washed again in PBST and covered with Fluoromount-G mounting medium (Southern Biotech). H3S10ph, H3K9me2, H4K5ac, H4K12ac specific polyclonal antibodies were from ABCAM or SEROTEC and were used in 1:100 or 1:200 dilutions. Ecdysone receptor antibody (EcRB, 1:50) was from the Developmental Studies Hybridoma Bank, University of Iowa. JIL-1-specific monoclonal antibody (5C9) used in 1:5 dilution was kindly provided by K. Johansen. Mouse anti-Pol II (7G5) was provided by Dr. Tora. Secondary antibodies Alexa Fluor488-conjugated goat-anti-mouse IgG and AlexaFluor555-conjugated goat-anti-rabbit IgG (Molecular Probes) were used in 1:500 dilutions.

Solution 1 (1000 µl)	56 µl 10 % NP-40 100 µl 10 X PBS 844 µl distilled H ₂ O
Solution 2 (500 µl)	100 µl NP-40 50 µl 10 X PBS 50 µl 37 % paraformaldehyde 300 µl distilled H ₂ O
Solution 3 (500 µl)	225 µl 100 %-os Acetic acid 50 µl 37 % paraformaldehyde 225 µl distilled H ₂ O
Solution 4 (1000 µl)	450 µl 100 % Acetic acid 550 µl distilled H ₂ O

37 % paraformaldehyde
0,185 g paraformaldehyde (SIGMA)
7 µl 1 M NaOH
500 µl distilled H₂O

Stained samples were examined with an OLYMPUS BX51 microscope and photos were taken with an Olympus DP70 camera using identical settings for mutant and control samples.

3.3.2. Immunostaining of polytene nuclei

Polytene nuclei of third instar salivary gland (smush preparation) were prepared as described by Zhang et. al., (2006) with minor modifications (175). Three to six pairs of late 3rd instar larval salivary glands were dissected in PBS, placed on a slide in 50 µl PBS, covered with a siliconized coverslip and gently squashed. The nuclei were fixed in 3.7% paraformaldehyde in PBT (PBS with 0.2% Titon X-100) at 4°C for 20 min and then brought to room temperature for 5 min. The fixed tissues were washed 2X 10 min in PBST and blocked

with 5% FCS in PBST for 1 h at 4°C. Immunostaining and detection were performed as described for polytene spreads. Stained nuclei were analyzed with an OLYMPUS BX51 microscope and photos were taken using an Olympus DP70 camera. All staining and data recording procedures were performed under identical conditions.

3.3.3. Immunostaining of larval tissue

For immunostaining of larval tissue samples (salivary glands, guts and imaginal discs), animals were dissected in PBS and fixed in 4% formaldehyde solution. Treatment with anti-JIL-1 primary antibody (1:5) overnight at 4 °C, was followed by 1h incubation with Alexa Fluor 488-conjugated anti-mouse secondary antibody 1:500 (Molecular Probes) at room temperature.

Stained samples were examined with an OLYMPUS BX51 microscope and photos were taken with an Olympus DP70 camera using identical settings for mutant and control samples.

3.4. Western blot

For protein analysis by immunoblot total protein samples were extracted from third instar larvae of the genotypes indicated in the figure legends, the concentration was measured using the Bradford reagent, 20-25 µg protein was separated on 15% SDS-PAGE and transferred by electroblotting to 0,2 µm nitrocellulose membrane. The membranes were blocked for 1 h in 5% dry milk in TBST (20 mM Tris-HCl, pH 7.4, 150 mM NaCl, 0.05% Tween 20) and incubated overnight with primary antibody diluted in 2% BSA TBST. For the detection of histone H3, H4, H4K12ac, H4K5ac and H3S10ph commercially available antibodies (ABCAM) were used. The JIL-1 5C9 monoclonal antibody was used at 1:50 dilution. The same membranes developed with H4K12ac or H3S10ph specific polyclonal primary antibodies were washed in TBST and reprobbed with anti-H4 monoclonal Ab or anti-H3 polyclonal Ab. Membranes were washed, incubated with horseradish peroxidase-conjugated anti-rabbit or anti-mouse secondary antibodies (DAKO), washed again extensively, and developed using the ECL (Millipore) kit following the manufacturer's recommendations.

3.5. Recombinant DNA

The transgene constructs *pCaSpeR4-DtlAda2aRpb4* (*P[DtlAdaRpb4]*), *pCaSpeR4-DtlRpb4* (*P[DtlRpb4]*), and *pCaSpeR4-DtlAda2a* (*P[DtlAda2a]*) were described earlier (2, 91, 120). *P[DtlAdaRpb4]* carries the entire *Ada2a/Rpb4/Dtl* locus; *P[DtlRpb4]* has a nonsense mutation in the *dAda2a* coding region, and from *P[DtlAda2a]*, the *Rpb4* region is deleted. The upstream activator sequence promoter-driven *dGcn5* transgene was generated by the insertion of a cDNA fragment from clone LD17356 (generated in the Berkeley EST sequencing project), encompassing the *dGcn5* coding region, into the P element insertion vector pUAST with the help of PCR. The structure of the plasmid thus obtained was verified by nucleotide sequencing.

3.6. RT-PCR and Quantitative real-time PCR

For the quantitative determination of transcripts of early-response ecdysone genes, BR-C, Eip74 and Eip75, larvae were staged at the second- to third-instar molt, and 42 h later (which corresponds to the time of spiracle eversion in wild-types) collected for RNA extraction. For the determination of *JIL-1* message of the different genotypes L3 wandering larvae were used. Total RNA was isolated with the QIAGEN RNeasy kit according to the manufacturer's instructions. First-strand cDNA was synthesized from 1 µg RNA using TaqMan Reverse Transcription Reagent (ABI). The relative abundances of Broad-Complex-, E74A-, and E75A-specific and *JIL-1* mRNAs were quantified by Q-RT-PCR (ABI Prism 7300) using 18S rRNA as control. C_T values were set against a calibration curve. The $\Delta\Delta C_T$ method was used for the calculation of the relative abundances (168). The sequences of specific primers are shown in Table 1.

TABLE 1. Oligonucleotides used for this study

Oligonucleotides	Sequence (5'-3')
18S Fw	GCCAGCTAGCAATTGGGTGTA
18S Rev	CCGGAGCCCAAAAAGCTT
BR-C Fw	GCCCTGGTGGAGTTCATCTA
BR-C Rev	CAGATGGCTGTGTGTGTCCT
Eip74A Fw	GTTGCCGGAACATTATGGAT
Eip74A Rev	ATCAGCCGAATTGTCAATCA
Eip75A Fw	GCGGTCCAGAATCAGCAG
Eip75A Rev	GAGGATGTGGAGGAGGATGA
JIL-1 Fw	TGCCACCAGCAATAGTACA
JIL-1 Rev	GCATACAATTTCCGGCATC

3.7. *In vitro* and *in vivo* ecdysone treatments

For *in vitro* ecdysone treatment, larvae were synchronized at the second- to third-instar molt and collected 24h later at mid-L3 stage. The salivary glands were removed and placed into Robb medium. Each gland was divided into two parts; one part was ecdysone treated, and the other was mock treated. For ecdysone treatment, 20M 20-OH-ecdysone (Sigma) was added to the medium and the lobes of the glands were incubated at 25°C for 2h. Following incubation, ecdysone and mock-treated control salivary glands were used to prepare polytene chromosome squashes. Chromosome preparations were visualized under a phase-contrast microscope and photographed, and the widths of the puffs in the treated samples were determined by comparison with a nearby band as reference. Data were analyzed by averaging the widths of puffs observed in ecdysone-treated glands. For *in vivo* ecdysone treatment, both wild-type and *dAda2a* mutant L3 larvae were placed on autoclaved yeast containing 1 mM 20-OH-ecdysone.

4. RESULTS

4.1. dADA2a role in H4 acetylation

The transcriptional adaptor protein ADA2 is a subunit of SAGA complex in yeast and forms a part of the catalytic acetyltransferase core with GCN5 and ADA3 (140). Whereas yeast has one version of ADA2, *Drosophila melanogaster* has two distinct ADA2 homologues, dADA2a and dADA2b (97, 110). By a combination of biochemical and cell biological studies, it was demonstrated that the two *Drosophila Ada2* homologues are present in functionally and structurally distinct multiprotein complexes (97, 110). dADA2b, is associated with SAGA-type GNAT complexes (97). The second variant, dADA2a, is part of newly characterize ATAC complex, which contains also dGCN5 and dADA3, and possible a dGCN5-independent HAT (68). *Arabidopsis*, mice and humans also possess homologues of *dAda2a* and *dAda2b*, suggesting that higher eukaryotes have two distinct subgroups of ADA2, which characterize functionally distinct multiprotein complexes involved in transcriptional regulation.

4.1.1. Characterization of *dAda2a* mutants

In order to facilitate the *in vivo* functional study of *Drosophila melanogaster* dADA2a protein, homozygous mutants were generated by remobilizing a P element localized close to the 5' end of the *dAda2a* gene (120). In the *l(3)S096713* line, a P element is located in the 90F cytological region, 107bp upstream of the transcription start site of *dAda2a* gene. By remobilizing the P element in *l(3)S096713* a small deletion (*d189*) that removed nucleotides +107 to -613 was isolated. The *d189* deletion removed the regulatory regions of the adjacent *dAda2a/Rpb4* and *Dtl* genes and resulted in an early larva lethal phenotype (Fig. 4.1.) (91, 120). With the use of transgenes corresponding to specific functions affected by the deletion, it was determined that the loss of Rpb4 and Dtl function results in L1 and L2 lethality, respectively (Fig. 4.1.) (91, 120, 121). When a transgene (P[*DtlRpb4*]) encompassing both transcription units with a stop codon in the *dAda2a* coding region is introduced into the *d189* background, the Rpb4 and Dtl functions are restored and the transgene carriers survive until late L3. A further transgene with an intact *dAda2a* region results in a complete phenotypic rescue, providing evidence that the L3 lethality is a result of the absence of the dADA2a function. P[*DtlRpb4*] transgene carrier *d189* homozygotes therefore represent clean *dAda2a* loss-of-function mutants (these will be referred to as *dAda2a^{d189}*) (Fig. 4.1.). As expected RT-

PCR analysis did not reveal *dAda2a*-specific transcript in the *dAda2a*^{d189}(*P[DtlRpb4]*) animals (data not shown).

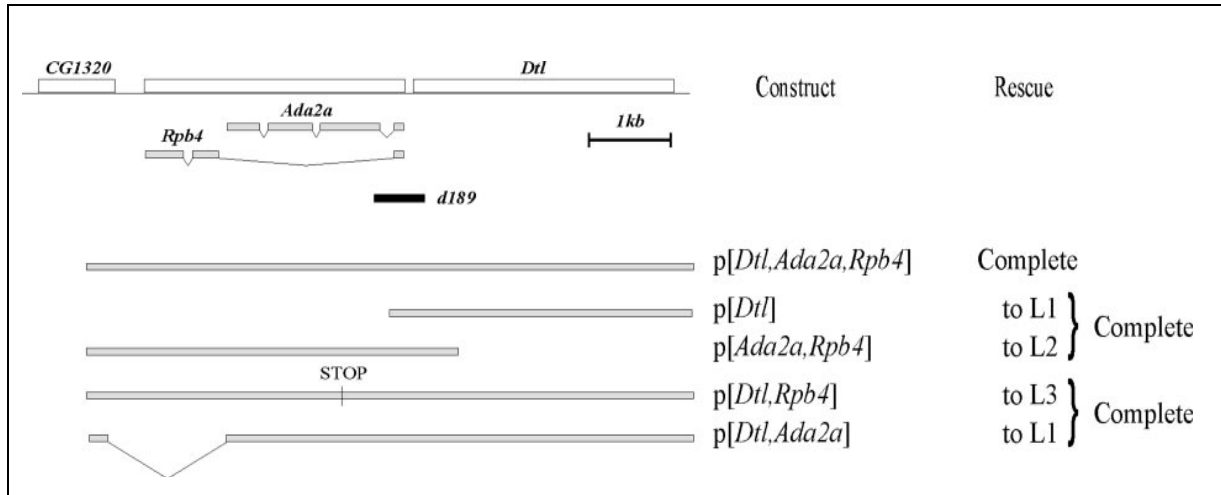


Fig. 4.1. Schematic view of the *Drosophila* 90F cytological region. The position of *d189* deletion and the genes affected by it (*Dtl*, *Ada2a*, *Rpb4*), as well as the regions present in the used transgene construct are shown. The rescue ability of particular transgenes and their combinations is indicated.

The phenotypic characterization of *dAda2a*^{d189} homozygotes revealed that the mutants survive for an extended period (up to 2 weeks) in the L3 stage but fail to pupariate or form only malformed structures covered with brownish cuticle (Fig. 4.2). During their extended L3 stage, *dAda2a* larvae feed and reach a size similar to that of their wild-type siblings but never start wandering. The imaginal discs, central nervous system, and gonads of *dAda2a*^{d189} larvae are significantly smaller than those of the wild-type controls (Fig. 4.3 and data not shown).

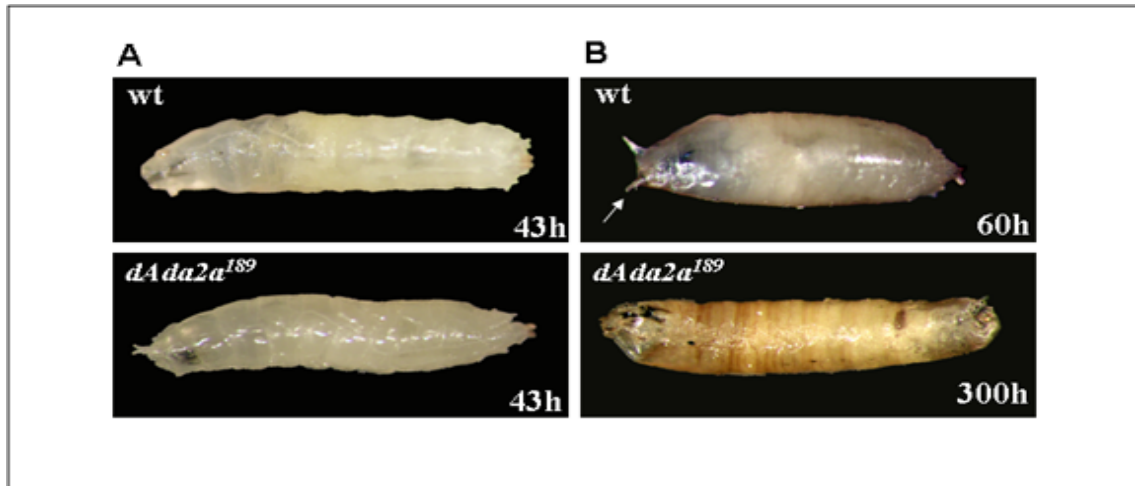


Fig. 4.2. *dAda2a*¹⁸⁹ mutants fail to pupariate or form malformed pupae. Third instar *dAda2a*¹⁸⁹ larvae reach similar size to those of the wild-type (wt) sibling but do not start wandering and fail to evert spiracle (white arrow), and only after 8 to 10 days in L3 do some of them form primitive pupa-like structures covered with brownish cuticle.

We also assessed the consequence of loss of *dAda2a* and *dGcn5* on polytene chromosome structure in interphase nuclei. Whereas wild-type polytene chromosomes show extended arm with a regular pattern of bands, the polytene chromosomes of *dAda2a*¹⁸⁹ animals were severely perturbed. These latter preparation display a distorted banding pattern, while the most affected is the X male chromosome with no remaining observable banding pattern or structure (Fig. 4.4.A). A transgene that expresses wild-type dADA2a protein restore the chromosome structure similar to the wild-type (Fig. 4.4.B). *dGcn5*-null mutants, *dGCN5*^{E333st}, have similar phenotypes regarding lethality, underdeveloped discs, and polytene chromosome structural defects (Fig. 4.3 and 4.4.) (31). A transgene corresponding to the wild-type *dGcn5* allele restores the normal polytene chromosome phenotype of *dGcn5* mutants; however, a transgene with a deletion in the HAT domain or in the region involved in ADA2 interaction fails to restore the normal chromosome structure of *dGcn5* mutants (Fig. 4.4.B).

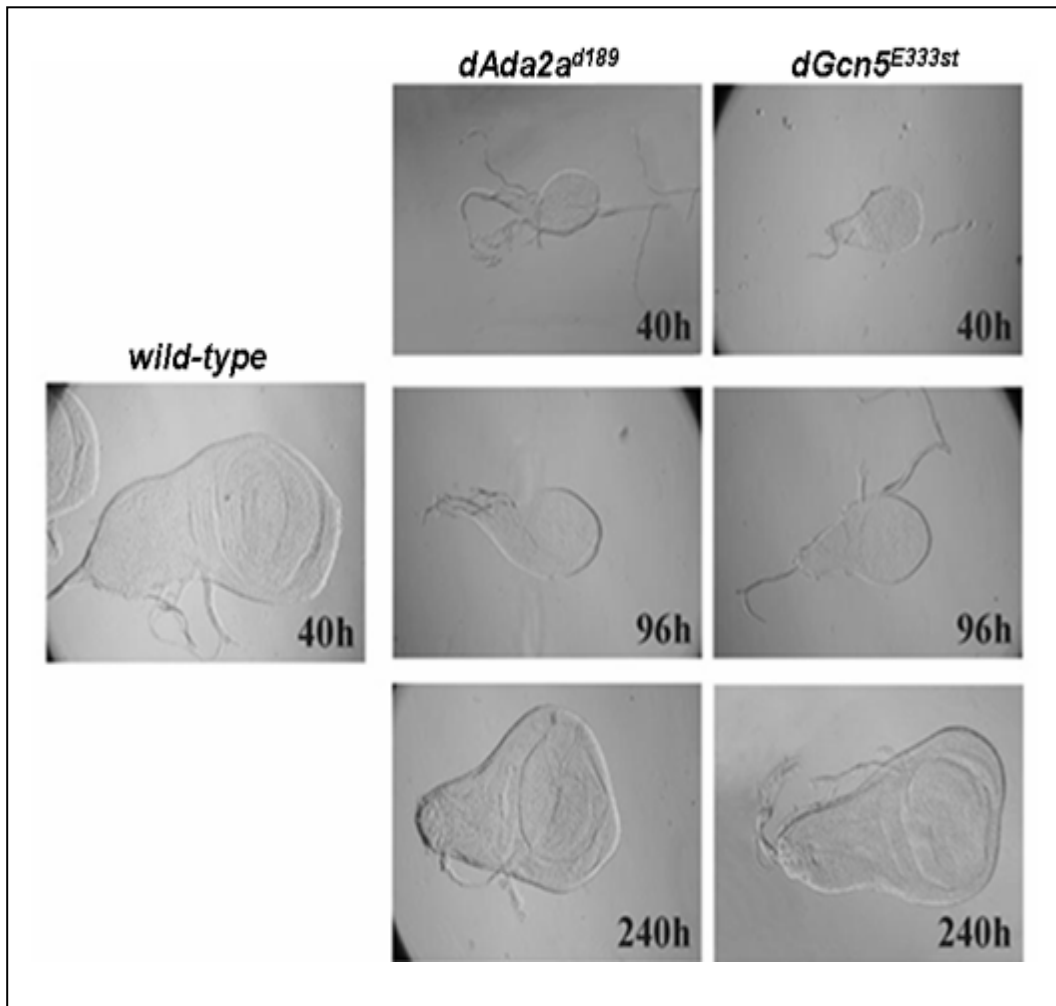


Fig. 4.3. Imaginal discs of *dAda2a^{d189}* and *dGcn5^{E333st}* third-instar larvae are underdeveloped compare with similar aged wild-type controls. During their extended L3 stage, the imaginal discs of *dAda2a^{d189}* and *dGcn5^{E333st}* grow and reach the size of the fully developed wild-type discs after 8 to 10 days of L2/L3 molting, but they are abnormal in regards to both their shape and their structure. The analyzed genotypes are indicated.

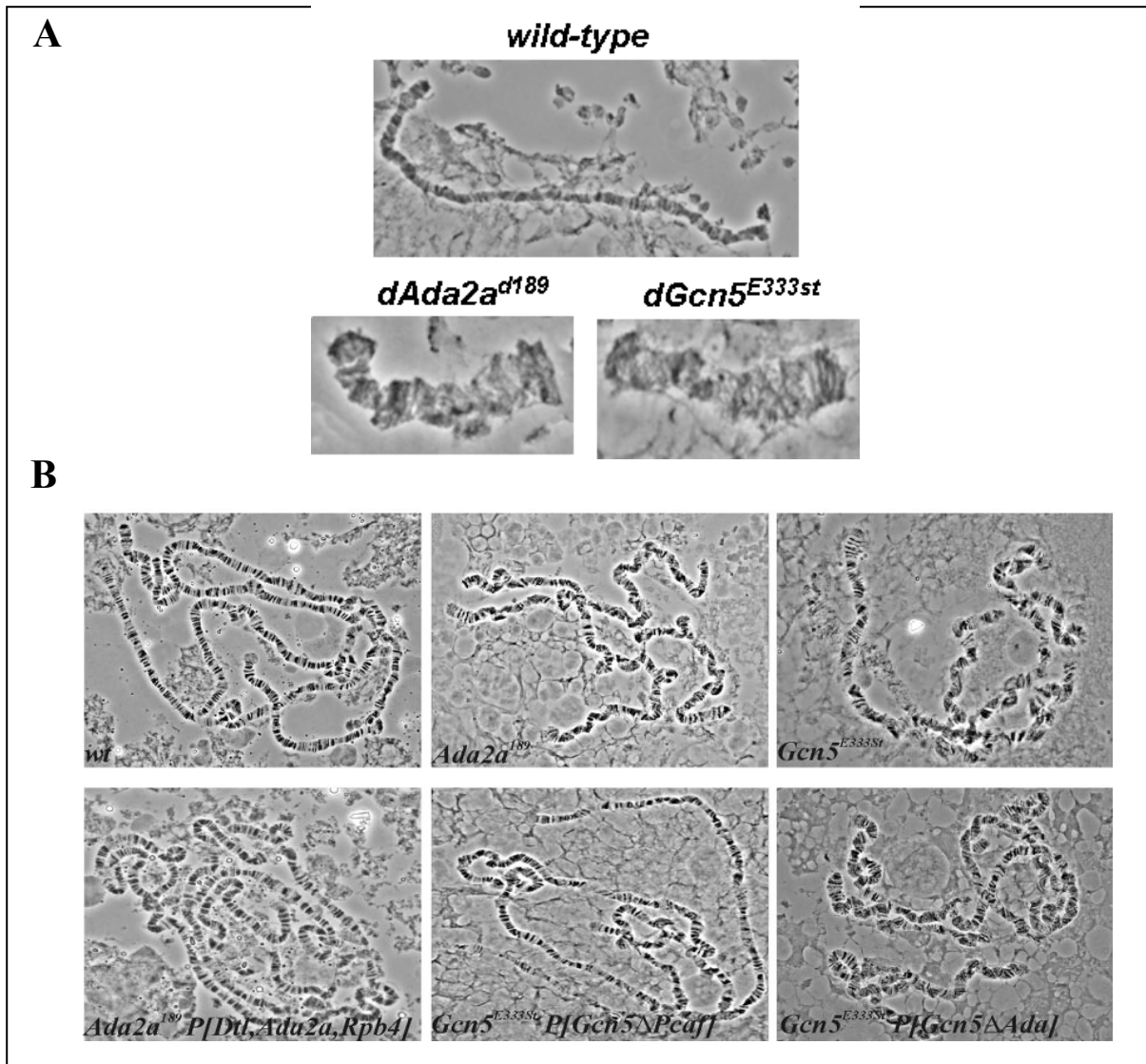


Fig. 4.4. Polytene chromosomes of *dAda2a^{d189}* and *dGcn5^{E333st}* mutants display similar abnormal structures with respect to condensation, short arm and distorted banding pattern. **A)** Male X chromosomes of *dAda2a^{d189}* and *dGcn5^{E333st}* (bottom) compared to wild-type (top). **B)** The structure of *dAda2a^{d189}* and *dGcn5^{E333st}* mutant chromosomes (top) is rescued by a wild-type *dAda2a* and *dGcn5* transgene (bottom, first and second picture), but not by an *dGcn5* transgene with deleted ADA interacting domain (bottom, third picture).

Thus, the polytene chromosomes phenotype suggests that dADA2a and dGCN5 proteins act together, probably as components of the ATAC complex, to regulate directly or through an indirect mechanism the chromatin structure.

4.1.2. Genetic interaction between *dAda2a* and *dGcn5*

In accord with the above conclusion, biochemical purification of dADA2a and dGCN5 indicated their coseparation as a part of the same complex, and Yeast Two Hybrid (YTH) experiments showed their physical interaction (110). In order to study whether genetic interaction between *dAda2a* and *dGcn5* can also be demonstrated, double mutants were generated using null and hypomorph *dAda2a* and *dGcn5* mutations. *dGcn5 dAda2a* double-null mutants or a combination of *dAda2a* null (*dAda2a^{d189}*) and a hypomorph *dGcn5* allele (*dGcn5^{C137T}*) (31) results in a phenotype stronger than that of either of the two mutations alone; *dAda2a^{d189} dGcn5^{C137T}* animals are L2 and early L3 lethal. The coexpression of an upstream activator sequence (UAS) promoter-driven *dGcn5* transgene and an act-GAL4 driver in a *dAda2a^{d189}* background results in a partial phenotypic rescue: *dAda2a^{d189} P[UAS-Gcn5] P[act-GAL4]* L3 larvae have polytene chromosomes that are indistinguishable from the wild-type in morphological features, and they form pupae, though they do not hatch (data not shown). These observations indicate a genetic interaction between *dAda2a* and *dGcn5*.

Several independent *dAda2a* transgene carrier lines that were established and carry the insertion of a genomic fragment encompassing the *Ada2a* locus with its regulatory region, fully rescues the *dAda2a^{d189}* phenotype. In line P[DtlAda2a]^{79/1}, however, the transgene expression results in only a partial phenotypic rescue, most probably because of the low level of expression determined by the site of integration. The *dAda2a^{d189} P[DtlAda2a]^{79/1}* genotype can be therefore considered a hypomorph *dAda2a* (*dAda2a^{hyp}*) allele (see Materials and Methods). Nearly 85% of *dAda2a^{hyp1}* animals with a wild-type *dGcn5* background hatch, but 30% of them display an outstretched wing (*os*) phenotype (Fig. 4.5.B). In a *+/dGcn5^{E333st}* heterozygous background, however, two-thirds of the *dAda2a^{hyp1}* animals perish as pupae or pharate adults, and 70% of those which emerge as adults have an *os* phenotype (Fig. 4.5.A, insert). In contrast, an excess amount of dGCN5 partially suppresses the phenotypic defects of the hypomorph *dAda2a* mutation; *dAda2a^{hyp2} P[UAS-Gcn5] P[act-GAL4]* adults emerge in higher numbers than do their control siblings without the *dGcn5* transgene (Fig. 4.5.B), and only a small proportion of them display the *os* phenotype (Fig. 4.5.B, insert). These results obtained from an analysis of the phenotypes of *dAda2a* transgene carriers, provide further support for the genetic interaction of *dAda2a* and *dGcn5*.

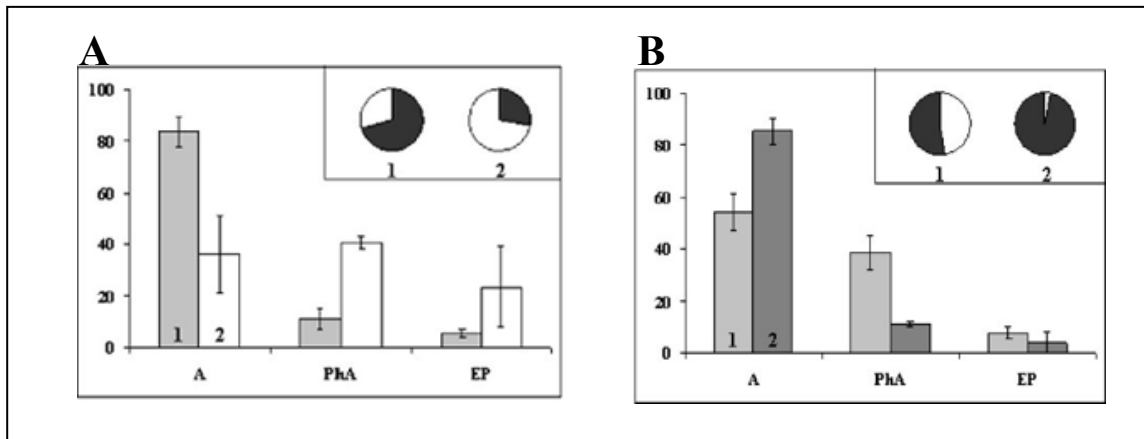


Fig. 4.5. **A)** The null *dGcn5^{E333st}* allele has a negative effect on the development of *dAda2a^{hyp1}*. The phenotype change is shown as the fraction of animals reaching adult (A), pharat adult (PhA), and early pupa (EP) stages in the wild-type (light gray bars) and *dGcn5* heterozygous background (white bars). **B)** The overexpression of *dGcn5* from a transgene (dark gray bars) has a positive effect on the development of *dAda2a^{hyp2}* (labels are described in panel A). The inserts show the fractions of adults displaying the outstretched wing (*os*, white) and wild-type (*wt*, black) phenotypes. Resulting from the different chromosomal background, the fractions of *dAda2a^{hyp1}* and *dAda2a^{hyp2}* adults in the two experiments (columns in panel B and C) are different. Error bars indicate deviations.

4.1.3. Failure in ecdysone response in *dAda2a* mutants

The phenotypic features of *dAda2a* mutants indicate a developmental block at the time of the larva-pupa transition. Since major developmental transitions during the onset of metamorphosis are triggered by the steroid hormone ecdysone, we wondered whether the induction of ecdysone-responsive genes in *dAda2a* mutants was affected. The first pulse of ecdysone, at the beginning of the prepupal stage (0 hour prepupa), induces the expression of a set of early genes. The Broad Complex (BR-C), E74 and E75 early genes are located within early puffs 2B5, 74EF, 75B, respectively (25, 47, 137). In the presence of ecdysone, early genes are transcribed for the next 4 hours. Most interestingly, the second ecdysone pulse, around 10 hours after pupariation, induces the same early genes BR-C, E74, E75.

Late larval and prepupal pulses of ecdysone trigger a sequential induction of puffs in the giant polytene chromosomes of the larval and prepupal salivary glands. The puffs correspond to a loose chromatin structure where genes are actively transcribed. Importantly, during normal development, puffs corresponding to the above regions are visible in the last stage of the third instar, from the beginning of the wandering phase, when the larvae stop feeding and prepare for puparium formation. To establish whether the *dAda2a* mutation has an effect on ecdysone-

induced puff formation, wild-type and *dAda2a*^{d189} larvae were staged at the second - to third instar molt and then sampled at regular intervals. Polytene chromosome squashes were prepared from salivary glands dissected from wandering wild-type animals and *dAda2a*^{d189} animals of similar age, and the presence and size of puffs in the cytological regions 2B5, 74EF, and 75B were determined (Fig. 4.6.). The size of the puffs present in the regions 2B5, 74EF, and 75B in the wild-type animals are significantly larger than those in the *dAda2a* mutants. The reduced size of early ecdysone- responsive puffs was also observed in *dGcn5* mutants (31) and *dAda3* (66).

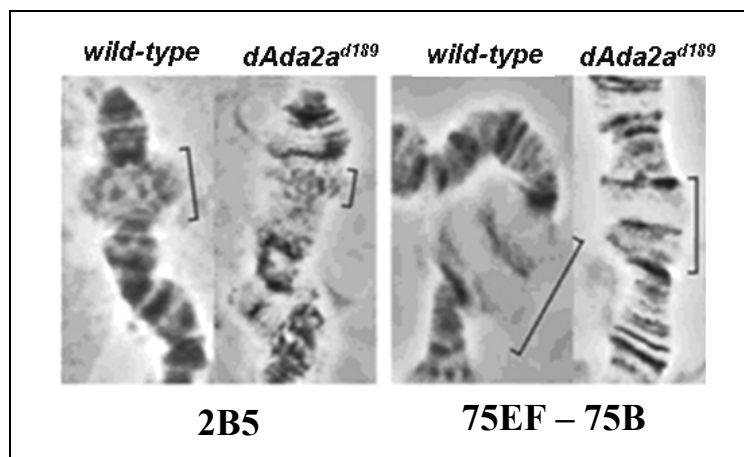


Fig. 4.6. The formation of ecdysone-induced early-response puffs is reduced in *dAda2a* mutants. Phase-contrast images of polytene chromosome region of wild-type control and *dAda2a*^{d189} third-instar larvae, depicting the cytological regions 2B5 (left) and 74EF-75B (right). Brackets show the regions corresponding to early response puffs.

Since the ecdysone levels change dynamically in this stage, and the response to the hormone is rapid, there is inevitably some degree of heterogeneity in the developmental age of the late third instars, which makes the timing of the comparison critical. This is of particular concern when the puffs of wild-type and *dAda2a* mutants are compared, since the development of the latter in the L3 stage is slowed down considerably compared with that of their control siblings. With this in mind, we also tested whether *dAda2a* mutants retained their abilities to form puffs in response to *in vitro* ecdysone treatment. For ectopic ecdysone treatment, salivary glands were dissected from mid-third-instar larvae and cultured in Robb medium at 25°C for 2 – 4 h either in the absence or in the presence of ecdysone. Polytene squashes were prepared from both the ecdysone treated and untreated salivary glands and the presence of puffs was

observed under phase-contrast microscope and photographed. The widths of the puffs from the wild-type and mutant treated samples were determined as the report between the size of the puff and a nearby reference band. Figure 4.7.A reveals that ecdysone treatment induces puff formation at 2B5, 74EF, and 75B in the salivary glands from both wild-type and mutant larvae. In the *dAda2a* mutants, the puffs are consistently smaller. Thus, the reduced abilities of these loci to be induced by ecdysone in late-third-instar *dAda2a* salivary glands can be overcome only partially by ectopic ecdysone treatment (Fig. 4.7.A). In accord with this observation, we found that an increase in the *in vivo* ecdysone level of *dAda2a* mutant L3 larvae results in a partial phenotypic rescue: animals whose control siblings remain in the L3 stage for more than 10 days mostly form deformed pupa-like structures when placed on ecdysone-containing medium for 1 day (Fig. 4.7.B).

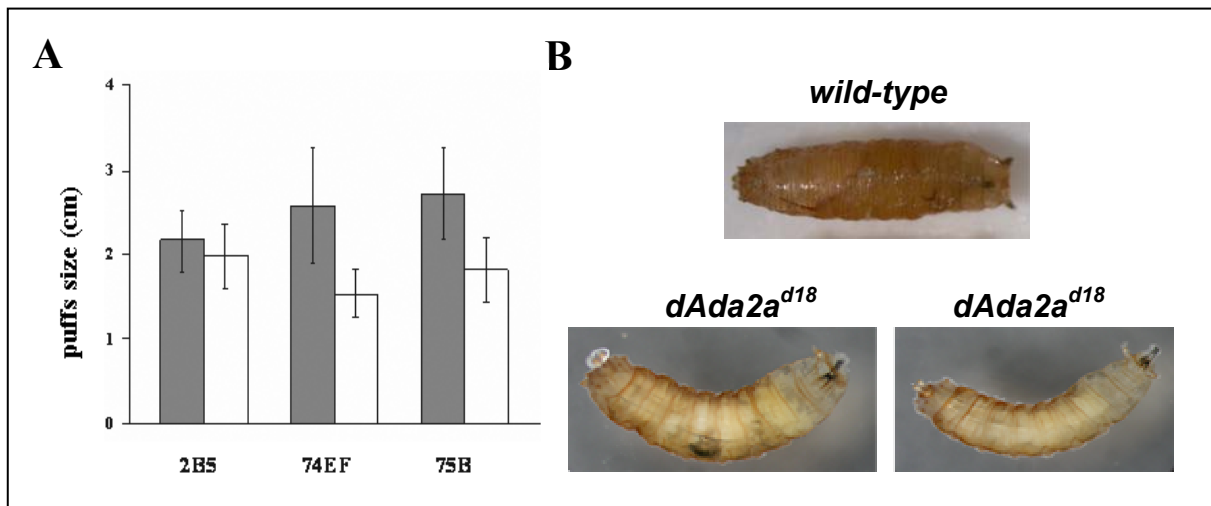


Fig. 4.7. *In vitro* and *in vivo* ecdysone treatment partially rescue the puff formation and the lethal phase in *dAda2a*^{d189} mutants. **A)** The average size of early puffs (expressed as the average width of puffs in arbitrary units) following ectopic ecdysone treatment is significantly smaller in the *dAda2a*^{d189} mutants (white bars) than in the wild-type controls (dark bars). The size of the puffs was determined as described in Materials and Methods. Each column represents the average of measurements of at least 20 dissected salivary glands. Error bars indicate deviations. **B)** *In vivo* ecdysone treatment lead to the formation of *dAda2a* mutant malformed pupae after 24 hours of ecdysone feeding. Ectopically ecdysone fed wild-type (top) and *dAda2a* mutant (bottom) larvae are shown.

To determine if the failure of the puff formation correlates with a failure in the expression of early ecdysone induced genes we compared the levels of hormone induced mRNA levels in mutant and wild-type animals. Early puffs at 2B5, 74EF, and 75B contain complex

transcription units (Broad-Complex, Eip74, and Eip75, respectively), each encoding a family of transcription factors. Q-RT-PCRs indicated that the mRNA level corresponding to a representative transcript from each locus is markedly decreased in the *dAda2a*^{d189} samples compared with that of the control late-L3 wild-type larvae (Fig. 4.8.A). The difference in the levels of the Eip74A message of the wild-type and *dAda2a*^{d189} mutants was consistently the highest upon repetition, reaching more than 2 log differences. These results indicate that the ecdysone-triggered transcription activation that directs developmental responses is severely attenuated in the *dAda2a*^{d189} mutants. A possible underlying reason of the reduced expression of ecdysone-induced genes could be that the lack of ADA2a interferes with the synthesis of ecdysone or with the expression of the ecdysone receptor (EcR). In order to test this assumption by RT-PCR we analyzed the expression of two EcR isoform messages. The results obtained show that the level of EcR was affected to a lesser extent by the loss of *dAda2a*, compared to the message level of studied ecdysone induced genes (Fig. 4.8.B).

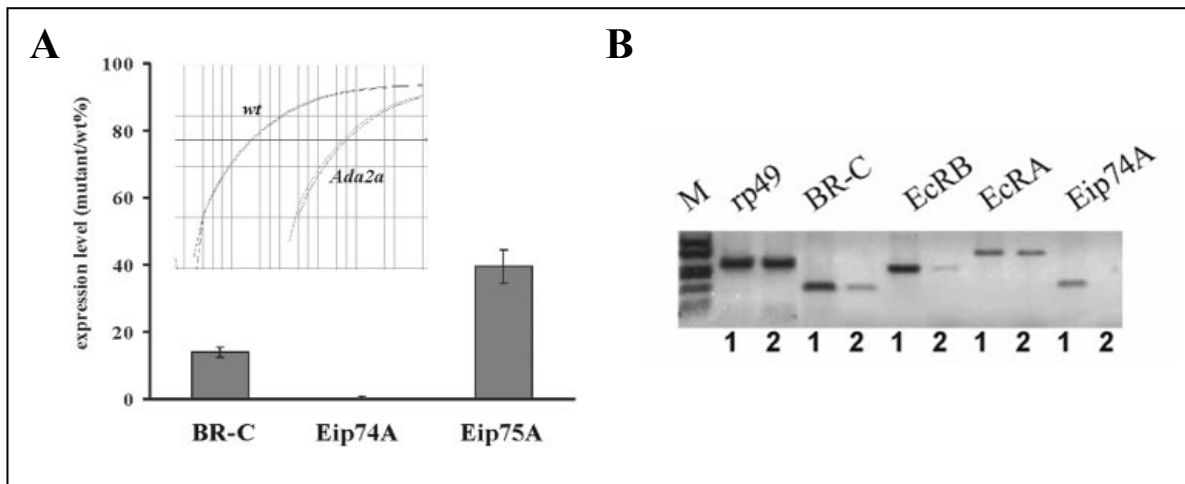


Fig. 4.8. **A)** The level of representative mRNAs transcribed in early puffs is decreased in the *dAda2a*^{d189} mutants. mRNA levels in L3 larvae were determined by quantitative RT-PCR and presented as the ratios between mutants and the wild type (wt). The insert illustrates the cycle threshold plot of a Q-PCR performed for the comparison of Eip74A mRNA levels in wild-type and in *dAda2a*^{d189} mutants. Two parallels were run and are shown for both samples. One division of the chart represents a twofold difference in the amount of PCR product. **B)** RT-PCR detection indicates reduced levels of ecdysone receptor subunit and ecdysoneinduced messages. 1, wild type; 2, *dAda2a*^{d189}. Note the reduced level of E74A and BR-C mRNA similar to that seen in panel C, while no change in the level of rp49 message is detectable.

In the next step we analyzed the binding of ecdysone receptor to chromosomes by immunostaining with EcR-specific monoclonal antibody. Results revealed decreased staining in *dAda2a*^{d189} mutants compared to the staining intensities observed in wild-type animals, which shows very intense staining in the puffs (Fig. 4.9.). A possible explanation for above results is that the ecdysone synthesis is affected by the lack of dADA2a or dGCN5 that leads to reduced binding of EcR to chromatin and expression of ecdysone-induced genes. Altogether, these data clearly indicate that the loss of the dADA2a function interferes with hormonal induction of a set of genes required for the progress of the *Drosophila* developmental program.

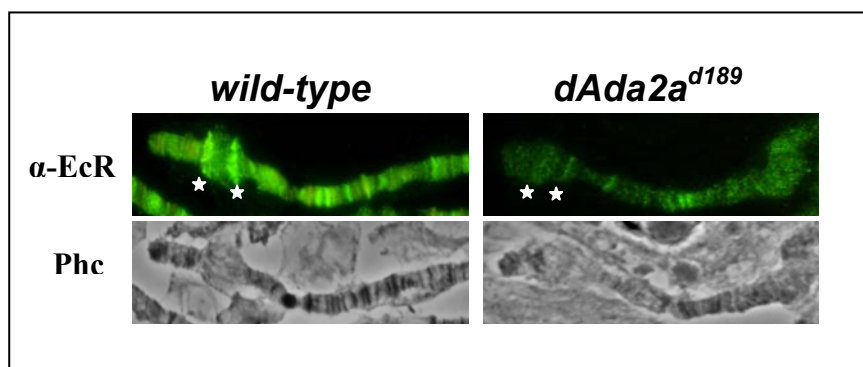


Fig. 4.9. *dAda2a*^{d189} mutant shows reduced EcR binding to chromosomes. Phase contrast (Phc) and EcR-specific antibody-stained images (green) of the end of X chromosomes of wild-type and *dAda2a*^{d189} are shown. White stars indicate the localization of EcR at the 2B5 cytological region.

4.1.4. Lack of dADA2a function results in decreased H4 acetylation

GCN5 (KAT2) is the catalytic component of several complexes which acetylates nucleosomal histones. In our and others laboratories it was recently determined that H3 acetylation at lysines 9 and 14 is significantly reduced in both *dAda2b* and *dGcn5* mutants of *Drosophila* (31, 120). *dAda2a* mutations, however, do not affect the acetylation of these lysine residues. Furthermore, the loss of either of the dADA2a or dADA2b functions does not change the acetylation of H3 lysine 18 or of H4 lysine 8 (120, 124). To extend these studies, we compared the acetylation of further lysine residues of H4 in *dAda2a*, *dAda2b*^{d842}, and *dGcn5* mutants. Using highly specific antibodies for H4 acetylated K5 (H4K5ac) and K12 (H4K12ac) we assessed the level of H4 acetylation level via immunostaining of polytene chromosomes. As a control, we used RNA Pol II monoclonal antibody specific for the largest subunit.

Fluorescent microscopic images of wild-type, *dAda2a*¹⁸⁹, *dAda2b*^{d842}, and *dGcn5*^{E333st} polytene chromosomes stained with antibodies recognizing Pol II and H4 acetylated at different lysine residues are presented in Fig. 4.10.A. All staining and data recording procedures were performed under identical conditions. The comparison of the staining intensities indicates that the levels of H4K12ac and H4K5ac are significantly less in the *dAda2a*¹⁸⁹ and *dGcn5*^{E333st} mutants than in the wild-type. Chromosomes of *dAda2b*^{d842} mutants do not reveal decreased acetylation of either of the two lysines of H4 tested in these experiments.

Similar to the immunostaining, the detection of H4 acetylated at K12 and K5 lysine residues in protein extracts of *dAda2a*¹⁸⁹, *dGcn5*^{E333st} and *dAda2b*^{d842} larvae by Western blotting also indicates significant reductions in the levels of H4K12ac and H4K5ac in the first two, but not in *dAda2b*^{d842} mutants (Fig. 4.10.B). In contrast, neither the loss of *dAda2a* nor the loss of *dGcn5* changed the level of H4K8ac to an extent detectable by immunostaining (data not shown) (31, 120). The acetylation of H3 at K9 and K14 has been shown to depend on ADA2b-containing GCN5 HAT complexes. Neither the acetylation of these sites nor the acetylation of H3K18 is affected by the loss of dADA2a. The structure of *dAda2a*^{d189} chromosomes makes it difficult to obtain a detailed staining pattern; nonetheless, a comparison of the H4K12ac and Pol II-specific antibody-stained wild-type and *dAda2a*^{d189} chromosome regions clearly reveals that some of the bands staining intensely for H4K12ac in the wild-type are missing in the *dAda2a* mutant (Fig. 4.11.B). Comparing the staining patterns obtained with Pol II-specific and H4K5ac- or H4K12ac-specific antibodies on wild-type chromosomes reveal that K5- and K12-acetylated H4 localized mostly in bands, less intensively stained by Pol II, although the acetylated H4 and Pol II stainings overlap at several positions. Notably, intensive staining of H4K5ac or H4K12ac is not detected in puffs or interband regions (Fig. 4.11.A).

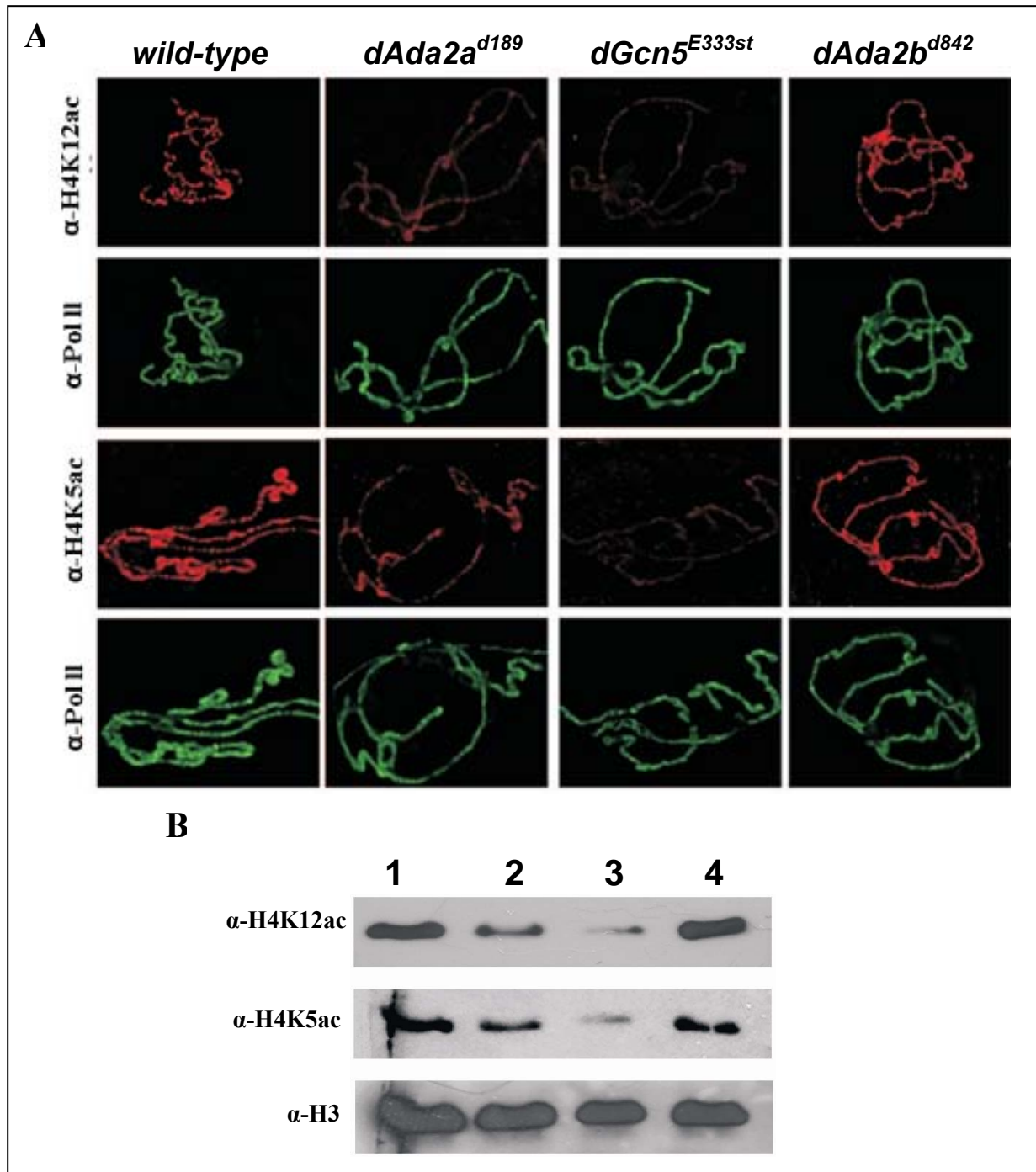


Fig. 4.10. The effects of *dAda2a*, *dGcn5* and *dAda2b* mutations on the H4K12 and H4K5 acetylation of polytene chromosomes. **A)** Chromosomes immunostained with polyclonal antibodies specific for individual acetylated lysine residues of H4 (red), as indicated on the left, and a Pol II-specific monoclonal antibody (Pol II 7G5, green) are shown. Genotypes are indicated at the top. The images demonstrating immunostaining in different mutants were obtained with identical data-recording settings. wt, wild-type. **B)** Western blot of protein extracts of wild-type (1), *dAda2a*^{d189} (2), *dGcn5*^{E333st} (3), and *dAda2b*^{d842} (4) L3 larvae developed with antibodies as indicated on the left. For the detection of H4K5ac and H3, the same blot was developed consecutively with the two specific antibodies.

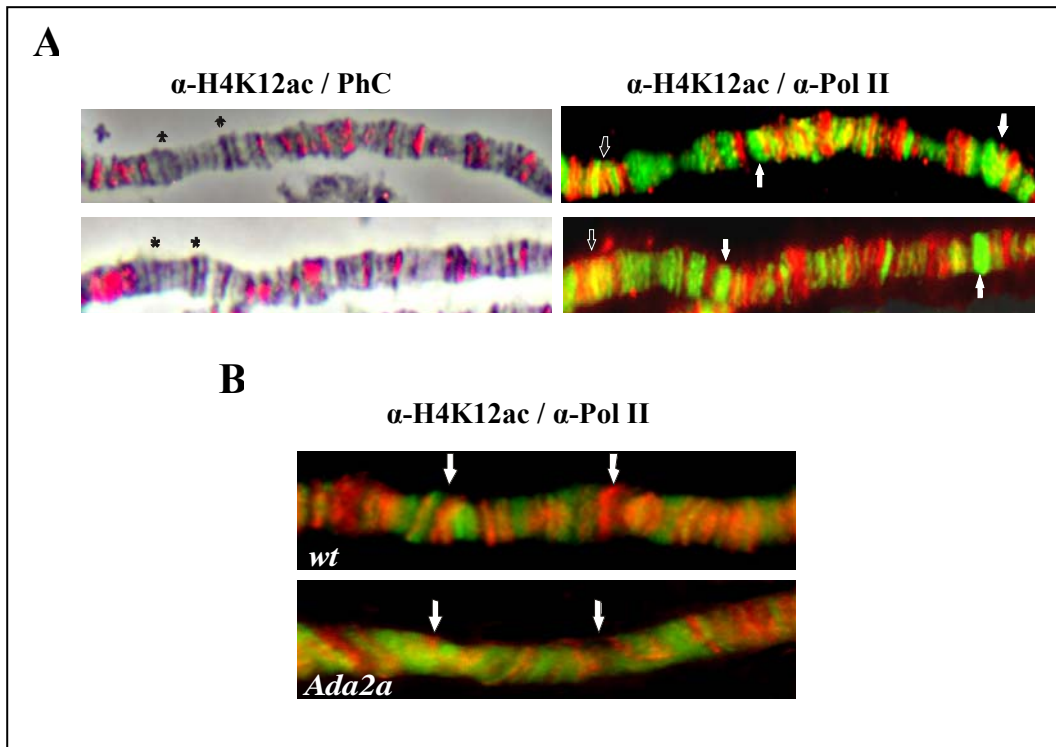


Fig. 4.11 A) Merged images of (left) phase-contrast and acetylated H4-stained (red) and (right) Pol II- (green) and acetylated H4-stained region of wild-type 3R chromosomes reveal similar distributions of H4K12ac and K5ac staining mostly in the condensed chromosomal regions. It may be noted that some of the stronger bands seen in the phase-contrast images do not display acetylated H4 staining (stars) and that acetylated H4 and Pol II colocalization is observable in a few regions (open arrowheads), while in other regions, strong polymerase-specific, but no acetylated H4, signal is detected (closed arrowheads). **B)** Identical regions of wild-type and *dAda2a*^{d189} chromosomes costained for H4K12ac (red) and Pol II (green). For better comparison, the H4K12ac signal on the *dAda2a*^{d189} chromosome is enhanced. Despite the distorted banding pattern of the *dAda2a* chromosome, similar distributions of H4K12ac are observable on wild-type and mutant chromosomes, though for specific bands, the H4K12ac signal on the *dAda2a* chromosome is absent or greatly reduced (arrows).

Taking advantage of animals that carry *dGcn5* transgenes with deletions we investigate if dADA2a is important for the catalytic activity of dGCN5. A full-length *dGcn5* transgene that was shown to restore the chromosome structure, restores the level of K12 acetylation to the level of the wild-type in *dGcn5* mutants, while transgenes with deletions in the ADA interaction or in the HAT domain do not (Fig. 4.12.A, B). *dAda2a*^{d189} and *dGcn5*^{E333st} chromosomes stained with H4K12ac- specific antibodies exhibit reduced staining intensities along the entire length of the chromosomes.

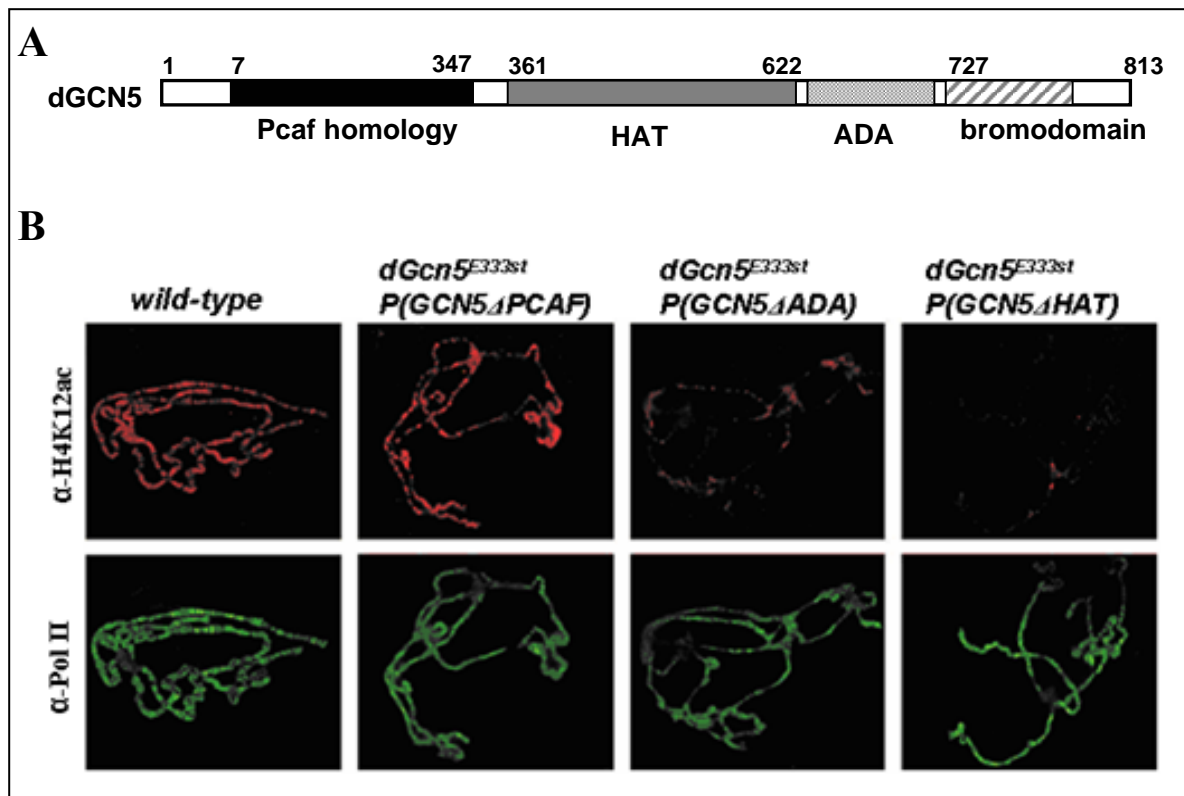


Fig. 4.12. A) Schematic view of the domains contained by the *Drosophila* GCN5 protein. B) H4K12ac (red) in *dGcn5^{E333st}* mutants is restored by a *dGcn5* transgene lacking the PCAF region, but not by the transgenes with mutations in the ADA interaction region or HAT domain. Images obtained with Abs specific for the largest subunit of Pol II (green) are shown as control.

Genetic loss of function of *dAda2a* as well as of *dGcn5* leads to a dramatic decondensation of the male X chromosome, indicating a role of this remodeling complex in higher-order chromosome structure. In *Drosophila* males the genes localized on X chromosomes are double transcribed and marked by an increased H4K16 acetylation. The H4K16ac is deposited by MOF HAT and is detectable only on the male X chromosome as a part of the dosage compensation (DCC) (2). H4K16 acetylation leads to the double transcription of the genes localized on the male chromosome and a more open structure of the male X compared to the autosomes. To test whether the alteration of the male X chromosome reflects an alteration of the DCC, we analyzed H4K16 chromosome acetylation in *dAda2a^{d189}* and *dGcn5^{E333st}* mutant males by chromosome immunostaining. Despite its bloated appearance, we found that X chromosome in these males is still highly acetylated on H4K16 residues, similar to the wild-type control (Fig. 4.13.).

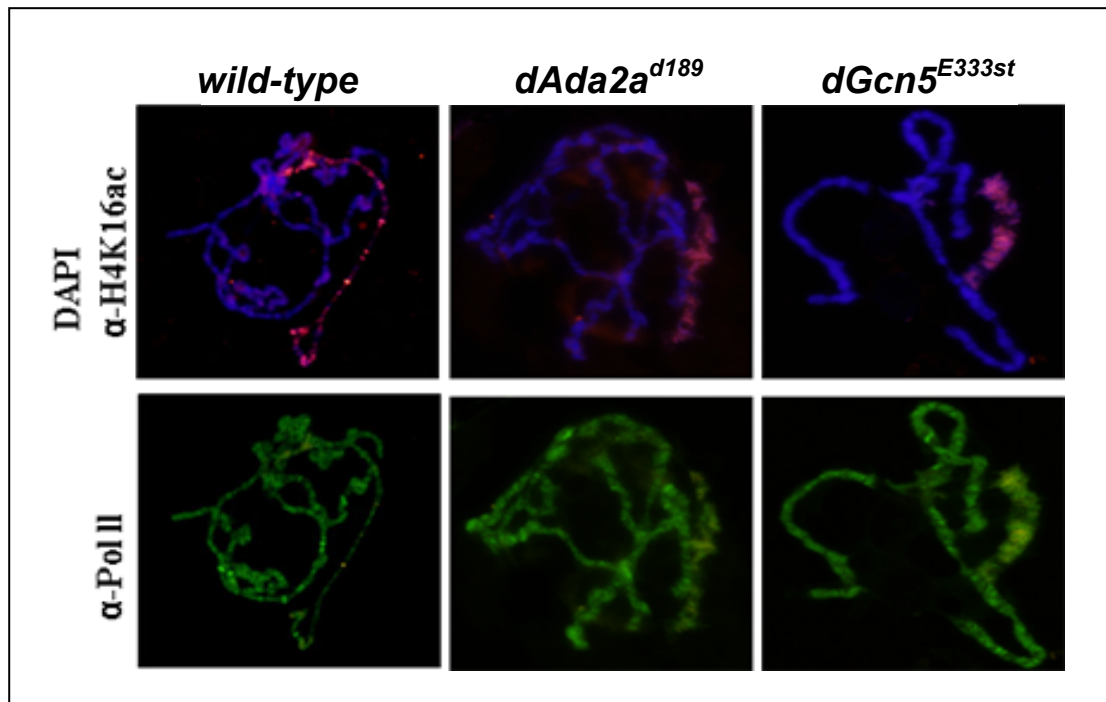


Fig. 4.13. Immunostaining of male polytene chromosomes with anti-H4K16ac specific Ab in wild-type, *dAda2a^{d189}* and *dGcn5^{E333st}* mutants. Merged picture of DAPI (blue) and H4K16ac (red) stained chromosomes (top) does not show any difference between the staining intensity of wild-type and mutant chromosomes. Pol II-specific antibody (green, bottom) is used as control.

The lack of detectable change of H4K16ac level in *dAda2a* mutants indicate that ADA2a is not involved in H4K16 acetylation, but affects X male chromosome structure by a different mechanism. Taken together, the above presented results strongly suggest that the two ADA2-type adaptor proteins present in *Drosophila* are part of two distinct HAT complexes, dSAGA and ATAC, with role in H3 acetylation at lysine K9 and K14 and H4 acetylation at lysines K5 and K12, respectively. In addition, ATAC complex play a role in maintenance of an ordered chromatin structure.

4.2. H4 acetylation is linked to JIL-1 kinase function

The interplay of different modifications means that deposition of one type of modification facilitates or inhibits the deposition of a subsequent one. It was observed that histone H3 phosphorylation at S10 can enhance acetylation of histone H3 at K14 (34, 105, 128) and inhibit methylation of histone H3 at K9 (49). In another example, the acetylation of histone H4 at K12 was suggested to be required for the methylation of histone H3 at K9 and the following HP1 recruitment to the centromeric regions of *Drosophila* chromosomes (152). Cross-talks between phosphorylation, acetylation and methylation thus clearly exist. Acetylation, and similarly phosphorylation and methylation of specific histone tail residues can be brought about by several distinct enzymes or protein complexes, which often have overlapping specificities (17, 100, 102). It is therefore expected that a particular (pre)established constellation of modifications can have different effects on the establishment of a subsequent modification, depending on the enzymes/complexes participating in the process.

In mutants of several *Drosophila* genes that play roles in histone posttranslational modifications, alterations in the higher order polytene chromosomes structure have been observed. Mutations affecting the JIL-1 kinase (166), subunits of the NURF chromatin remodeling complex (*iswi* and *nurf* alleles) (6, 7, 46) and as well as other chromatin-associated proteins such as HP1, (SU(VAR)2-5), SU(VAR)3-7 (142) and Chromator/Chriz (52, 127) each result in chromatin structural defects. Since similar chromosome structural defects were observed in ATAC subunit mutants (*dAda2a*, *dAda3*, *dGcn5*), but not in SAGA HAT complex specific *dAda2b* mutants (120) we set out to test whether the similar phenotypes of JIL-1 and ATAC mutant chromosomes reflect a functional interaction between the ATAC HAT complex and the JIL-1 kinase, but not between the SAGA complex and JIL-1 kinase.

4.2.1. Decreased H3S10ph level in mutants deficient in ATAC function

In order to determine whether interdependence between JIL-1 and ATAC functions exists first we studied the levels of ATAC-deposited histone H4K12 acetylation and JIL-1-deposited histone H3S10 phosphorylation in *JIL-1* and ATAC subunit mutants. Immunoblots developed with antibodies specific for H4 acetylated at K12 residue demonstrate a dramatically decreased level of H4K12ac in total protein extracts of *dAda2a*^{d189} and *dGcn5*^{E333st} mutants, while the level of H4K12ac in *dAda2b*^{d842} and *JIL-1*^{z2} mutants is similar to that observed in wild-type sample (Fig. 4.14.A). On the contrary, the level of histone H3S10-phosphorylation,

as determined by immunoblots using H3S10ph-specific antibodies, is greatly reduced in *dAda2a*^{d189} and *dGcn5*^{E333st} mutants, but is comparable to the control in the SAGA-specific *dAda2b*^{d842} mutant samples (Fig. 4.14.B). Immunostaining of salivary gland polytene chromosomes of *dGcn5*^{E333st} and *dAda*^{d189} mutants corroborate the results of immunoblots in that the staining intensity displayed with H3S10ph-specific antibodies by both *dAda*^{d189} and *dGcn5*^{E333st} chromosomes is greatly reduced compared to wild-type or *dAda2b*^{d842} chromosomes (Fig. 4.14.C). Similarly, in the absence of the ADA3 protein, a subunit of both ATAC and SAGA complexes, a significant decrease in the level of H3S10ph was also detected by immunoblotting or chromosome immunostaining (66).

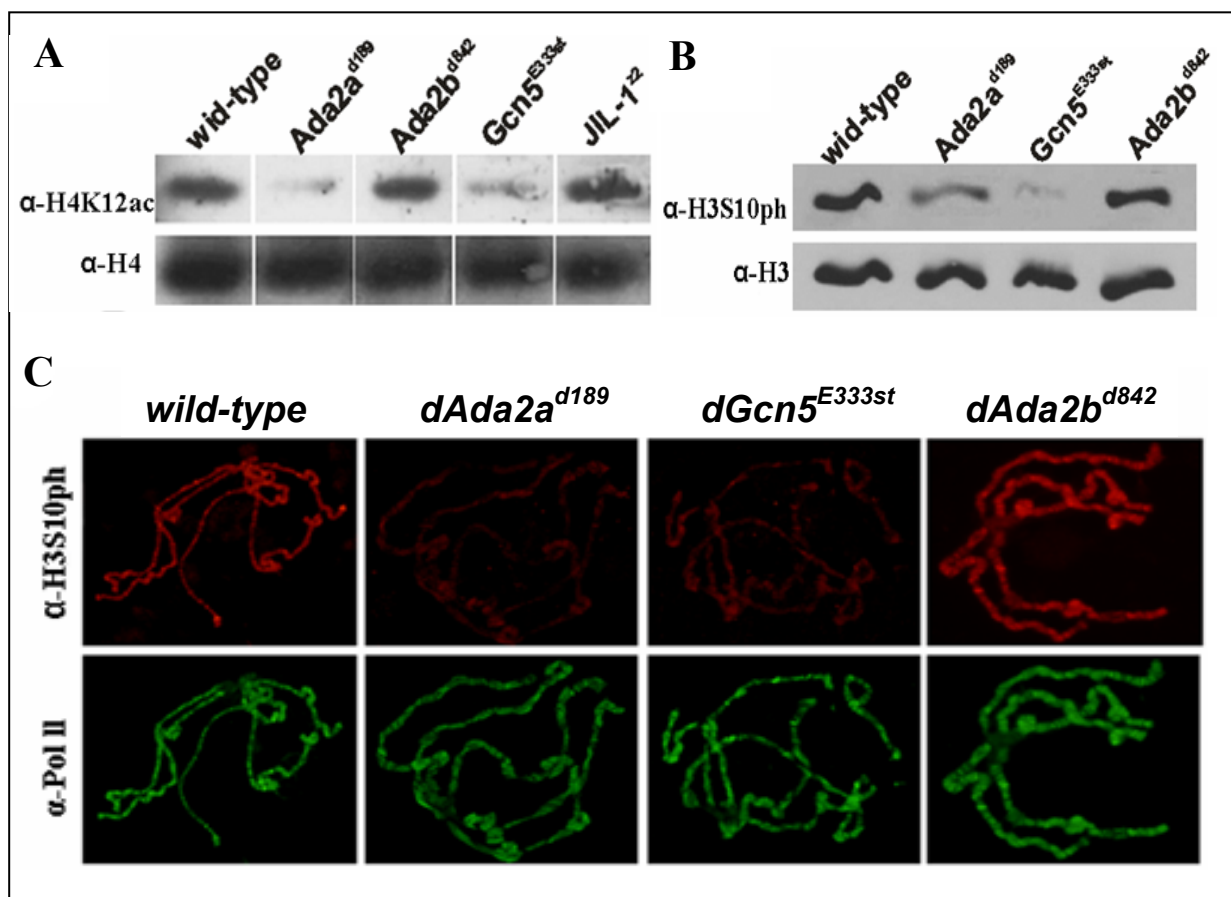


Fig. 4.14. Total protein extract of indicated genotypes immunoprobed with: **A)** Specific antibodies for H4K12ac (top) and H4 (bottom) and **B)** Antibodies specific for H3S10ph (top) and H3 (bottom). **C)** Double labeling of polytene squashes with antibodies against H3S10ph (red) and the largest subunit of the RNA polymerase II (green).

Since the combination of western blot and immunofluorescence analysis showed the loss of phosphorylation in ATAC mutants, we decided to determine whether the HAT activity of GCN5 was required to enhance H3 phosphorylation by JIL-1. For this, we studied the level of

H3S10ph in animals in which partial GCN5 functions were provided by transgenes. Polytene chromosome staining of transgene carrier larvae revealed that GCN5 transgenes lacking the HAT catalytic or the ADA2-interacting domain fail to restore H3S10 phosphorylation level in *dGcn5^{E333st}* null mutants (Fig. 4.15). Combined, these data strongly suggest that the loss of histone H4 acetylation by ATAC decreases H3 phosphorylation by JIL-1.

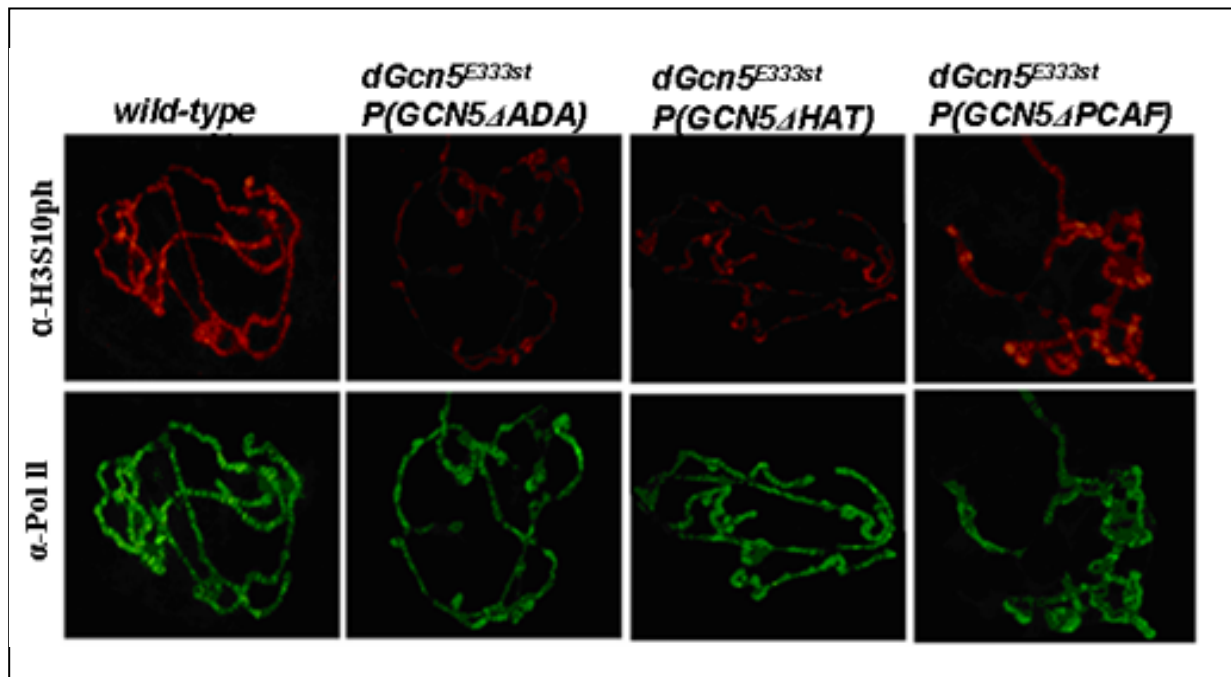


Fig. 4.15. Polytene chromosome squashes of *dGcn5^{E333st}* third-instar larvae expressing a *dGcn5* transgene with mutations in the ADA interacting, HAT and PCAF homology domains, double stained with antibodies specific for H3S10ph (red) and for the C-terminal domain of the largest subunit of RNA polymerase II (Pol II 7G5) (green).

4.2.2. JIL-1 overexpression restores H3S10ph and suppresses phenotypic features of ATAC mutants

The functional failure of ATAC might lead to a decreased level of H3S10ph because H4 tails with acetylated K12 play a direct role in the enhancement of JIL-1 function, or through several indirect mechanisms which might be triggered, among others, by an altered chromatin structure or by altered JIL-1 activity. In an attempt to gain information on the underlying mechanism of ATAC and JIL-1 interplay we studied the effect of the ectopic overproduction of JIL-1 in ATAC mutants. In order to perform these experiments *dAda2a^{d189}* and *dGcn5^{E333st}* mutants animals were crossed with animals carrying the JIL-1EGFP transgene driven by a

heat-shock promoter. Animals heterozygous for JIL-1EGFP and homozygous for *dAda2a* or *dGcn5* mutations were analyzed. By analyzing the lethal phase of these animals we observed that *dAda2a*^{d189} or *dGcn5*^{E333st} null mutants, which do not evert spiracle and have a lethal phase in late third-instar larval stage, everted spiracle and formed pupae with high frequency upon JIL-1 overproduction (Fig. 4.16.A.). The effect of JIL-1 overproduction is also well observable in the change of the chromosome structure of ATAC mutants. The bloated phenotype of male X chromosomes characteristic for each ATAC mutant studied (*dAda2a*, *dAda3* and *dGcn5*) is significantly suppressed by JIL-1 overproduction (Fig. 4.16.C). We noticed a less striking but clearly observable improvement in the structure of autosomes of ATAC mutants overexpressing JIL-1, both males and females. A JIL-1 transgene overexpressed in *dAda2a* and *dGcn5* hypomorph mutants also, increased survival of hypomorph *dAda2a* or *dGcn5* mutants, as shown by the elevated number of hatching JIL-1 transgene carrier *dAda2a* or *dGcn5*^{C14Ti} adults, compared to the number of animals without a JIL-1 transgene (Fig. 4.16.B).

As expected, both immunofluorescens and Western blot experiments showed that the expression of the hs-promoter driven JIL-1EGFP transgene in *dAda2a*^{d189} and *dGcn5*^{E333st} mutants restored histone H3S10ph level comparable to normal (Fig. 4.17.A, B). These data thus strongly suggest that the similar chromatin structure distortions seen both in ATAC and JIL-1 mutants, most clearly in the structure of male X, have at least in part an identical underlying cause in the reduced level of phosphorylated histone H3S10. Furthermore, the suppressive effect that JIL-1 overproduction exerts on the phenotype of ATAC mutants also suggests that the reduced level of ATAC-specific histone H4K5 and K12 acetylation does not prevent, but rather only hinders JIL-1 phosphorylation of histone H3S10. The observations that JIL-1 overexpression decreased the effects of ATAC subunit mutations concerning either lethal phase, chromosome structural distortions or level of phosphorylation, suggests that ATAC and JIL-1 function in the same pathway, where ATAC complex acts upstream the JIL-1 kinase.

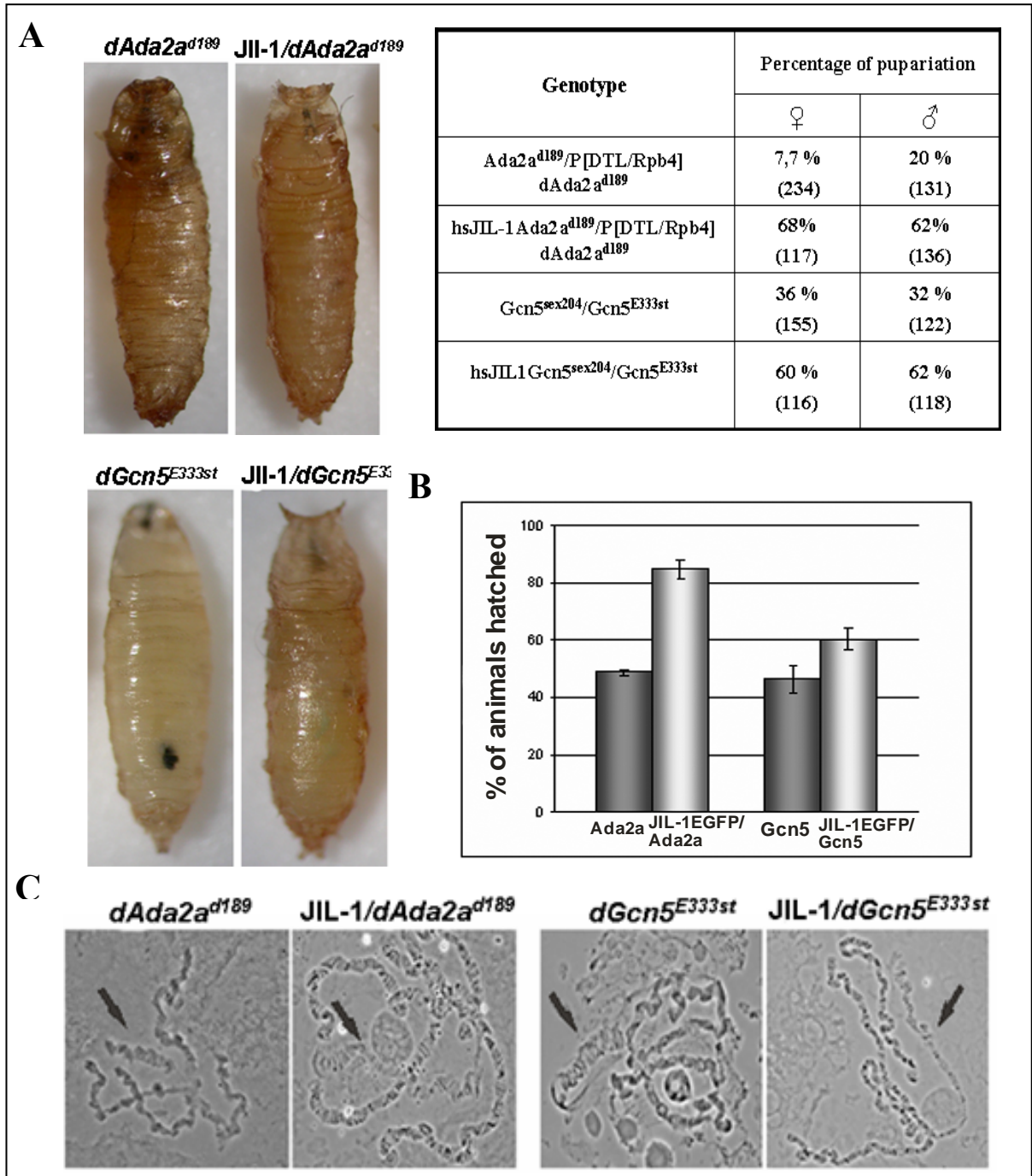


Fig. 4.16. A) Lethal phases of *dAda2a^{d189}*, *JIL-1EGFP/dAda2a^{d189}*, *dGcn5^{E333st}* and *JIL-1EGFP/dGcn5^{E333st}* animals. The percentages of animals perishing in the indicated stages are shown. In parentheses the number of third instar larvae of the particular genotype and sex is given. The sex of the animals was determined by observing the presence of testes in L3. **B)** The hatching rate of hypomorph *dAda2a* and *dGcn5* mutants in the absence and the presence of a *JIL-1EGFP* transgene. **C)** Phase contrast images of *dAda2a^{d189}*, *JIL-1EGFP/dAda2a^{d189}*, *dGcn5^{E333st}* and *JIL-1EGFP/dGcn5^{sex204/E333st}* polytene chromosomes of late third-instar male larvae. The black arrows indicate the male X chromosomes.

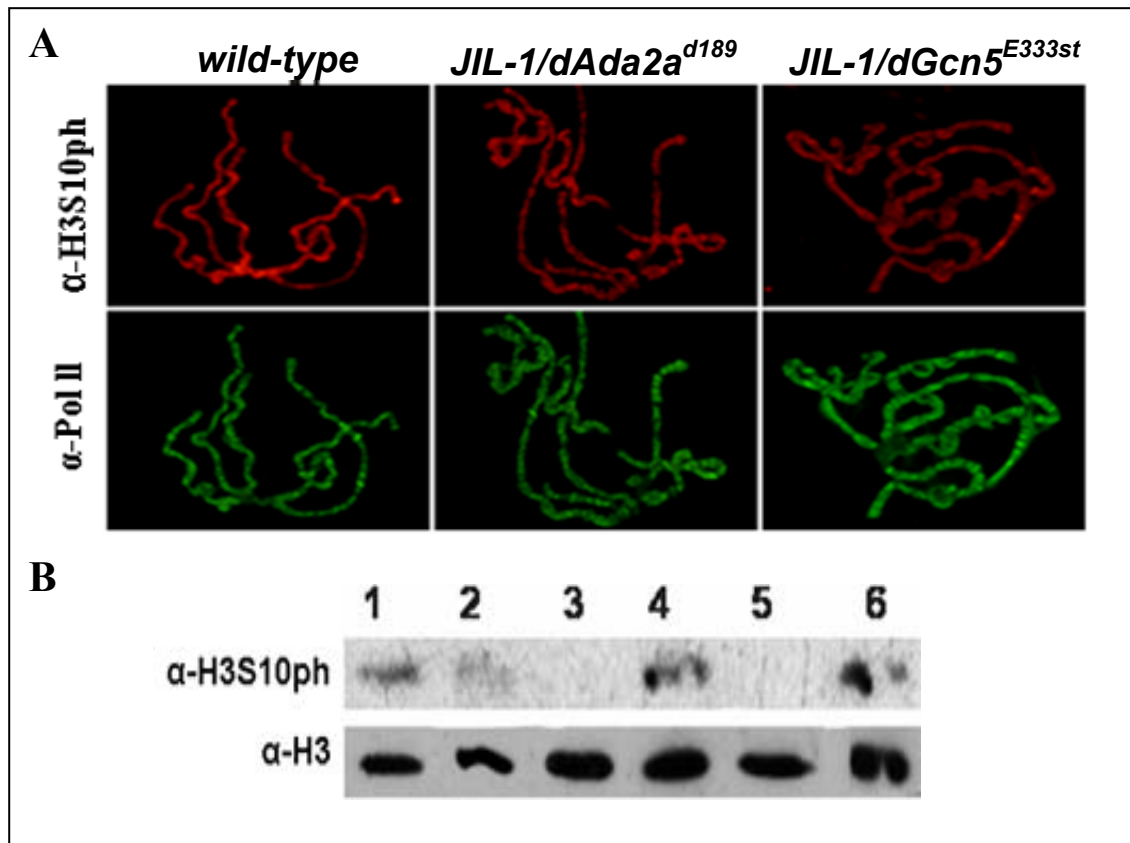


Fig. 4.17. **A)** Polytene chromosome squashes of wild-type and JIL-1 transgene expressor *dAda2a^{d189}* and *dGcn5^{E333st}* third-instar larvae double stained with H3S10ph (red) and Pol II specific Abs (green). **B)** Immunoblot of total protein extract of 1. wild-type, 2. JIL-1EGFP, 3. *dAda2a^{d189}*, 4. JIL-1EGFP/*dAda2a^{d189}*, 5. *dGcn5^{E333st}* and 6. JIL-1EGFP/*dGcn5^{E333st}* developed with H3S10ph and H3 specific antibodies.

4.2.3. Mutations of ATAC subunits enhance the spreading of histone H3K9 dimethylation by SU(VAR)3-9

Zhang et al. reported that the loss of JIL-1 function results in the spreading of the major heterochromatin markers H3K9me2 and HP1 to ectopic locations on the polytene chromosomes arms (177). While by reducing the dose of *Su(var)3-9* gene *JIL-1* null mutants were rescued to a large degree, no improvement was observed by reducing SU(VAR)2-5 activity (44). As phosphorylation of histone H3S10 by JIL-1 was shown to counteract histone H3K9 dimethylation and heterochromatin formation, we reasoned that if ATAC mutations indeed hinder JIL-1 function, then in ATAC mutants a spreading of H3K9me2 mark should be observed and mutations of *Su(var)3-9*, the gene encoding the H3K9 dimethyltransferase, should suppress the effect of ATAC mutations. In order to test this assumption we examined

the distribution of histone H3K9 dimethylation in ATAC mutants and studied the phenotype of *dAda2a*^{d189}/*Su(var)3-9* and *dGcn5*^{E333st}/*Su(var)3-9* double mutants. Immunostaining of polytene chromosome squashes with H3K9me2-specific antibodies revealed a spread of signal on *dAda2a*^{d189} and *dGcn5*^{E333st} mutant chromosomes similarly to that observed on *JIL-1*^{z2} chromosomes (Fig. 4.18). While on control samples (*w*¹¹¹⁸) the H3K9me2 positive signal is detectable mostly at centromeric regions, on the 4th chromosomes and at a few bands on autosomes, on *dAda2a*^{d189} and *dGcn5*^{E333st} chromosomes the staining on the autosome arms in both males and females is readily detectable (Fig. 4.18.A). Using the polytene salivary gland 'smush' preparation stained with anti-H3K9me2 specific antibody, the spreading of H3K9 dimethylation in ATAC mutants is even more obvious (Fig. 4.18.B).

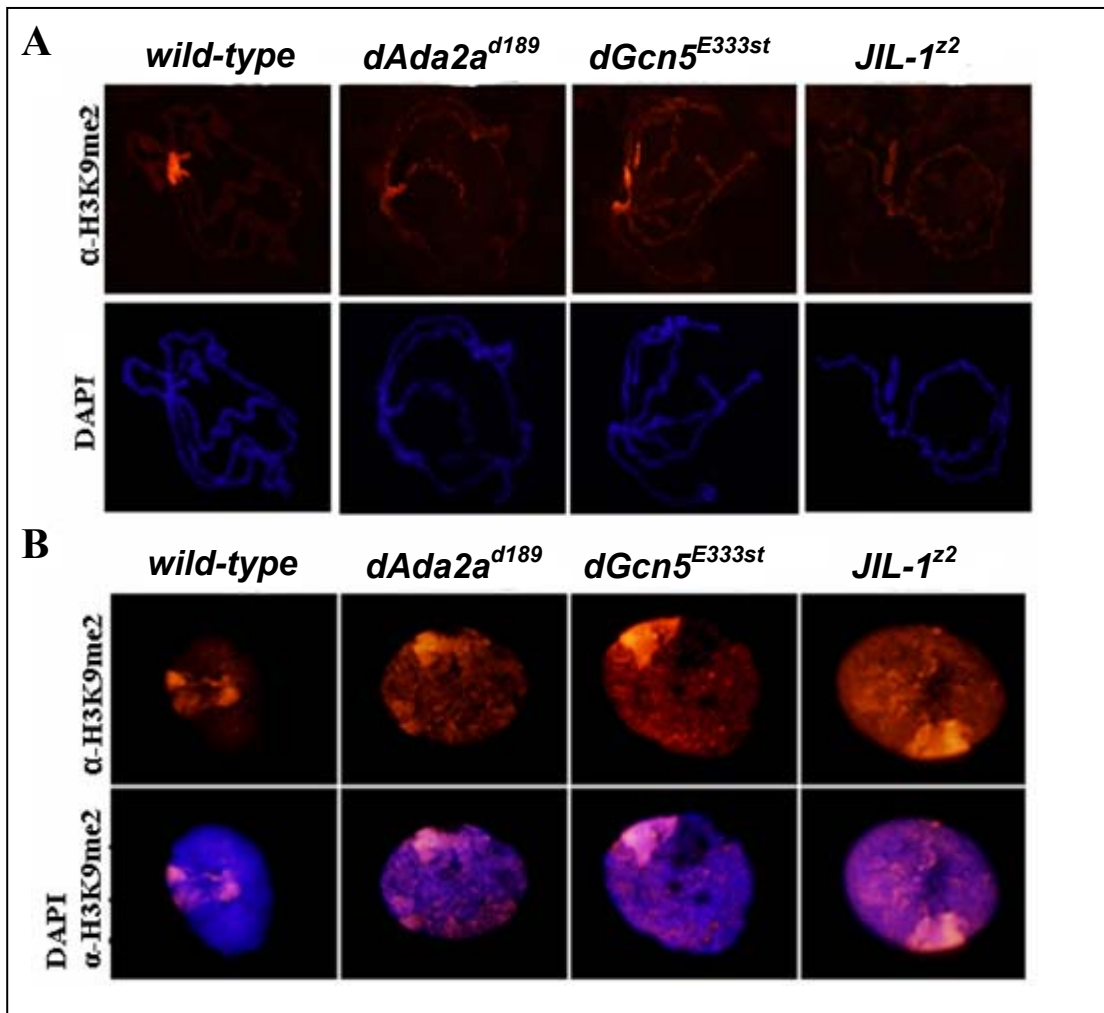


Fig. 4.18. ATAC subunits mutation leads to H3K9me2 spreading. **A)** Polytene chromosome squashes of *dAda2a*^{d189}, *dGcn5*^{E333st} and *JIL-1*^{z2} null homozygous third-instar larvae stained with H3K9me2-specific Antibody (red) and DAPI (blue). **B)** Polytene nuclei of *dAda2a*^{d189}, *dGcn5*^{E333st} and *JIL-1*^{z2} null homozygous larvae stained with H3K9me2-specific antibody (red) and DAPI (blue).

For testing the genetic interaction between *Su(var)3-9* and ATAC subunit mutants we studied the effect of *dAda2a* and *dGcn5* deficiency in *Su(var)3-9¹* and *Su(var)3-9²* heterozygous backgrounds. Because all three genes, *Su(var)3-9*, *dAda2a* and *dGcn5* are located on the third chromosome, first we recombined the *Su(var)3-9¹* and *Su(var)3-9²* alleles onto *d189* or *dGcn5^{sex204}*. Subsequently, the *Su(var)3-9 d189/TM6C* or *Su(var)3-9 dGcn5^{sex204}/TM6C* animals were crossed to *P[DtlRpb4] d189/TM6C* and *dGcn5^{E333st}/TM6C* generating *Su(var)3-9 d189/P[DtlRpb4] d189* or *Su(var)3-9 dGcn5^{sex204}/dGcn5^{E333st}* progeny homozygous for *dAda2a* or *dGcn5* mutation and heterozygous for *Su(var)3-9*. Both of these *Su(var)3-9* alleles are null and gave the same results in that a decreased level of SU(VAR)3-9 increased the survival of ATAC mutants permitting development to P4-P5 stages in high frequency and up to pharate adult stage in small numbers (Fig. 4.19.A). The effect of the decreased level of SU(VAR)3-9 had a stronger influence on *dAda2a* than *dGcn5* null mutants. Similarly, *Su(var)3-9* heterozygosis improved the chromosome structure of the studied ATAC mutants (Fig. 4.19.B).

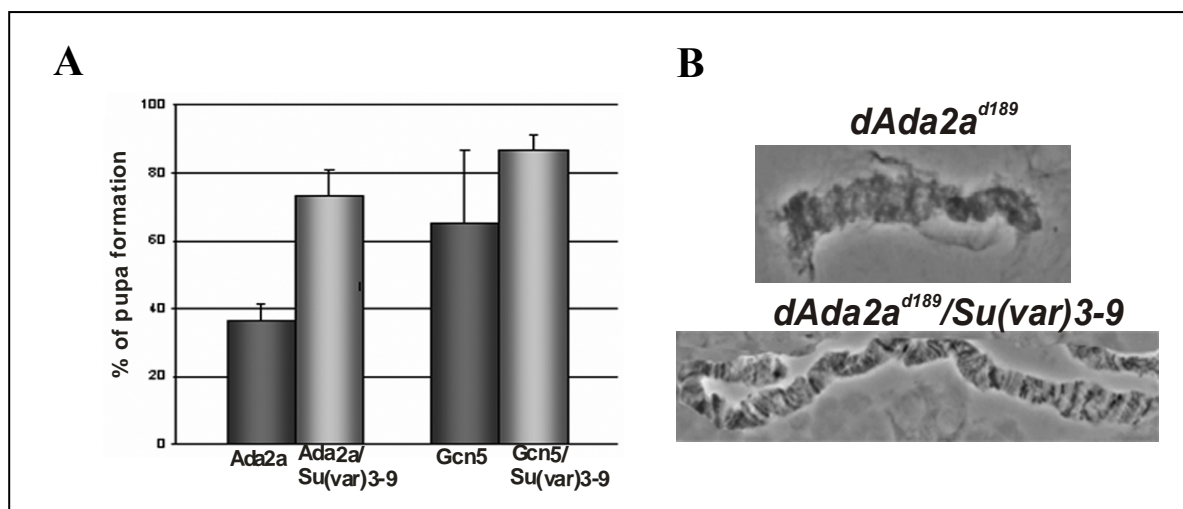


Fig. 4.19. A) *Su(var)3-9* heterozygosis increases the viability of *dAda2a^{d189}* or *dGcn5^{E333st}* null animals. The percentages of animals perishing at the indicated developmental stages are shown. The number of animals in each category was over 350. **B)** Male X chromosomes of *dAda2a^{d189}* single mutant (top) and *dAda2a^{d189}/Su(var)3-9* double mutant (bottom). *Su(var)3-9* heterozygous background improves the structure of male X chromosomes of *dAda2a^{d189}* null mutants.

4.2.4. Loss of H4K12 acetylation decreases JIL-1 localization to chromatin

The reason for the reduced level of H3S10 phosphorylation in mutants affecting ATAC subunits could be that *JIL-1* is one of the numerous genes down-regulated in the absence of H4K12 acetylation and the low level of JIL-1 protein cannot sustain normal level H3S10 phosphorylation. To test this possibility we studied the expression of *JIL-1* in ATAC mutants. First, we compared the JIL-1 mRNA levels in *JIL-1*, *JIL-1/+*, *dGcn5^{E333st}*, *dAda2a^{d189}* and *dAda3²* mutants and *w¹¹¹⁸* controls by Q-RT-PCR (Fig. 4.20.A). We found the level of JIL-1-specific mRNA in all three ATAC mutants tested to be slightly decreased, corresponding to approximately 60% of the control samples. As expected, in homozygous *JIL-1* null mutants we detected a dramatic decrease in the level of specific message, while in *JIL-1/+* heteroallelic combinations, which display wild-type phenotype, we detected JIL-1 mRNA at a level similar to ATAC mutants, corresponding to a 60% of wild-type levels. Next we compared the JIL-1 protein levels in wild-type, *dAda2a^{d189}* and *dAda2b^{d842}* samples by immunoblot and found that JIL-1 was present at similar levels in total protein extracts of all three samples (Fig. 4.20.B).

By immunostaining of tissue samples with JIL-1-specific antibody we also detected comparable signal intensities in *dAda2a^{d189}*, *dAda3²* or *dGcn5^{E333st}* and wild-type larvae. Preparation of whole salivary gland showed that JIL-1 localizes into the nucleus and completely overlaps with DAPI stained nuclei (Fig. 4.21.A). A comparison of JIL-1-specific staining intensities of wild-type and *JIL-1*, and ATAC mutant chromosomes, however, revealed a more severe decrease in the level of JIL-1 localization to *dAda2a^{d189}* and *dGcn5^{E333st}* chromosomes (Fig. 4.21.B). Remarkably, JIL-1 binding to *dAda2a* and *dGcn5* chromosomes is not lost completely and a weak signal all along the chromosome arms and particularly on the dosage compensated male X chromosomes is well discernable (data not shown and Fig. 4.22). The much gentle “smush” preparation technique for polytene nuclei staining provided similar results. Noteworthy, that the difference in staining intensity between wild-type and ATAC mutant samples was repeatedly smaller on the “smush” preparations than the chromosome spreads prepared using harsher conditions. (Fig. 4.21.B, compare top and bottom). In contrast, polytene chromosome spreads and “smush” preparations of JIL-1 heterozygotes displayed staining intensities with JIL-1 specific Abs indistinguishable from wild-type controls (Fig. 4.21.B). The sharp difference in JIL-1 specific staining of ATAC mutants was repeatedly seen both in male and female chromosomes (not shown and Fig. 4.21.B top). This observations lead to the conclusion that the level of JIL-1 mRNA or the protein is not affected by the loss of ATAC subunits, but in the absence of H4 acetylation the JIL-1 proper binding to chromosomes is impeded.

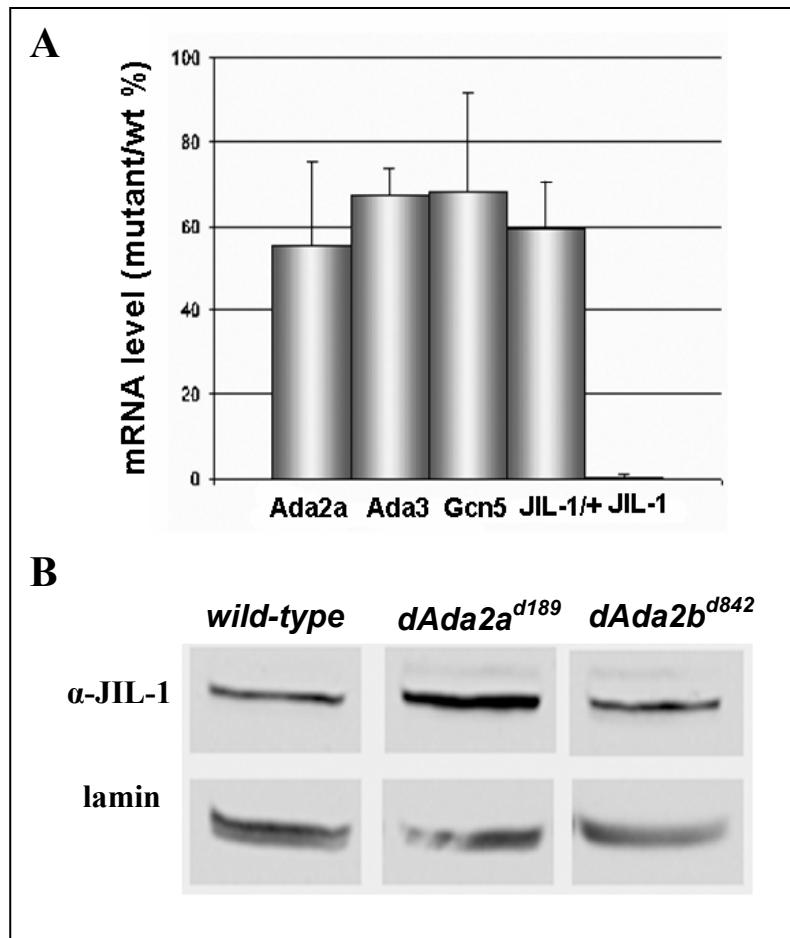


Fig. 4.20. A) The level of JIL-1 mRNA in ATAC mutant subunits and *JIL-1* mutants determined by Q-PCR, showed as the report between mutant and wild type (wt). **B)** Total protein extract of third-instar larvae immunoprobed with antibodies specific for JIL-1 and lamin as control. The genotypes are indicated.

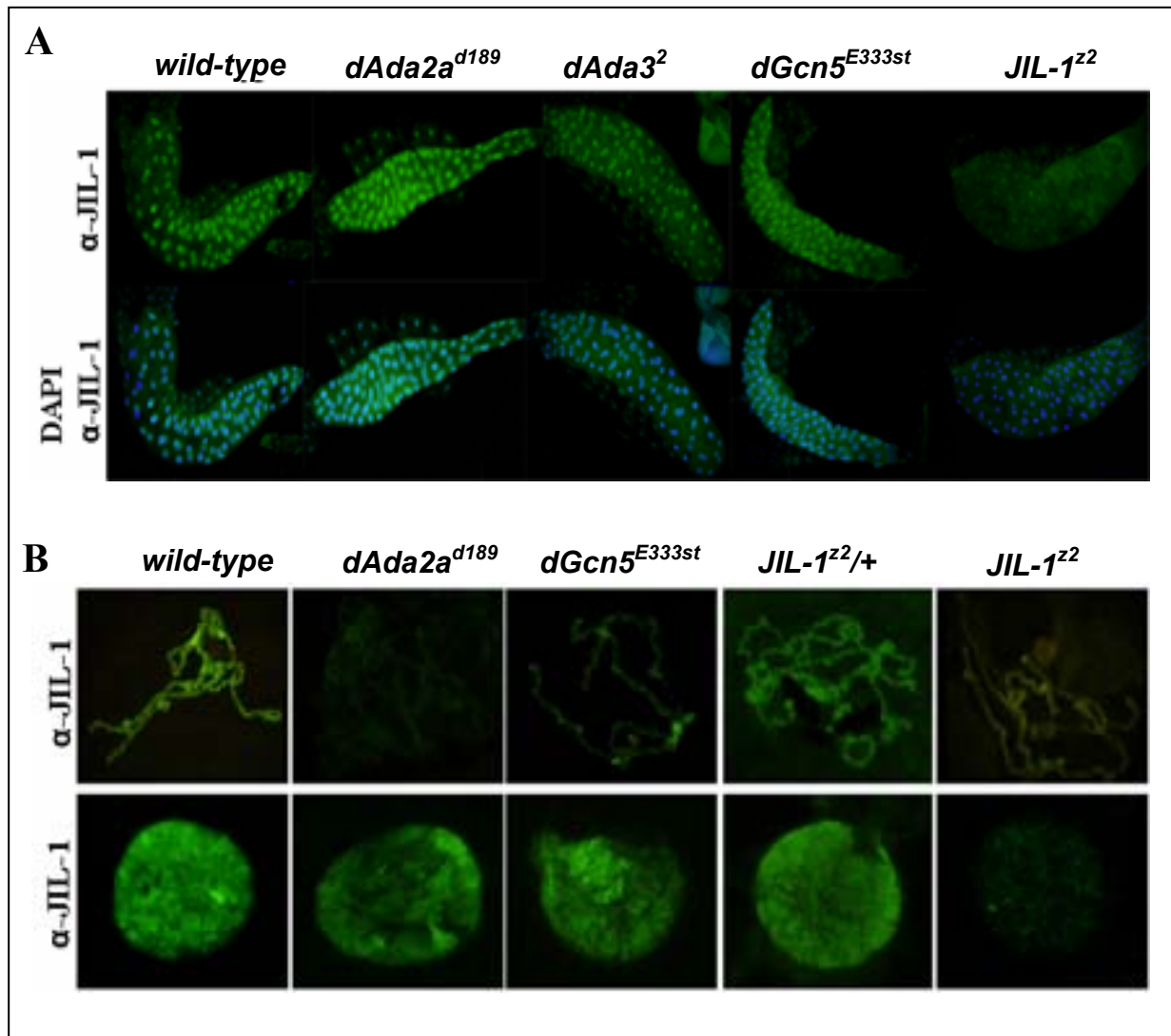


Fig. 4.21. **A)** Immunostaining of salivary glands of ATAC mutant subunits and JIL-1 null mutant with JIL-1-specific antibody (top). Merged image of DAPI and JIL-1 stained salivary glands (bottom). **B)** Immunostaining of polytene chromosomal spreads (top) and „smush” preparations (bottom) of wild-type and *dAda2a*^{d189}, *dGcn5*^{E333st}, *JIL-1/+* and *JIL-1*^{z2} third-instar larvae with JIL-1-specific antibody. Female chromosomes are shown.

Expression of a PCAF homology region deleted GCN5 transgene, which complemented H4K5/12 acetylation and H3S10 phosphorylation in *Gcn5* null mutants restored also JIL-1 localization to polytene chromosomes, while a HAT domain deleted *dGcn5* transgene which failed in the rescue of H4 acetylation and H3S10 phosphorylation was also defective in restoring JIL-1 chromosomal localization (Fig. 4.22.).

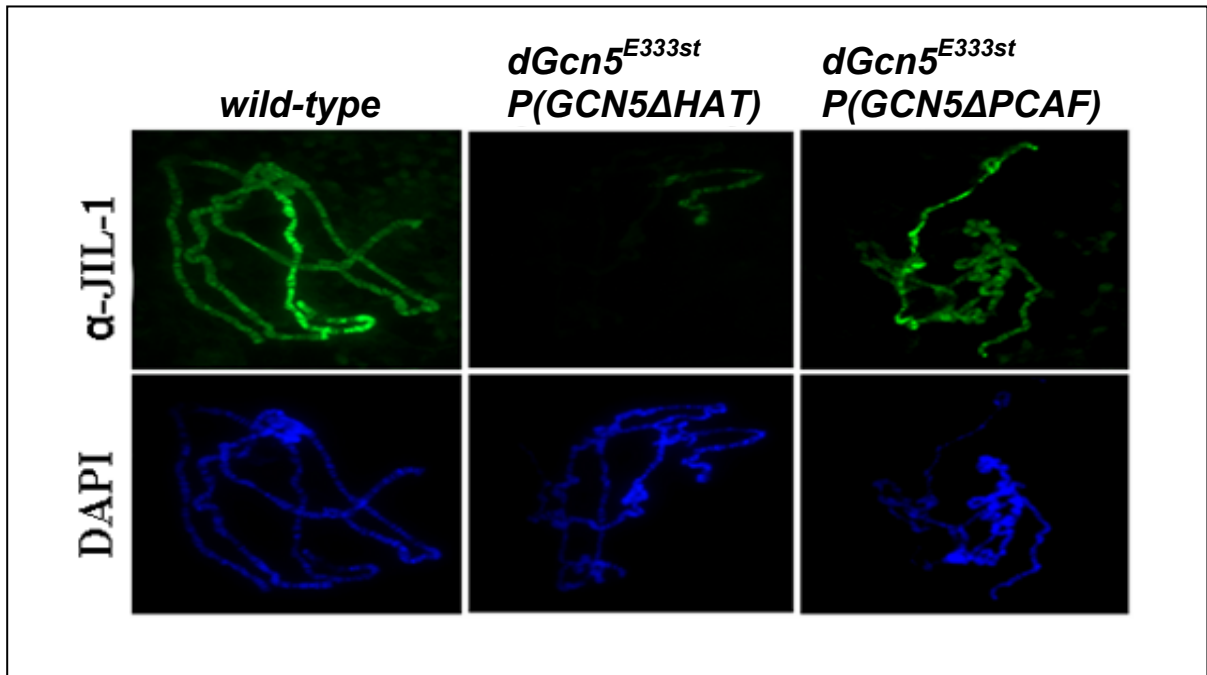


Fig. 4.22. Male chromosomes spreads immunostained with specific JIL-1 antibody (top) and DAPI (bottom). A transgene encoding *dGcn5* with mutation in the HAT domain does not rescued the JIL-1 binding to chromosomes, while the transgene lacking PCAF homology domain does. Male X chromosome shows an increased JIL-1 staining compared to the autosomes (top).

The data presented above strongly suggest that the loss of histone H4 acetylation by ATAC decreases H3 phosphorylation deposited by JIL-1 kinase. *In vivo* experiments using *Drosophila* single and double mutants demonstrated that there is genetic interaction between ATAC and both *JIL-1* and *Su(var)3-9* alleles. In the absence of ATAC or JIL-1, H3K9 dimethylation deposited by SU(VAR)3-9 enzyme spreads along chromosome arms leading to a more condensed chromatin and gene silencing.

5. DISCUSSIONS

This work describes the involvement of *Drosophila* dADA2a protein in H4 acetylation for the first time. Previous independent studies showed the colocalization of GCN5 and ADA2 in HAT complexes. First, yeast complexes containing both GCN5 and ADA2 were separated biochemically and their HAT activities were demonstrated (32, 64, 65). Another transcriptional adaptor protein, dADA3 was purified together with dADA2a and dGCN5 and was shown to be part of the catalytic acetyltransferase core of HAT complexes (9, 145). Recently, two dGCN5-containing complexes were partially separated from *Drosophila* cell extracts (97, 110). One of them is dSAGA and contains dGCN5, dADA2b and dADA3. The other complex, ATAC was isolated by Guelman et al. and show to contain both dGCN5 and dADA2a, as well as dADA3 (68). More recently, Suganuma and colleagues demonstrated that ATAC complex contain another HAT subunit, ATAC2, with role in H4K16ac and demonstrated that ATAC complex stimulates nucleosome sliding (151). At the time this work started, no direct proof of the functional interaction of *Drosophila* dGCN5 with dADA2a protein has been reported. Previous genetic analysis clearly demonstrated that the two dADA2s are functionally distinct and both Pankotai et al. and, independently, Qi et al. have shown that dADA2b, is involved in histone H3 acetylation (120, 124). Those studies, however, did not indicate dADA2a involvement in histone modification. Carre et al. recently reported that a deletion variant of *dGcn5* (*dGcn5ΔAda*), lacking the domain believed to be involved in GCN5-ADA2 interaction, appeared normally distributed on polytene chromosomes and restored H3 acetylation in *dGcn5* mutants. However, *dGcn5* mutants were not rescued by the *dGcn5ΔAda* transgene and were arrested at puparium formation (31). The observations detailed above prompted us to search for direct evidence of the dGCN5-dADA2a interaction *in vivo*. To achieve this, first we studied the genetic interaction of *dGcn5^{E333st}* and *dAda2a^{d189}*. Our observation that the characteristic phenotypic features of the *dAda2a^{d189}* mutants are suppressed or enhanced, depending on the *dGcn5* genetic background, indicates an *in vivo* functional interplay between the two proteins. The finding that the level of dGCN5 alters the manifestation of a hypomorph *dAda2a* allele (Fig. 4.5) and vice versa is in accord with the proposed ADA2a-GCN5 functional link, the former playing a role in facilitating the HAT activity of the latter. As expected from this scenario, the effect resulting from a change in the level of dGCN5 is compensated by a change in the opposite direction in the dADA2a level or, vice versa, changes in dADA2a level are compensated by changes in the level of dGCN5.

The similar phenotypes of *dGcn5*^{E333st} and *dAda2a*^{d189} mutants, with characteristic developmental defects at the larva-pupa transition (Fig. 4.2., Fig. 4.3), indicate that the two proteins play essential roles in the regulatory hierarchy controlled by the steroid hormone ecdysone at the end of the third-larval instar. The puff formation at chromosomal regions containing early ecdysone response genes is defective in both *dAda2a* and *dGcn5* mutants (Fig. 4.6.), supporting this conclusion and indicating a lack of appropriate transcriptional activation upon the appearance of the regulatory signal. The reduced level of puff formation correlates with the failure in hormone induced gene activation, as indicated by the drastically reduced level of mRNAs corresponding to the early ecdysone-induced genes (Fig. 4.8). The lack of transcription induction is not simply a result of a decreased hormone level, since *dAda2a* mutants are defective in puff formation even if the hormone is ectopically provided (Fig. 4.7.A). Furthermore, the localization of EcR to polytene chromosomes was also affected. One possible explanation for the reduced puff formation and the decreased expression of ecdysone induced genes is that the EcR receptor expression is also affected by the lack of dADA2a. This was not the case, since RT-PCR experiment revealed that only the mRNA of EcRB isoform was slightly reduced, while that of EcR isoform A was not affected. Another possible explanation for the reduced binding of EcR to polytene chromosomes is that the ligand, ecdysone, is missing. A defective ATAC complex might alter the synthesis of ecdysone hormone or the expression of genes required for ecdysone synthesis. In independent studies, analysis of microarray data revealed that most of the ecdysone induced genes are downregulated in ATAC mutants, while some of the genes involved in the ecdysone synthesis were either down- or upregulated (data not shown). Similar observations, blockage during metamorphosis, reduction of puff formation and expression of ecdysone induced genes and decrease binding of EcR to polytene chromosomes were observed in the absence of dADA3 protein (66). Overall, we conclude from these observations that the lack of the ATAC complex components, dGCN5, dADA2a and dADA3, reduces transcription activation at specific loci. The effect is gene specific since the lack of these proteins did not affect the expression of all the tested ecdysone induced genes, and in other cases, an increase in the mRNA level in the absence of dADA2a can be observed (120).

Another characteristic of all the three ATAC mutant subunits is the alteration of the polytene chromosome structure. In the *dAda2a*, *dAda3* and *dGcn5* null mutants the chromosomes banding pattern is affected, a misalignment and intermixing of interband and banded regions and the extensive coiling and folding of the chromatides is observed. The male X chromosome is particularly affected and no remnants of banded regions are discernable (Fig.

4.4.A). In contrast, *dAda2b* mutants display normal chromosomal structure. These observations suggest the involvement of ATAC complex in chromatin organization. Mutation of ATAC subunits may have a direct effect on chromatin structure due to the loss of H4 acetylation, or indirectly can influence its organization through the regulation of different processes that use the chromatin as the physiological substrate. Studies on plants and mammalian cells revealed that the H4 acetylation, mainly acetylation at K5 and K12 residues, within the euchromatin and heterochromatin domains is linked with DNA replication, rather than with DNA transcription (16, 81). We can not exclude the possibility that acetylation of the K5 and K12 residues in the H4 tail takes place before the formation of the histone core and these posttranslational modifications are required for an ordered chromatin assembly. This might explain the alteration of chromatin observed in the absence of the ATAC complex. However, H4 acetylation by the same or different enzyme seems to be required also for specific gene activation.

The specificity of recombinant yGCN5 and partially purified GCN5-containing HAT complexes for particular lysine residues of the core histones has been analyzed on both free and nucleosomal histone substrates (21, 65). These studies indicated that yGCN5 has a preference for the lysines of H3, and that the components of the GCN5-containing complexes influence both HAT activity and specificity. From these studies, it was concluded that the major targets of yGCN5 HAT are the lysines of nucleosomal H3. However, other studies also suggested the involvement of yGCN5-containing complexes in the acetylation of histones other than H3. By analyzing the *in vivo* effects of changes in the specific lysines in the N-termini of the histones in the absence and in the presence of yGCN5, Zhang et al. found that the loss of GCN5 caused a diminution of acetylation at each of the four lysines in the N terminus of H4 (176). Recently, Pankotai et al. and Qi et al. observed that the lack of *dAda2b* greatly reduced the K9 and K14 acetylation of H3, while not affecting H4 acetylation (120, 124). In concert with these data, Carre et al. reported that mutations of *dGcn5* reduced H3K9 and K14 acetylation but had no effect on the acetylation of H4K8 (31). The combination of immunostainings and Western blots presented here show that, in *dAda2a* and *dGcn5* mutants, the extent of H4K12 and K5 acetylation is significantly reduced (Fig. 4.10) (31, 120, 124). Homozygous *dGcn5* mutants expressing transgenes with a deletion in the ADA-interacting region or in the HAT domain fail in rescuing the H4 acetylation (Fig. 4.12). As expected, polytene chromosomes of *dAda3*-null mutants display reduced levels of H3K9ac and H3K14ac, and also H4K5ac and H4K12ac staining, suggesting that similar to dGCN5, dADA3 has an essential role in both dSAGA and ATAC HAT complexes (66). These results are in

agreement with the recently obtained data by Guleman et al. that characterized the new *Drosophila* ADA2a-containing complex, ATAC. In an *in vitro* HAT assay ATAC complex was shown to acetylates mainly nucleosomal H4 (68). We did not observed a significant change in K9-, K14- and K18-acetylated H3 or K8 acetylated H4 on polytene *dAda2a* chromosomes. Earlier studies in *Drosophila* showed that acetylation of H4 at lysine K5, K8 and K12 have a different pattern of expression during embryogenesis and CBP HAT is required for H4K8 acetylation (106).

In *Drosophila* males, the dosage compensation complex (DCC) containing MLE, MSL1, MSL3 and the male-specific MSL-2 protein, recruits the MOF histone acetyltransferase to the X chromosome, resulting in a specific hyperacetylation of H4K16 residues which ensures a 2-fold increase of X-linked genes (2). To test whether the decondensation of the X chromosome reflects an alteration of the DCC, we analyzed H4K16 chromosome acetylation in *dAda2a*^{d189} and *dGcn5*^{E333st} mutant males. Although the structure of male X chromosome in these males is altered, the acetylation level of H4K16 residues was not changed compared to the wild type. This alteration of male X chromosomes structure, repeatedly observed, is proposed to reflect a higher sensitivity of the male X chromosome conferred by the activity of the dosage compensation machinery.

According to previous findings when polytene chromosomes were immunoprobed for dADA2a, dADA2b, dADA3 and dGCN5, all proteins stained mostly the euchromatic interband regions. dADA3 and dGCN5 displayed full colocalization, while dADA2a and dADA2b colocalized to only a few bands on polytene chromosomes, whereas most of the signals were not overlapping (97). Remarkably, a significant portion of dADA2a containing complexes localized to decondensed chromosome puffs. In contrast, the staining of wild-type chromosomes with anti-H4K5ac and anti-H4K12ac antibodies indicates that regions with high DNA content are enriched in these types of modifications (Fig. 4.11.A). Strong staining is also visible in the centromeric heterochromatic region for both H4K5ac and H4K12ac. One possible explanation would be that the HAT complexes are necessary for a basic level of acetylation distributed along the chromosomes more visible in the band, while the chromosome immunostaining method is not sensitive enough to detect the basic level of acetylation in the euchromatic regions. In addition, dADA3, dADA2a, dADA2b or dGCN5 as a part of the same or different complexes are necessary for specific gene activation, and they are detectable in euchromatic regions. The colocalization of Pol II- and K5- or K12-acetylated H4 staining occurs in some regions along the chromosome, but, as a general rule, intensely transcribed loci are not enriched in the acetylation deposited by dADA2a-containing complexes (Fig. 4.11.A).

A similar distribution of dADA2b-dependent acetylation of H3 (K14 and K9) and its loss in *dAda2b* mutants were observed earlier (120, 124). Depending on the surroundings, like the presence of transcription factors, chromatin remodeling factors or specific signals, the acetylation of different residues is changed in order to activate or inhibit the expression of genes. The precise pattern of histone acetylation and its effect on gene expression is not completely understood yet. Maintaining a balance between acetylated and deacetylated regions is important in targeted promoter modification, where specific modifications occur in a background of global acetylation and deacetylation that not only reduces basal transcription, but also allows a rapid return to the initial state of acetylation when targeting is removed. According to the data available from studies on yeast, Arabidopsis and mammalian cells, similar to the H3 acetylation, in the active genes H4 acetylation seems to accumulate at the promoter regions, also.

Taken together, these data indicate that dADA2a and dADA2b are functionally similar in playing roles in histone acetylation distributed along the chromosomes in rough proportion with the DNA content. However, dADA2a and dADA2b participate in dGCN5-containing complexes that acetylate specific residues of H4 and H3, respectively. dADA2a and dADA2b also differ in that the complexes containing them participate in the transcriptional activation of distinct sets of genes: the hormone induction of early-response genes requires the dADA2a function (Fig. 4.7), while dADA2b is involved in p53-mediated processes among others (120). Accordingly, we propose dual functions for dADA2a-containing complexes: the deposition of uniformly distributed H4 acetylation along the chromosomes and the targeted acetylation of histones at specific loci. A decrease in the former might contribute to the observed structural change in *dAda2a* chromosomes, while a loss of the latter function results in an altered transcription activity at specific loci. Our data clearly indicate that, regarding the first function, dADA2a- and dADA2b-containing complexes have distinct preferences for H4 and H3, respectively. Whether the same specificity of dADA2a and dADA2b-containing complexes exists in promoter-specific modifications remains to be determined. Guelman et al. reported the identification of a novel dADA2a-containing HAT complex, ATAC, in *Drosophila* (68). In an *in vitro* acetylation assay, ATAC was found to display strong nucleosomal H4 activity. The specificity of ATAC for *in vivo* histone acetylation is at present unknown. Therefore, it is an intriguing possibility that *in vivo* the dADA2b-containing SAGA complexes acetylate H3 lysines, while the dADA2a-containing ATAC complexes target lysines at the N terminus of H4. It should be noted, however, that in the ATAC complex, the presence of an additional protein with a putative HAT domain, designated as ATAC2, was also detected (151). ATAC2

is required for *Drosophila* viability and in its absence the mutant animals die in the L2 larval stage. Staining of *atac2* mutant embryos with specific antibodies for H4K12ac or H4K5ac did not show a significant change in the acetylation level, while the H4K16 acetylation was reduced. It is possible that ATAC2 does not influence the H4K5 and K12 acetylation, or since they die in a latter stage, due to the maternal effect in these animals the acetylation of K5 and K12 residues is still detectable (151). Very recently the human ATAC (hATAC) complex was purified and some of the subunits were identified due to their homology with the *Drosophila* subunits (167). By an *in vitro* HAT assay Wang and colleagues showed that hATAC mainly acetylates nucleosomal H3.

Alternatively, the obtained results together with the existing data might also suggest the possibility that dADA2a, and perhaps also dADA2b, participates in gene-specific transcription regulation independently of dGCN5. Indeed, several independent observations indicate the presence of dADA2a independently of dGCN5, which might reflect a dGCN5-independent role for dADA2a. On glycerol gradient sedimentation of *Drosophila* embryo extract, a significant fraction of dADA2a did not cosediment with dGCN5 but was present in fractions corresponding to smaller *M_w* complexes (110). Immunocolocalization studies on polytene chromosomes revealed that dADA2a was enriched at many sites independently of dGCN5, and only a little overlap was observed between the two proteins (97). Furthermore, the amount of dADA2a and dGCN5 does not seem to be tightly linked at different stages of *Drosophila* development (97). Our observation that *dGcn5 dAda2a* double mutants cause a stronger phenotype than that of either null mutant alone can also be interpreted as an indication of separate functions of the two proteins.

The observations that *dAda2* and *dGcn5* (and also *dAda2b*) mutants survive until the late-larva stage suggest that the uniformly deposited acetylation by the complexes containing these factors either is not essential or can be accomplished without these factors or can be compensated for by other acetyltransferases. On the other hand, the gene-specific effects of dGCN5- and dADA2a-containing complexes, which lead to the onset of the metamorphosis program or those carried out by dADA2b containing complexes in regulating p53-mediated processes, cannot be compensated for. It is interesting that the partial phenotypic rescue resulting from the increased ecdysone level in hormone-fed larvae indicates further complexity in the gene regulatory circuits: while these animals form cuticle readily in response to the hormone pulse, no response in the development in their imaginal discs is apparent and they perish as malformed pupae. A dual role for yGcn5 in promoter-targeted acetylation and in maintaining low levels of uniform acetylation in surrounding regions has also been proposed

by Howe et al. (75). Our findings on the role of Drosophila ADA2-GCN5-containing complexes are in full accord with their suggestion and also with observations that yeast cells can tolerate large decreases in histone acetylation without affecting the cell viability (75).

In several mutants affecting subunits of ATAC HAT complex we observed chromatin structural changes similar to those seen in *JIL-1*, *Iswi*, *NURF* and *Su(var)2-5* mutants. Significantly, while *dAda2a*, *dAda3* and *dGcn5* mutants display distorted chromosome phenotype, *dAda2b* null mutants do not. The presence of dADA2a and dADA2b are characteristic for the ATAC, and dSAGA HAT complexes, respectively (35, 68), we therefore hypothesized that the altered chromatin structure resulted from a failure of the former complex. In order to test if the same chromosomal alteration seen in mutants of ATAC complex and *JIL-1*, reflect a functional interplay between the two we analyzed the level of H4K12 acetylation deposited by ATAC in *JIL-1* mutants and, vice versa, the level of H3S10 phosphorylation deposited by *JIL-1* in ATAC mutants. While the H4K12ac was not affected by the loss of *JIL-1* function, a severe reduction in the H3S10ph was detected in the ATAC mutants. In addition, ectopic expression of the histone kinase *JIL-1* in ATAC mutants restores H3S10 phosphorylation level and also restores the polytene chromosome structure close to normal.

With the experiments presented here we provide support to this hypothesis and suggest why the reduced level of H4 acetylation by ATAC leads to chromosome structural alterations. Our data indicate that the chromosome structural defects observed in ATAC mutants are, at least in part, due to a reduced S10 phosphorylated histone H3 level. This observation suggests that the direct cause of altered chromosome structure is not only the lack of H4 acetylation per se, but also the concomitant loss of H3 phosphorylation in the absence of ATAC function. In agreement with this, we observed a significantly reduced level of *JIL-1* kinase associated with ATAC mutant chromosomes. The decreased *JIL-1* function in ATAC mutants provides explanation for the observed genetic interaction between ATAC and *Su(var)3-9* mutants, and for the observation that the histone H3K9 dimethyl mark deposited by *SU(VAR)3-9* extends in ATAC mutants (44, 177).

We find it unlikely that a low level of *JIL-1* kinase expression would be the underlying cause of the severely decreased histone H3S10 phosphorylation level in ATAC mutants. Several independent observations argue against this: first, we observed only a 40% reduction in the *JIL-1*-specific mRNA level in ATAC mutants. In the same experiments we found that *JIL-1/+* heteroallelic combinations produced a similar reduced amount of *JIL-1* message like the ATAC mutant subunits, but they develop and live as the wild-type siblings. In contrast with the small difference in *JIL-1* mRNA level ATAC mutants show marked decreases in H3S10ph

level and JIL-1 localization to chromatin, and display bloated male X chromosome phenotype, while *JIL-1/+* heteroallelic combinations are indistinguishable from wild-types in all in these features. Previous studies have also shown that the level of histone H3S10 phosphorylation in *JIL-1/+* heterozygotes is comparable to that of wild-type larvae (177) and that hypomorph *JIL-1* mutants, producing approximately one tenth of the normal level of JIL-1 protein, affect the chromosome structure only moderately (166). A second argument is that we did not observe a significant reduction in the JIL-1 protein level in ATAC mutants by either immunoblots or immunostaining of tissue samples. In contrast with this, we repeatedly observed that the localization of JIL-1 to the chromatin of ATAC mutants was severely attenuated. We therefore favor the idea that the JIL-1 protein present in ATAC mutants is functionally restricted and unable to perform H3S10 phosphorylation effectively. A functional failure of JIL-1 could arise from its altered interaction with the chromatin hypoacetylated at histone H4K5/K12. Being devoid of these modifications, a less open chromatin might have restricted accessibility, or the lack of H4K5/K12 acetylation marks might have a specific effect on JIL-1-chromatin interaction. Very recent data of Bao and colleagues, demonstrated that the C-terminal domain of JIL-1 kinase is necessary for interaction with H3 tail, but it does not affect the kinase activity (10). We also can assume, that the altered chromatin structure seen in ATAC mutants impairs the interaction of JIL-1 with H3 histone, and the subsequent phosphorylation. We noticed the preferential association of JIL-1 to the histone H4K16 hyperacetylated chromatin of male X chromosomes. The mechanism of JIL-1 binding to H4K16-acetylated chromatin is, however, believed through its association with dosage compensation complex proteins (83).

Cross-talk between histone acetylation, methylation and phosphorylation have been described before. Several studies have linked histone H3 acetylation at the K9 or K14 residues with H3S10ph. H3 phosphorylation at S10 can enhance acetylation of histone H3 at K14 (34, 105), and inhibit methylation of histone H3 at lysine K9 (128). However, the relationship of H4 acetylation and H3 phosphorylation has not been observed before, and might seem surprising. JIL-1 is associated primarily with transcriptionally active interband regions, while H4K12 acetylation is observed mostly on compacted chromosomal regions (98). However, neither JIL-1 nor the ATAC complex reside exclusively at eu- or heterochromatic regions and roles in chromatin condensation and decondensation have been proposed for both H3S10 phosphorylation and H4K12 acetylation (17, 79, 119, 152). In addition immunostaining of polytene chromosomes showed that dADA2a, dADA3 and dGCN5 localize mostly to interband regions (97). In ATAC mutants the expression of a great number of genes is significantly altered (30, 66) demonstrating the role of histone H4K5/K12 acetylation in

transcription regulation. On the other hand, acetylation of H4K12 has been suggested to play a key role in the formation of heterochromatin following H2Av replacement (152). According to this model, H4K12 acetylation triggers deacetylation and methylation of H3K9 which in turn serves as signal for HP1 binding. In contrast with this model, we did not observe that a decrease of H4K12 acetylation provoked a decrease in the level of H3K9me2. On the contrary, our data suggest that a change of H4K12ac level indirectly causes a change in the opposite direction in the level of H3K9me2, through the modulation of H3S10 phosphorylation level. In accord with our observations, Grau et al. demonstrated that dADA3 is an enhancer of variegation of X chromosome rearrangements and in its absence the heterochromatin spreads. In the absence of dADA3 an enhanced variegation of the *Drosophila* pigment eye was observed, while increased level of dADA3 protein has a suppressive effect (66). Similarly, Deng et al., demonstrated that ectopic expression of JIL-1 kinase and increased H3S10ph causes chromatin decondensation (43). According to these observations, it is most probable that the lack of ATAC complex leads to heterochromatin formation, rather to chromatin loosening. At present we cannot offer a convincing argument to resolve the discrepancy between these two observations and we should assume that depending on the specific chromosomal regions and particularly on the already existing histone modifications, the acetylation of H4K5/K12 can have different effects.

Many studies have linked the functions of ATP-utilizing chromatin-remodeling factors and histone-modifying enzymes. In an independent work, not discussed in detail in this study, we also demonstrated the interplay between the NURF and the ATAC complexes in chromatin structure organization. We demonstrated the genetic interaction between mutations affecting subunits of the NURF chromatin remodeling and ATAC HAT complexes. We also analyzed the level of ISWI in ATAC mutants, and vice-versa, the level of dADA2a and dGCN5 in ISWI mutants. In none of the cases the expression of the analyzed genes was affected. ISWI binding to polytene chromosome was also not affected by the loss of the ATAC components. Using an ISWI-specific antibody we tested the ISWI binding to chromosomes and compared to wild-type no change was detected, or in some cases a small increase in the level of the staining intensity was observed. Strikingly, *Iswi* mutation impairs the binding of dADA2a to chromosomes and, as a consequence, both *Iswi* and *Nurf301* mutations strongly reduce acetylation of H4 histone K12 residues. Analysis of microarray data revealed that both ATAC and NURF complexes regulated same set of genes, including the ecdysone induced genes, heat-shock genes, engrailed and *Ubx* (30). These observations lead to the hypothesis that

NURF is required for the recruitment of ATAC to chromatin and subsequent acetylation of H4 histone.

Combined, these observations thus indicate a cascade of interdependent steps in chromatin structure modification, involving an ATP-dependent chromatin remodeling complex, a histone H4-specific acetyltransferase complex, and the balanced action of a histone H3-specific kinase and methyltransferase. The bloated male X phenotype, characteristic for mutations affecting either NURF, ATAC or JIL-1, and the genetic interactions among these and also with *Su(var)3-9* mutants, as described here and in earlier reports (177), provide a strong support for the *in vivo* existence of such a cascade.

The results discussed above suggest the existence of a complex multistep model for chromatin remodeling, shown in figure 5.1. As the first step, the H4 acetylation at K5 and K12 is deposited by ATAC complex, alteration that would facilitate the recruitment of JIL-1 kinase followed by H3S10 phosphorylation. These modifications lead to chromatin structural changes favorable for gene transcription. On the other hand, in the absence of a functional ATAC complex, the function of JIL-1 is impaired also, permitting the spreading of H3K9me2 deposited by SU(VAR)3-9 methyltransferase and chromatin compaction.

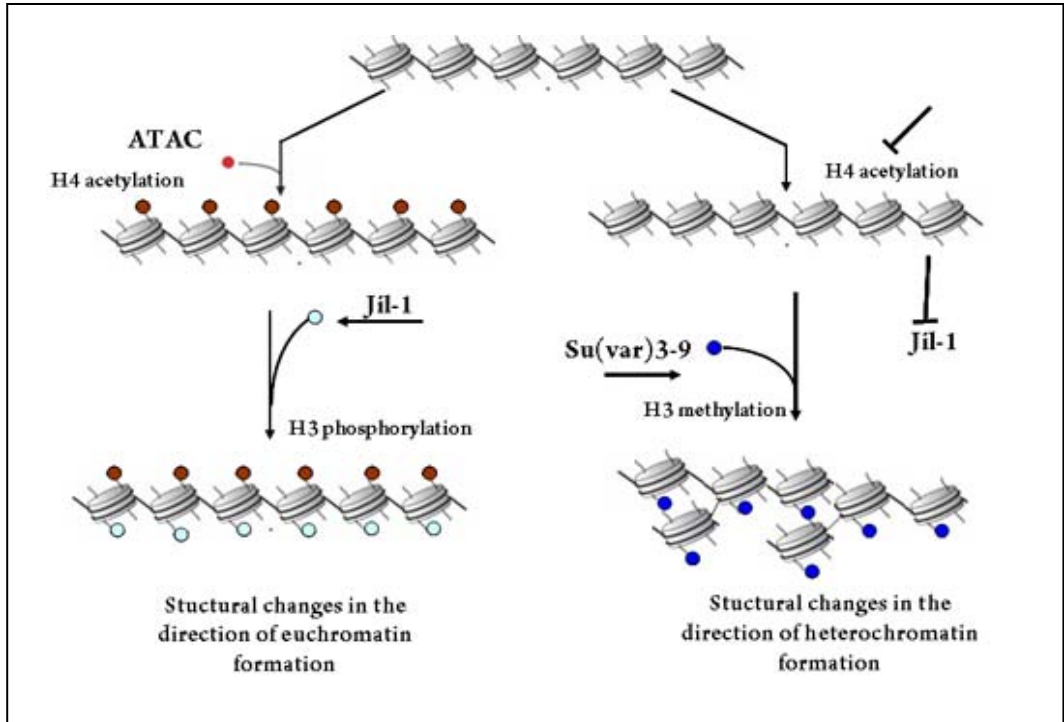


Fig. 5.1. Possible pathway for euchromatin and heterochromatin formation. H4 acetylation by ATAC triggers phosphorylation of H3S10 by JIL-1 kinase that leads to euchromatin formation. In the absence of H4 acetylation, JIL-1 kinase cannot properly phosphorylate H3S10, permitting the spreading of H3K9 dimethylation by SU(VAR)3-9 methyltransferase.

6. SUMMARY

Numerous enzymes and protein complexes are known to bring about changes in the state of chromatin by different mechanisms with resultant effects on gene expression. One class of complexes, alter the DNA packaging in an ATP-dependent manner. Another class of chromatin structure regulating factors acts by covalently modifying histone proteins. The various modifications include phosphorylation, ubiquitination, ADP-ribosylation, methylation, sumoylation and frequently acetylation, catalyzed by histone acetyltransferases (HATs). In many cases HAT enzymes are components of complexes which also contain among others, ADA-type adaptors.

Recently our laboratory, in parallel with several others, has showed that contrary to the single ADA2 adaptor protein present in *Saccharomyces cerevisiae*, different Gcn5-containing HAT complexes of *Drosophila melanogaster* cells contain two related ADA2 proteins encoded by genes referred to as *dAda2a* and *dAda2b*. In several other metazoan organisms, including mouse, human and Arabidopsis, there are also two ADA2-type coactivators. Biochemical separation of ADA2-containing *D. melanogaster* complexes indicated that dADA2a is present in a smaller (0.8 MDa) and dADA2b in a larger (2MDa) complex which corresponds to the *Drosophila* homologue of yeast SAGA complex. In a number of independent studies it was shown that in the absence of dADA2b or dGCN5, in other words, in the absence of functional dSAGA, the acetylation of histone H3K9 and K14 is greatly reduced, while the H4K8 acetylation is not affected.

In this work we provide evidence that the dADA2a protein is a specific component of the smaller *Drosophila* HAT complex which during the course of this work became identified as ATAC. We demonstrate the genetic interaction between *dAda2a* and *dGcn5* genes and show their role in H4 acetylation. Finally, we describe the functional interplay between components of the ATAC complex and factors responsible for two other types of modifications that take place at the chromatin: histone phosphorylation by the JIL-1 kinase and methylation by SU(VAR)3-9.

We provide several lines of evidence for the functional linkage between dADA2a and dGCN5. We show their physical and genetic interaction by analyzing the phenotype of specific single and double mutants. The loss of either *dGcn5* or *dAda2a* function results in similar chromosome structural and developmental defects. *dGcn5/dAda2a* double-null mutants or a combination of *dAda2a* and *dGcn5* hypomorph alleles result in a phenotype stronger than that

of either of the two mutations alone. The overexpression of dGCN5 protein by the use of an act-GAL4 driver in *dAda2a* mutant background results in a partial rescue. Furthermore, the phenotypic features of *dAda2a* mutants indicate a developmental block at the time of larva-pupa transition similarly as it was shown by others for *dGcn5* mutants. In accord with this, by analyzing the puff formation at sites containing ecdysone induced genes and using RT-PCR and Q-PCR to measure specific mRNA levels we demonstrate that the expression of several ecdysone-induced genes such as BR-C, Eip74 and Eip75 are downregulated in the absence of dADA2a protein.

Immunostaining of *Drosophila* polytene chromosome and Western Blot analysis revealed a significantly decreased level of K5 and K12 acetylated histone H4 in *dAda2a* and *dGcn5* mutants, while the acetylation established by dADA2b-containing GCN5 complexes at H3K9 and K14 was unaffected. These results, for the first time in the literature, clearly establish the *D. melanogaster* ATAC as a histone H4-specific HAT complex.

We noticed that another important characteristic of ATAC subunit mutants (*dAda2a*, *dAda3* and *dGcn5*) is the altered structure of the polytene chromosomes observed as disturbed banding pattern and distortions shown most clearly by the male X chromosome. Similar alterations of polytene chromosome structure were observed by others in the absence of JIL-1, the kinase that phosphorylates H3 at serine 10. In order to determine if there is an interdependence between JIL-1 and ATAC functions we studied the levels of ATAC-deposited histone H4K12 acetylation and JIL-1-deposited histone H3S10 phosphorylation in *JIL-1* and ATAC subunit mutants and found that H3S10 phosphorylation in ATAC mutants was severely decreased, while no change was detectable in the level of H4K12-Ac in *JIL-1* mutants. Thus, phosphorylation by JIL-1 depends on ATAC function. Further experiments support this observation, the increase of the JIL-1 protein level by the use of JIL-1EGFP transgene in *dAda2a* and *dGcn5* mutants restored the H3S10 phosphorylation level close to normal and increased the survival of *dAda2a* and *dGcn5* null and hypomorph animals. Significantly, the effect of JIL-1 overproduction is also well observable in the change of chromosome structure of ATAC mutants as the bloated phenotype of male X chromosome characteristic for each ATAC mutant studied (*dAda2a*, *dGcn5* and *dAda3*) was significantly suppressed by JIL-1 overproduction.

As phosphorylation of histone H3S10 by JIL-1 counteracts heterochromatin formation resulting from histone H3K9 dimethylation by SU(VAR)3-9 dimethyltransferase, we assumed that H4 acetylation at K5 and K12 also has an effect on heterochromatin spreading. In concert with this assumption, immunostaining of polytene nuclei or chromosome spreads with

H3K9me2 specific antibodies revealed a spread of signal on *dAda2a* and *dGcn5* mutant chromosomes similarly to that observed on *JIL-1* chromosomes. For testing the genetic interaction between *Su(var)3-9* and ATAC subunit mutants we studied the effect of *dAda2a* and *dGcn5* deficiency in *Su(var)3-9* heterozygous backgrounds and showed that a decreased level of SU(VAR)3-9 increased the survival and improved the chromosome structure of ATAC mutants.

In order to explain the mechanism of ATAC and JIL-1 functional interaction we analyzed the expression of JIL-1 in ATAC mutants by determining the JIL-1 mRNA and protein levels and showed that the JIL-1 was expressed in ATAC mutants to similar level as in wild-type controls. However, the binding of the JIL-1 protein to the chromatin containing a low level of acetylated H4 was significantly reduced.

In a set of independent experiments we showed functional interaction between the histone modifying ATAC and the nucleosome remodeling NURF complexes. Using appropriate mutants strains we showed that there is genetic interaction between genes encoding ATAC subunits and the NURF subunit ISWI. In addition, immunostaining of polytene chromosomes with dADA2a-specific Ab revealed that the ADA2a binding to *Iswi* chromosomes was strongly reduced. In agreement with this data, immunoblot analysis and chromosome immunostaining showed a significant decreased of K12 acetylated H4 level of salivary gland polytene chromosomes of *Iswi* and *Nurf301* mutants.

Taken together, these results strongly suggest a functional interaction of nucleosome remodeling and histone acetyltransferase complexes and histone kinase and methyltransferase. Our data demonstrate that the function of NURF complex is required for the binding of ATAC to chromatin and for subsequent acetylation of H4K12 residues. A reduced level of histone H4K12 acetylation by ATAC attenuates the phosphorylation of histone H3S10 by JIL-1 due to a reduced level of JIL-1 binding to hypoacetylated chromatin that permits the spreading of H3K9 dimethylation by SU(VAR)3-9 .

7. ABBREVIATIONS

ACF	ATP-utilizing chromatin assembly and remodeling factor
ADA	Alteration Deficiency in Activation
AIR2-Ipl1	Aurora/Ipl1-Related protein
ATAC	Ada Two A containing Complex
ATP	Adenosil-triphosphat
BRG1	Brahma-related gene 1
BSA	Bovine albumin serum
CARM1	Coactivator-associated arginine methyltransferase 1
CHRAC	Chromatin-accessibility complex
CREB p300/BP	CREB p300 binding protein
Cy	Curly
Dtl	Drosophila tat like protein
EGFP	Enhanced green fluorescent protein
FCS	Fetal calf serum
GCN5	General control nonderepressible-5'
GNAT	Gcn5-containing N-acetyltransferase complex
H3K14ac (K9)	Histone 3 acetylated at lysine 14 (lysine 9)
H3S10ph	Histone 3 phosphorylated at serine 10
H4K5ac (K12)	Histone 4 acetylated at lysine 5 (lysine 12)
HAT	Histone Acetyltransferase
HCF	Host cell factor
HDAC	Histone deacetylase
HMG17, HMG1	High mobility group protein 17, 1
HMTase	Histone methyltransferase
HPI	Heterochromatic protein 1
Hu	Humeral
IGBMC	Institut de Génétique et de Biologie Moléculaire et Cellulaire
ISWI	Imitation switch
ING	Inhibitor of growth
MOF	Males absent on the first
MORF	Monocytic leukemia zinc finger protein-related factor
MOZ	Monocytic leukemia zinc finger protein

MyoD	Myogenic determination
MYST	MOZ, Ybf2/Sas3, Sas2 and Tip60 acetyltransferase superfamily
NPC	Nuclear pore complex
NuA4	Nucleosome acetyltransferase of H4
NURF	Nucleosome remodeling factor
PCAF	p300/CBP-associating factor
PCR	Polimerase chain reaction
PP1	Protein phosphatase 1
Rpb4	RNA polimerase β 4
PRMT	Protein arginine methyltransferase
SAGA	Spt-Ada-Gcn-acetyltransferase
SANT	Swi3, Ada2, NCoR, TFIIB
Sb	Stubble
SDS-PAGE	Sodium-dodecyl-sulfate polyacrilamide gel electrophoresis
SNF	Sucrose non-fermenting
SWI/SNF	Switching/sucrose nonfermenting
SWIRM	Swi3p, Rsc8p and Moira
SU(VAR)3-9	Supressor of position-effect variegation 3-9
TAF10	TBP-associated factor 10
Tb	Tubby
TBP	TATA binding protein
UAS	Upstream Activation Sequences
w	White

8. BIBLIOGRAPHY

1. **Ait-Si-Ali, S., S. Ramirez, P. Robin, D. Trouche, and A. Harel-Bellan.** 1998. A rapid and sensitive assay for histone acetyl-transferase activity. *Nucleic Acids Res* **26**:3869-70.
2. **Akhtar, A.** 2003. Dosage compensation: an intertwined world of RNA and chromatin remodelling. *Curr Opin Genet Dev* **13**:161-9.
3. **Akhtar, A., and P. B. Becker.** 2000. Activation of transcription through histone H4 acetylation by MOF, an acetyltransferase essential for dosage compensation in *Drosophila*. *Mol Cell* **5**:367-75.
4. **Aletta, J. M., T. R. Cimato, and M. J. Ettinger.** 1998. Protein methylation: a signal event in post-translational modification. *Trends Biochem Sci* **23**:89-91.
5. **Allard, S., R. T. Utley, J. Savard, A. Clarke, P. Grant, C. J. Brandl, L. Pillus, J. L. Workman, and J. Cote.** 1999. NuA4, an essential transcription adaptor/histone H4 acetyltransferase complex containing Esa1p and the ATM-related cofactor Tra1p. *Embo J* **18**:5108-19.
6. **Badenhorst, P., M. Voas, I. Rebay, and C. Wu.** 2002. Biological functions of the ISWI chromatin remodeling complex NURF. *Genes Dev* **16**:3186-98.
7. **Badenhorst, P., H. Xiao, L. Cherbas, S. Y. Kwon, M. Voas, I. Rebay, P. Cherbas, and C. Wu.** 2005. The *Drosophila* nucleosome remodeling factor NURF is required for Ecdysteroid signaling and metamorphosis. *Genes Dev* **19**:2540-5.
8. **Baker, S. P., and P. A. Grant.** 2007. The SAGA continues: expanding the cellular role of a transcriptional co-activator complex. *Oncogene* **26**:5329-40.
9. **Balasubramanian, R., M. G. Pray-Grant, W. Selleck, P. A. Grant, and S. Tan.** 2002. Role of the Ada2 and Ada3 transcriptional coactivators in histone acetylation. *J Biol Chem* **277**:7989-95.
10. **Bao, X., W. Cai, H. Deng, W. Zhang, R. Krencik, J. Girton, J. Johansen, and K. M. Johansen.** 2008. The COOH-terminal domain of the JIL-1 histone H3S10 kinase interacts with histone H3 and is required for correct targeting to chromatin. *J Biol Chem* **283**:32741-50.
11. **Bao, Y., and X. Shen.** 2007. SnapShot: chromatin remodeling complexes. *Cell* **129**:632.
12. **Barak, O., M. A. Lazzaro, W. S. Lane, D. W. Speicher, D. J. Picketts, and R. Shiekhattar.** 2003. Isolation of human NURF: a regulator of *Engrailed* gene expression. *Embo J* **22**:6089-100.
13. **Barlev, N. A., A. V. Emelyanov, P. Castagnino, P. Zegerman, A. J. Bannister, M. A. Sepulveda, F. Robert, L. Tora, T. Kouzarides, B. K. Birshtein, and S. L. Berger.** 2003. A novel human Ada2 homologue functions with Gcn5 or Brg1 to coactivate transcription. *Mol Cell Biol* **23**:6944-57.
14. **Barlev, N. A., V. Poltoratsky, T. Owen-Hughes, C. Ying, L. Liu, J. L. Workman, and S. L. Berger.** 1998. Repression of GCN5 histone acetyltransferase activity via bromodomain-mediated binding and phosphorylation by the Ku-DNA-dependent protein kinase complex. *Mol Cell Biol* **18**:1349-58.
15. **Becker, P. B., and W. Horz.** 2002. ATP-dependent nucleosome remodeling. *Annu Rev Biochem* **71**:247-73.
16. **Benson, L. J., Y. Gu, T. Yakovleva, K. Tong, C. Barrows, C. L. Strack, R. G. Cook, C. A. Mizzen, and A. T. Annunziato.** 2006. Modifications of H3 and H4 during chromatin replication, nucleosome assembly, and histone exchange. *J Biol Chem* **281**:9287-96.

17. **Berger, S. L.** 2007. The complex language of chromatin regulation during transcription. *Nature* **447**:407-12.
18. **Berger, S. L., B. Pina, N. Silverman, G. A. Marcus, J. Agapite, J. L. Regier, S. J. Triezenberg, and L. Guarente.** 1992. Genetic isolation of ADA2: a potential transcriptional adaptor required for function of certain acidic activation domains. *Cell* **70**:251-65.
19. **Bone, J. R., J. Lavender, R. Richman, M. J. Palmer, B. M. Turner, and M. I. Kuroda.** 1994. Acetylated histone H4 on the male X chromosome is associated with dosage compensation in *Drosophila*. *Genes Dev* **8**:96-104.
20. **Bouazoune, K., and A. Brehm.** 2006. ATP-dependent chromatin remodeling complexes in *Drosophila*. *Chromosome Res* **14**:433-49.
21. **Brown, C. E., T. Lechner, L. Howe, and J. L. Workman.** 2000. The many HATs of transcription coactivators. *Trends Biochem Sci* **25**:15-9.
22. **Brownell, J. E., and C. D. Allis.** 1995. An activity gel assay detects a single, catalytically active histone acetyltransferase subunit in *Tetrahymena* macronuclei. *Proc Natl Acad Sci U S A* **92**:6364-8.
23. **Brownell, J. E., J. Zhou, T. Ranalli, R. Kobayashi, D. G. Edmondson, S. Y. Roth, and C. D. Allis.** 1996. *Tetrahymena* histone acetyltransferase A: a homolog to yeast Gcn5p linking histone acetylation to gene activation. *Cell* **84**:843-51.
24. **Burgio, G., G. La Rocca, A. Sala, W. Arancio, D. Di Gesu, M. Collesano, A. S. Sperling, J. A. Armstrong, S. J. van Heeringen, C. Logie, J. W. Tamkun, and D. F. Corona.** 2008. Genetic identification of a network of factors that functionally interact with the nucleosome remodeling ATPase ISWI. *PLoS Genet* **4**:e1000089.
25. **Burtis, K. C., C. S. Thummel, C. W. Jones, F. D. Karim, and D. S. Hogness.** 1990. The *Drosophila* 74EF early puff contains E74, a complex ecdysone-inducible gene that encodes two ets-related proteins. *Cell* **61**:85-99.
26. **Cai, W., X. Bao, H. Deng, Y. Jin, J. Girton, J. Johansen, and K. M. Johansen.** 2008. RNA polymerase II-mediated transcription at active loci does not require histone H3S10 phosphorylation in *Drosophila*. *Development* **135**:2917-25.
27. **Candau, R., and S. L. Berger.** 1996. Structural and functional analysis of yeast putative adaptors. Evidence for an adaptor complex in vivo. *J Biol Chem* **271**:5237-45.
28. **Candau, R., P. A. Moore, L. Wang, N. Barlev, C. Y. Ying, C. A. Rosen, and S. L. Berger.** 1996. Identification of human proteins functionally conserved with the yeast putative adaptors ADA2 and GCN5. *Mol Cell Biol* **16**:593-602.
29. **Candau, R., J. X. Zhou, C. D. Allis, and S. L. Berger.** 1997. Histone acetyltransferase activity and interaction with ADA2 are critical for GCN5 function in vivo. *Embo J* **16**:555-65.
30. **Carre, C., A. Ciurciu, O. Komonyi, C. Jacquier, D. Fagegaltier, J. Pidoux, H. Tricoire, L. Tora, I. M. Boros, and C. Antoniewski.** 2008. The *Drosophila* NURF remodelling and the ATAC histone acetylase complexes functionally interact and are required for global chromosome organization. *EMBO Rep* **9**:187-92.
31. **Carre, C., D. Szymczak, J. Pidoux, and C. Antoniewski.** 2005. The histone H3 acetylase dGcn5 is a key player in *Drosophila melanogaster* metamorphosis. *Mol Cell Biol* **25**:8228-38.
32. **Carrozza, M. J., R. T. Utley, J. L. Workman, and J. Cote.** 2003. The diverse functions of histone acetyltransferase complexes. *Trends Genet* **19**:321-9.
33. **Chen, D., H. Ma, H. Hong, S. S. Koh, S. M. Huang, B. T. Schurter, D. W. Aswad, and M. R. Stallcup.** 1999. Regulation of transcription by a protein methyltransferase. *Science* **284**:2174-7.

34. **Cheung, P., K. G. Tanner, W. L. Cheung, P. Sassone-Corsi, J. M. Denu, and C. D. Allis.** 2000. Synergistic coupling of histone H3 phosphorylation and acetylation in response to epidermal growth factor stimulation. *Mol Cell* **5**:905-15.
35. **Ciurciu, A., O. Komonyi, T. Pankotai, and I. M. Boros.** 2006. The *Drosophila* histone acetyltransferase Gcn5 and transcriptional adaptor Ada2a are involved in nucleosomal histone H4 acetylation. *Mol Cell Biol* **26**:9413-23.
36. **Clapier, C. R., G. Langst, D. F. Corona, P. B. Becker, and K. P. Nightingale.** 2001. Critical role for the histone H4 N terminus in nucleosome remodeling by ISWI. *Mol Cell Biol* **21**:875-83.
37. **Clarke, A. S., J. E. Lowell, S. J. Jacobson, and L. Pillus.** 1999. Esa1p is an essential histone acetyltransferase required for cell cycle progression. *Mol Cell Biol* **19**:2515-26.
38. **Clarke, S.** 1993. Protein methylation. *Curr Opin Cell Biol* **5**:977-83.
39. **Corona, D. F., C. R. Clapier, P. B. Becker, and J. W. Tamkun.** 2002. Modulation of ISWI function by site-specific histone acetylation. *EMBO Rep* **3**:242-7.
40. **Cuthbert, G. L., S. Daujat, A. W. Snowden, H. Erdjument-Bromage, T. Hagiwara, M. Yamada, R. Schneider, P. D. Gregory, P. Tempst, A. J. Bannister, and T. Kouzarides.** 2004. Histone deimination antagonizes arginine methylation. *Cell* **118**:545-53.
41. **de la Barre, A. E., V. Gerson, S. Gout, M. Creaven, C. D. Allis, and S. Dimitrov.** 2000. Core histone N-termini play an essential role in mitotic chromosome condensation. *Embo J* **19**:379-91.
42. **Delattre, M., A. Spierer, C. H. Tonka, and P. Spierer.** 2000. The genomic silencing of position-effect variegation in *Drosophila melanogaster*: interaction between the heterochromatin-associated proteins Su(var)3-7 and HP1. *J Cell Sci* **113 Pt 23**:4253-61.
43. **Deng, H., X. Bao, W. Cai, M. J. Blacketer, A. S. Belmont, J. Girton, J. Johansen, and K. M. Johansen.** 2008. Ectopic histone H3S10 phosphorylation causes chromatin structure remodeling in *Drosophila*. *Development* **135**:699-705.
44. **Deng, H., X. Bao, W. Zhang, J. Girton, J. Johansen, and K. M. Johansen.** 2007. Reduced levels of Su(var)3-9 but not Su(var)2-5 (HP1) counteract the effects on chromatin structure and viability in loss-of-function mutants of the JIL-1 histone H3S10 kinase. *Genetics* **177**:79-87.
45. **Deng, H., W. Zhang, X. Bao, J. N. Martin, J. Girton, J. Johansen, and K. M. Johansen.** 2005. The JIL-1 kinase regulates the structure of *Drosophila* polytene chromosomes. *Chromosoma* **114**:173-82.
46. **Deuring, R., L. Fanti, J. A. Armstrong, M. Sarte, O. Papoulas, M. Prestel, G. Daubresse, M. Verardo, S. L. Moseley, M. Berloco, T. Tsukiyama, C. Wu, S. Pimpinelli, and J. W. Tamkun.** 2000. The ISWI chromatin-remodeling protein is required for gene expression and the maintenance of higher order chromatin structure in vivo. *Mol Cell* **5**:355-65.
47. **DiBello, P. R., D. A. Withers, C. A. Bayer, J. W. Fristrom, and G. M. Guild.** 1991. The *Drosophila* Broad-Complex encodes a family of related proteins containing zinc fingers. *Genetics* **129**:385-97.
48. **Dutnall, R. N., S. T. Tafrov, R. Sternglanz, and V. Ramakrishnan.** 1998. Structure of the histone acetyltransferase Hat1: a paradigm for the GCN5-related N-acetyltransferase superfamily. *Cell* **94**:427-38.
49. **Eberharter, A., and P. B. Becker.** 2004. ATP-dependent nucleosome remodelling: factors and functions. *J Cell Sci* **117**:3707-11.
50. **Eberharter, A., I. Vetter, R. Ferreira, and P. B. Becker.** 2004. ACF1 improves the effectiveness of nucleosome mobilization by ISWI through PHD-histone contacts. *Embo J* **23**:4029-39.

51. **Ebert, A., G. Schotta, S. Lein, S. Kubicek, V. Krauss, T. Jenuwein, and G. Reuter.** 2004. Su(var) genes regulate the balance between euchromatin and heterochromatin in *Drosophila*. *Genes Dev* **18**:2973-83.
52. **Eggert, H., A. Gortchakov, and H. Saumweber.** 2004. Identification of the *Drosophila* interband-specific protein Z4 as a DNA-binding zinc-finger protein determining chromosomal structure. *J Cell Sci* **117**:4253-64.
53. **Eissenberg, J. C., and S. C. Elgin.** 2000. The HP1 protein family: getting a grip on chromatin. *Curr Opin Genet Dev* **10**:204-10.
54. **Eissenberg, J. C., T. C. James, D. M. Foster-Hartnett, T. Hartnett, V. Ngan, and S. C. Elgin.** 1990. Mutation in a heterochromatin-specific chromosomal protein is associated with suppression of position-effect variegation in *Drosophila melanogaster*. *Proc Natl Acad Sci U S A* **87**:9923-7.
55. **Ekwall, K., T. Olsson, B. M. Turner, G. Cranston, and R. C. Allshire.** 1997. Transient inhibition of histone deacetylation alters the structural and functional imprint at fission yeast centromeres. *Cell* **91**:1021-32.
56. **Elfring, L. K., C. Daniel, O. Papoulas, R. Deuring, M. Sarte, S. Moseley, S. J. Beek, W. R. Waldrip, G. Daubresse, A. DePace, J. A. Kennison, and J. W. Tamkun.** 1998. Genetic analysis of brahma: the *Drosophila* homolog of the yeast chromatin remodeling factor SWI2/SNF2. *Genetics* **148**:251-65.
57. **Ferreira, R., A. Eberharter, T. Bonaldi, M. Chioda, A. Imhof, and P. B. Becker.** 2007. Site-specific acetylation of ISWI by GCN5. *BMC Mol Biol* **8**:73.
58. **Fischle, W., Y. Wang, and C. D. Allis.** 2003. Binary switches and modification cassettes in histone biology and beyond. *Nature* **425**:475-9.
59. **Fischle, W., Y. Wang, S. A. Jacobs, Y. Kim, C. D. Allis, and S. Khorasanizadeh.** 2003. Molecular basis for the discrimination of repressive methyl-lysine marks in histone H3 by Polycomb and HP1 chromodomains. *Genes Dev* **17**:1870-81.
60. **Gangaraju, V. K., and B. Bartholomew.** 2007. Mechanisms of ATP dependent chromatin remodeling. *Mutat Res* **618**:3-17.
61. **Gary, J. D., and S. Clarke.** 1998. RNA and protein interactions modulated by protein arginine methylation. *Prog Nucleic Acid Res Mol Biol* **61**:65-131.
62. **Georgakopoulos, T., and G. Thireos.** 1992. Two distinct yeast transcriptional activators require the function of the GCN5 protein to promote normal levels of transcription. *Embo J* **11**:4145-52.
63. **Giet, R., and D. M. Glover.** 2001. *Drosophila* aurora B kinase is required for histone H3 phosphorylation and condensin recruitment during chromosome condensation and to organize the central spindle during cytokinesis. *J Cell Biol* **152**:669-82.
64. **Grant, P. A., L. Duggan, J. Cote, S. M. Roberts, J. E. Brownell, R. Candau, R. Ohba, T. Owen-Hughes, C. D. Allis, F. Winston, S. L. Berger, and J. L. Workman.** 1997. Yeast Gcn5 functions in two multisubunit complexes to acetylate nucleosomal histones: characterization of an Ada complex and the SAGA (Spt/Ada) complex. *Genes Dev* **11**:1640-50.
65. **Grant, P. A., A. Eberharter, S. John, R. G. Cook, B. M. Turner, and J. L. Workman.** 1999. Expanded lysine acetylation specificity of Gcn5 in native complexes. *J Biol Chem* **274**:5895-900.
66. **Grau, B., C. Popescu, L. Torroja, D. Ortuno-Sahagun, I. Boros, and A. Ferrus.** 2008. Transcriptional adaptor ADA3 of *Drosophila melanogaster* is required for histone modification, position effect variegation, and transcription. *Mol Cell Biol* **28**:376-85.
67. **Gregory, P. D., A. Schmid, M. Zavari, L. Lui, S. L. Berger, and W. Horz.** 1998. Absence of Gcn5 HAT activity defines a novel state in the opening of chromatin at the PHO5 promoter in yeast. *Mol Cell* **1**:495-505.

68. **Guelman, S., T. Suganuma, L. Florens, S. K. Swanson, C. L. Kiesecker, T. Kusch, S. Anderson, J. R. Yates, 3rd, M. P. Washburn, S. M. Abmayr, and J. L. Workman.** 2006. Host cell factor and an uncharacterized SANT domain protein are stable components of ATAC, a novel dAda2A/dGcn5-containing histone acetyltransferase complex in *Drosophila*. *Mol Cell Biol* **26**:871-82.
69. **Hamiche, A., J. G. Kang, C. Dennis, H. Xiao, and C. Wu.** 2001. Histone tails modulate nucleosome mobility and regulate ATP-dependent nucleosome sliding by NURF. *Proc Natl Acad Sci U S A* **98**:14316-21.
70. **Hans, F., and S. Dimitrov.** 2001. Histone H3 phosphorylation and cell division. *Oncogene* **20**:3021-7.
71. **Hassa, P. O., S. S. Haenni, M. Elser, and M. O. Hottiger.** 2006. Nuclear ADP-ribosylation reactions in mammalian cells: where are we today and where are we going? *Microbiol Mol Biol Rev* **70**:789-829.
72. **Hassan, A. H., P. Prochasson, K. E. Neely, S. C. Galasinski, M. Chandy, M. J. Carrozza, and J. L. Workman.** 2002. Function and selectivity of bromodomains in anchoring chromatin-modifying complexes to promoter nucleosomes. *Cell* **111**:369-79.
73. **Hettmann, C., and D. Soldati.** 1999. Cloning and analysis of a *Toxoplasma gondii* histone acetyltransferase: a novel chromatin remodelling factor in Apicomplexan parasites. *Nucleic Acids Res* **27**:4344-52.
74. **Hilfiker, A., D. Hilfiker-Kleiner, A. Pannuti, and J. C. Lucchesi.** 1997. mof, a putative acetyl transferase gene related to the Tip60 and MOZ human genes and to the SAS genes of yeast, is required for dosage compensation in *Drosophila*. *Embo J* **16**:2054-60.
75. **Howe, L., D. Auston, P. Grant, S. John, R. G. Cook, J. L. Workman, and L. Pillus.** 2001. Histone H3 specific acetyltransferases are essential for cell cycle progression. *Genes Dev* **15**:3144-54.
76. **Hsu, J. Y., Z. W. Sun, X. Li, M. Reuben, K. Tatchell, D. K. Bishop, J. M. Grushcow, C. J. Brame, J. A. Caldwell, D. F. Hunt, R. Lin, M. M. Smith, and C. D. Allis.** 2000. Mitotic phosphorylation of histone H3 is governed by Ipl1/aurora kinase and Glc7/PP1 phosphatase in budding yeast and nematodes. *Cell* **102**:279-91.
77. **Iizuka, M., and B. Stillman.** 1999. Histone acetyltransferase HBO1 interacts with the ORC1 subunit of the human initiator protein. *J Biol Chem* **274**:23027-34.
78. **Ito, T.** 2007. Role of histone modification in chromatin dynamics. *J Biochem (Tokyo)* **141**:609-14.
79. **Ito, T., M. Bulger, M. J. Pazin, R. Kobayashi, and J. T. Kadonaga.** 1997. ACF, an ISWI-containing and ATP-utilizing chromatin assembly and remodeling factor. *Cell* **90**:145-55.
80. **Jaquet, Y., M. Delattre, A. Spierer, and P. Spierer.** 2002. Functional dissection of the *Drosophila* modifier of variegation Su(var)3-7. *Development* **129**:3975-82.
81. **Jasencakova, Z., A. Meister, J. Walter, B. M. Turner, and I. Schubert.** 2000. Histone H4 acetylation of euchromatin and heterochromatin is cell cycle dependent and correlated with replication rather than with transcription. *Plant Cell* **12**:2087-100.
82. **Jenuwein, T., G. Laible, R. Dorn, and G. Reuter.** 1998. SET domain proteins modulate chromatin domains in eu- and heterochromatin. *Cell Mol Life Sci* **54**:80-93.
83. **Jin, Y., Y. Wang, J. Johansen, and K. M. Johansen.** 2000. JIL-1, a chromosomal kinase implicated in regulation of chromatin structure, associates with the male specific lethal (MSL) dosage compensation complex. *J Cell Biol* **149**:1005-10.
84. **Jin, Y., Y. Wang, D. L. Walker, H. Dong, C. Conley, J. Johansen, and K. M. Johansen.** 1999. JIL-1: a novel chromosomal tandem kinase implicated in transcriptional regulation in *Drosophila*. *Mol Cell* **4**:129-35.

85. **John, S., L. Howe, S. T. Tafrov, P. A. Grant, R. Sternglanz, and J. L. Workman.** 2000. The something about silencing protein, Sas3, is the catalytic subunit of NuA3, a yTAF(II)30-containing HAT complex that interacts with the Spt16 subunit of the yeast CP (Cdc68/Pob3)-FACT complex. *Genes Dev* **14**:1196-208.
86. **Jones, R. S., and W. M. Gelbart.** 1993. The Drosophila Polycomb-group gene Enhancer of zeste contains a region with sequence similarity to trithorax. *Mol Cell Biol* **13**:6357-66.
87. **Kamine, J., B. Elangovan, T. Subramanian, D. Coleman, and G. Chinnadurai.** 1996. Identification of a cellular protein that specifically interacts with the essential cysteine region of the HIV-1 Tat transactivator. *Virology* **216**:357-66.
88. **Kaszas, E., and W. Z. Cande.** 2000. Phosphorylation of histone H3 is correlated with changes in the maintenance of sister chromatid cohesion during meiosis in maize, rather than the condensation of the chromatin. *J Cell Sci* **113 (Pt 18)**:3217-26.
89. **Katsanis, N., M. L. Yaspo, and E. M. Fisher.** 1997. Identification and mapping of a novel human gene, HRMT1L1, homologous to the rat protein arginine N-methyltransferase 1 (PRMT1) gene. *Mamm Genome* **8**:526-9.
90. **Klein, R. R., and R. L. Houtz.** 1995. Cloning and developmental expression of pea ribulose-1,5-bisphosphate carboxylase/oxygenase large subunit N-methyltransferase. *Plant Mol Biol* **27**:249-61.
91. **Komonyi, O., G. Papai, I. Enunlu, S. Muratoglu, T. Pankotai, D. Kopitova, P. Maroy, A. Udvardy, and I. Boros.** 2005. DTL, the Drosophila homolog of PIMT/Tgs1 nuclear receptor coactivator-interacting protein/RNA methyltransferase, has an essential role in development. *J Biol Chem* **280**:12397-404.
92. **Koonin, E. V., S. Zhou, and J. C. Lucchesi.** 1995. The chromo superfamily: new members, duplication of the chromo domain and possible role in delivering transcription regulators to chromatin. *Nucleic Acids Res* **23**:4229-33.
93. **Kouzarides, T.** 2007. Chromatin modifications and their function. *Cell* **128**:693-705.
94. **Kuo, M. H., J. E. Brownell, R. E. Sobel, T. A. Ranalli, R. G. Cook, D. G. Edmondson, S. Y. Roth, and C. D. Allis.** 1996. Transcription-linked acetylation by Gcn5p of histones H3 and H4 at specific lysines. *Nature* **383**:269-72.
95. **Kuo, M. H., J. Zhou, P. Jambeck, M. E. Churchill, and C. D. Allis.** 1998. Histone acetyltransferase activity of yeast Gcn5p is required for the activation of target genes in vivo. *Genes Dev* **12**:627-39.
96. **Kurshakova, M. M., A. N. Krasnov, D. V. Kopytova, Y. V. Shidlovskii, J. V. Nikolenko, E. N. Nabirochkina, D. Spehner, P. Schultz, L. Tora, and S. G. Georgieva.** 2007. SAGA and a novel Drosophila export complex anchor efficient transcription and mRNA export to NPC. *Embo J* **26**:4956-65.
97. **Kusch, T., S. Guelman, S. M. Abmayr, and J. L. Workman.** 2003. Two Drosophila Ada2 homologues function in different multiprotein complexes. *Mol Cell Biol* **23**:3305-19.
98. **Labrador, M., and V. G. Corces.** 2003. Phosphorylation of histone H3 during transcriptional activation depends on promoter structure. *Genes Dev* **17**:43-8.
99. **Lachner, M., D. O'Carroll, S. Rea, K. Mechtler, and T. Jenuwein.** 2001. Methylation of histone H3 lysine 9 creates a binding site for HP1 proteins. *Nature* **410**:116-20.
100. **Lee, K. K., and J. L. Workman.** 2007. Histone acetyltransferase complexes: one size doesn't fit all. *Nat Rev Mol Cell Biol* **8**:284-95.
101. **Lerach, S., W. Zhang, X. Bao, H. Deng, J. Girton, J. Johansen, and K. M. Johansen.** 2006. Loss-of-function alleles of the JIL-1 kinase are strong suppressors of position effect variegation of the wm4 allele in Drosophila. *Genetics* **173**:2403-6.

102. **Li, B., M. Carey, and J. L. Workman.** 2007. The role of chromatin during transcription. *Cell* **128**:707-19.
103. **Lin, W. J., J. D. Gary, M. C. Yang, S. Clarke, and H. R. Herschman.** 1996. The mammalian immediate-early TIS21 protein and the leukemia-associated BTG1 protein interact with a protein-arginine N-methyltransferase. *J Biol Chem* **271**:15034-44.
104. **Liu, L. P., J. Q. Ni, Y. D. Shi, E. J. Oakeley, and F. L. Sun.** 2005. Sex-specific role of *Drosophila melanogaster* HP1 in regulating chromatin structure and gene transcription. *Nat Genet* **37**:1361-6.
105. **Lo, W. S., R. C. Trievel, J. R. Rojas, L. Duggan, J. Y. Hsu, C. D. Allis, R. Marmorstein, and S. L. Berger.** 2000. Phosphorylation of serine 10 in histone H3 is functionally linked in vitro and in vivo to Gcn5-mediated acetylation at lysine 14. *Mol Cell* **5**:917-26.
106. **Ludlam, W. H., M. H. Taylor, K. G. Tanner, J. M. Denu, R. H. Goodman, and S. M. Smolik.** 2002. The acetyltransferase activity of CBP is required for wingless activation and H4 acetylation in *Drosophila melanogaster*. *Mol Cell Biol* **22**:3832-41.
107. **Luger, K., A. W. Mader, R. K. Richmond, D. F. Sargent, and T. J. Richmond.** 1997. Crystal structure of the nucleosome core particle at 2.8 Å resolution. *Nature* **389**:251-60.
108. **Marcus, G. A., N. Silverman, S. L. Berger, J. Horiuchi, and L. Guarente.** 1994. Functional similarity and physical association between GCN5 and ADA2: putative transcriptional adaptors. *Embo J* **13**:4807-15.
109. **Martens, J. A., and F. Winston.** 2003. Recent advances in understanding chromatin remodeling by Swi/Snf complexes. *Curr Opin Genet Dev* **13**:136-42.
110. **Muratoglu, S., S. Georgieva, G. Papai, E. Scheer, I. Enunlu, O. Komonyi, I. Cserpan, L. Lebedeva, E. Nabirochkina, A. Udvardy, L. Tora, and I. Boros.** 2003. Two different *Drosophila* ADA2 homologues are present in distinct GCN5 histone acetyltransferase-containing complexes. *Mol Cell Biol* **23**:306-21.
111. **Murnion, M. E., R. R. Adams, D. M. Callister, C. D. Allis, W. C. Earnshaw, and J. R. Swedlow.** 2001. Chromatin-associated protein phosphatase 1 regulates aurora-B and histone H3 phosphorylation. *J Biol Chem* **276**:26656-65.
112. **Nagy, Z., and L. Tora.** 2007. Distinct GCN5/PCAF-containing complexes function as co-activators and are involved in transcription factor and global histone acetylation. *Oncogene* **26**:5341-57.
113. **Nakayama, J., J. C. Rice, B. D. Strahl, C. D. Allis, and S. I. Grewal.** 2001. Role of histone H3 lysine 9 methylation in epigenetic control of heterochromatin assembly. *Science* **292**:110-3.
114. **Nathan, D., K. Ingvarsdottir, D. E. Sterner, G. R. Bylebyl, M. Dokmanovic, J. A. Dorsey, K. A. Whelan, M. Krsmanovic, W. S. Lane, P. B. Meluh, E. S. Johnson, and S. L. Berger.** 2006. Histone sumoylation is a negative regulator in *Saccharomyces cerevisiae* and shows dynamic interplay with positive-acting histone modifications. *Genes Dev* **20**:966-76.
115. **Nelson, C. J., H. Santos-Rosa, and T. Kouzarides.** 2006. Proline isomerization of histone H3 regulates lysine methylation and gene expression. *Cell* **126**:905-16.
116. **Neuwald, A. F., and D. Landsman.** 1997. GCN5-related histone N-acetyltransferases belong to a diverse superfamily that includes the yeast SPT10 protein. *Trends Biochem Sci* **22**:154-5.
117. **Nowak, S. J., and V. G. Corces.** 2000. Phosphorylation of histone H3 correlates with transcriptionally active loci. *Genes Dev* **14**:3003-13.

118. **Nowak, S. J., and V. G. Corces.** 2004. Phosphorylation of histone H3: a balancing act between chromosome condensation and transcriptional activation. *Trends Genet* **20**:214-20.
119. **Oki, M., H. Aihara, and T. Ito.** 2007. Role of histone phosphorylation in chromatin dynamics and its implications in diseases. *Subcell Biochem* **41**:319-36.
120. **Pankotai, T., O. Komonyi, L. Bodai, Z. Ujfaludi, S. Muratoglu, A. Ciurciu, L. Tora, J. Szabad, and I. Boros.** 2005. The homologous *Drosophila* transcriptional adaptors ADA2a and ADA2b are both required for normal development but have different functions. *Mol Cell Biol* **25**:8215-27.
121. **Papai, G., O. Komonyi, Z. Toth, T. Pankotai, S. Muratoglu, A. Udvardy, and I. Boros.** 2005. Intimate relationship between the genes of two transcriptional coactivators, ADA2a and PIMT, of *Drosophila*. *Gene* **348**:13-23.
122. **Peters, A. H., S. Kubicek, K. Mechtler, R. J. O'Sullivan, A. A. Derijck, L. Perez-Burgos, A. Kohlmaier, S. Opravil, M. Tachibana, Y. Shinkai, J. H. Martens, and T. Jenuwein.** 2003. Partitioning and plasticity of repressive histone methylation states in mammalian chromatin. *Mol Cell* **12**:1577-89.
123. **Pile, L. A., and I. L. Cartwright.** 2000. GAGA factor-dependent transcription and establishment of DNase hypersensitivity are independent and unrelated events in vivo. *J Biol Chem* **275**:1398-404.
124. **Qi, D., J. Larsson, and M. Mannervik.** 2004. *Drosophila* Ada2b is required for viability and normal histone H3 acetylation. *Mol Cell Biol* **24**:8080-9.
125. **Qian, C., Q. Zhang, S. Li, L. Zeng, M. J. Walsh, and M. M. Zhou.** 2005. Structure and chromosomal DNA binding of the SWIRM domain. *Nat Struct Mol Biol* **12**:1078-85.
126. **Ragvin, A., H. Valvatne, S. Erdal, V. Arskog, K. R. Tufteland, K. Breen, O. Y. AM, A. Eberharter, T. J. Gibson, P. B. Becker, and R. Aasland.** 2004. Nucleosome binding by the bromodomain and PHD finger of the transcriptional cofactor p300. *J Mol Biol* **337**:773-88.
127. **Rath, U., Y. Ding, H. Deng, H. Qi, X. Bao, W. Zhang, J. Girton, J. Johansen, and K. M. Johansen.** 2006. The chromodomain protein, Chromator, interacts with JIL-1 kinase and regulates the structure of *Drosophila* polytene chromosomes. *J Cell Sci* **119**:2332-41.
128. **Rea, S., F. Eisenhaber, D. O'Carroll, B. D. Strahl, Z. W. Sun, M. Schmid, S. Opravil, K. Mechtler, C. P. Ponting, C. D. Allis, and T. Jenuwein.** 2000. Regulation of chromatin structure by site-specific histone H3 methyltransferases. *Nature* **406**:593-9.
129. **Rea, S., G. Xouri, and A. Akhtar.** 2007. Males absent on the first (MOF): from flies to humans. *Oncogene* **26**:5385-94.
130. **Reuter, G., J. Gausz, H. Gyurkovics, B. Friede, R. Bang, A. Spierer, L. M. Hall, and P. Spierer.** 1987. Modifiers of position-effect variegation in the region from 86C to 88B of the *Drosophila melanogaster* third chromosome. *Mol Gen Genet* **210**:429-36.
131. **Roth, S. Y., J. M. Denu, and C. D. Allis.** 2001. Histone acetyltransferases. *Annu Rev Biochem* **70**:81-120.
132. **Ruiz-Garcia, A. B., R. Sendra, M. Galiana, M. Pamblanco, J. E. Perez-Ortin, and V. Tordera.** 1998. HAT1 and HAT2 proteins are components of a yeast nuclear histone acetyltransferase enzyme specific for free histone H4. *J Biol Chem* **273**:12599-605.
133. **Ruiz-Garcia, A. B., R. Sendra, M. Pamblanco, and V. Tordera.** 1997. Gcn5p is involved in the acetylation of histone H3 in nucleosomes. *FEBS Lett* **403**:186-90.

134. **Ryder, E., M. Ashburner, R. Bautista-Llacer, J. Drummond, J. Webster, G. Johnson, T. Morley, Y. S. Chan, F. Blows, D. Coulson, G. Reuter, H. Baisch, C. Apelt, A. Kauk, T. Rudolph, M. Kube, M. Klimm, C. Nickel, J. Szidonya, P. Maroy, M. Pal, A. Rasmuson-Lestander, K. Ekstrom, H. Stocker, C. Hugentobler, E. Hafen, D. Gubb, G. Pflugfelder, C. Dorner, B. Mechler, H. Schenkel, J. Marhold, F. Serras, M. Corominas, A. Punset, J. Roote, and S. Russell.** 2007. The DrosDel deletion collection: a Drosophila genomewide chromosomal deficiency resource. *Genetics* **177**:615-29.
135. **Schotta, G., A. Ebert, V. Krauss, A. Fischer, J. Hoffmann, S. Rea, T. Jenuwein, R. Dorn, and G. Reuter.** 2002. Central role of Drosophila SU(VAR)3-9 in histone H3-K9 methylation and heterochromatic gene silencing. *Embo J* **21**:1121-31.
136. **Schurter, B. T., S. S. Koh, D. Chen, G. J. Bunick, J. M. Harp, B. L. Hanson, A. Henschen-Edman, D. R. Mackay, M. R. Stallcup, and D. W. Aswad.** 2001. Methylation of histone H3 by coactivator-associated arginine methyltransferase 1. *Biochemistry* **40**:5747-56.
137. **Segraves, W. A., and D. S. Hogness.** 1990. The E75 ecdysone-inducible gene responsible for the 75B early puff in Drosophila encodes two new members of the steroid receptor superfamily. *Genes Dev* **4**:204-19.
138. **Shilatifard, A.** 2006. Chromatin modifications by methylation and ubiquitination: implications in the regulation of gene expression. *Annu Rev Biochem* **75**:243-69.
139. **Shogren-Knaak, M., H. Ishii, J. M. Sun, M. J. Pazin, J. R. Davie, and C. L. Peterson.** 2006. Histone H4-K16 acetylation controls chromatin structure and protein interactions. *Science* **311**:844-7.
140. **Silverman, N., J. Agapite, and L. Guarente.** 1994. Yeast ADA2 protein binds to the VP16 protein activation domain and activates transcription. *Proc Natl Acad Sci U S A* **91**:11665-8.
141. **Smith, E. R., J. M. Belote, R. L. Schiltz, X. J. Yang, P. A. Moore, S. L. Berger, Y. Nakatani, and C. D. Allis.** 1998. Cloning of Drosophila GCN5: conserved features among metazoan GCN5 family members. *Nucleic Acids Res* **26**:2948-54.
142. **Spierer, A., C. Seum, M. Delattre, and P. Spierer.** 2005. Loss of the modifiers of variegation Su(var)3-7 or HP1 impacts male X polytene chromosome morphology and dosage compensation. *J Cell Sci* **118**:5047-57.
143. **Stassen, M. J., D. Bailey, S. Nelson, V. Chinwalla, and P. J. Harte.** 1995. The Drosophila trithorax proteins contain a novel variant of the nuclear receptor type DNA binding domain and an ancient conserved motif found in other chromosomal proteins. *Mech Dev* **52**:209-23.
144. **Sterner, D. E., and S. L. Berger.** 2000. Acetylation of histones and transcription-related factors. *Microbiol Mol Biol Rev* **64**:435-59.
145. **Sterner, D. E., P. A. Grant, S. M. Roberts, L. J. Duggan, R. Belotserkovskaya, L. A. Pacella, F. Winston, J. L. Workman, and S. L. Berger.** 1999. Functional organization of the yeast SAGA complex: distinct components involved in structural integrity, nucleosome acetylation, and TATA-binding protein interaction. *Mol Cell Biol* **19**:86-98.
146. **Sterner, D. E., X. Wang, M. H. Bloom, G. M. Simon, and S. L. Berger.** 2002. The SANT domain of Ada2 is required for normal acetylation of histones by the yeast SAGA complex. *J Biol Chem* **277**:8178-86.
147. **Strahl, B. D., and C. D. Allis.** 2000. The language of covalent histone modifications. *Nature* **403**:41-5.
148. **Strahl, B. D., S. D. Briggs, C. J. Brame, J. A. Caldwell, S. S. Koh, H. Ma, R. G. Cook, J. Shabanowitz, D. F. Hunt, M. R. Stallcup, and C. D. Allis.** 2001.

- Methylation of histone H4 at arginine 3 occurs in vivo and is mediated by the nuclear receptor coactivator PRMT1. *Curr Biol* **11**:996-1000.
149. **Strahl, B. D., R. Ohba, R. G. Cook, and C. D. Allis.** 1999. Methylation of histone H3 at lysine 4 is highly conserved and correlates with transcriptionally active nuclei in *Tetrahymena*. *Proc Natl Acad Sci U S A* **96**:14967-72.
 150. **Straub, T., I. K. Dahlsveen, and P. B. Becker.** 2005. Dosage compensation in flies: mechanism, models, mystery. *FEBS Lett* **579**:3258-63.
 151. **Suganuma, T., J. L. Gutierrez, B. Li, L. Florens, S. K. Swanson, M. P. Washburn, S. M. Abmayr, and J. L. Workman.** 2008. ATAC is a double histone acetyltransferase complex that stimulates nucleosome sliding. *Nat Struct Mol Biol* **15**:364-72.
 152. **Swaminathan, J., E. M. Baxter, and V. G. Corces.** 2005. The role of histone H2Av variant replacement and histone H4 acetylation in the establishment of *Drosophila* heterochromatin. *Genes Dev* **19**:65-76.
 153. **Takechi, S., and T. Nakayama.** 1999. Sas3 is a histone acetyltransferase and requires a zinc finger motif. *Biochem Biophys Res Commun* **266**:405-10.
 154. **Tang, J., J. D. Gary, S. Clarke, and H. R. Herschman.** 1998. PRMT 3, a type I protein arginine N-methyltransferase that differs from PRMT1 in its oligomerization, subcellular localization, substrate specificity, and regulation. *J Biol Chem* **273**:16935-45.
 155. **Tschiersch, B., A. Hofmann, V. Krauss, R. Dorn, G. Korge, and G. Reuter.** 1994. The protein encoded by the *Drosophila* position-effect variegation suppressor gene *Su(var)3-9* combines domains of antagonistic regulators of homeotic gene complexes. *Embo J* **13**:3822-31.
 156. **Tse, C., E. I. Georgieva, A. B. Ruiz-Garcia, R. Sendra, and J. C. Hansen.** 1998. Gcn5p, a transcription-related histone acetyltransferase, acetylates nucleosomes and folded nucleosomal arrays in the absence of other protein subunits. *J Biol Chem* **273**:32388-92.
 157. **Tsukiyama, T., C. Daniel, J. Tamkun, and C. Wu.** 1995. ISWI, a member of the SWI2/SNF2 ATPase family, encodes the 140 kDa subunit of the nucleosome remodeling factor. *Cell* **83**:1021-6.
 158. **Tsukiyama, T., and C. Wu.** 1995. Purification and properties of an ATP-dependent nucleosome remodeling factor. *Cell* **83**:1011-20.
 159. **Turner, B. M.** 2000. Histone acetylation and an epigenetic code. *Bioessays* **22**:836-45.
 160. **Varga-Weisz, P. D., M. Wilm, E. Bonte, K. Dumas, M. Mann, and P. B. Becker.** 1997. Chromatin-remodelling factor CHRAC contains the ATPases ISWI and topoisomerase II. *Nature* **388**:598-602.
 161. **Wang, G. G., C. D. Allis, and P. Chi.** 2007. Chromatin remodeling and cancer, Part I: Covalent histone modifications. *Trends Mol Med* **13**:363-72.
 162. **Wang, H., Z. Q. Huang, L. Xia, Q. Feng, H. Erdjument-Bromage, B. D. Strahl, S. D. Briggs, C. D. Allis, J. Wong, P. Tempst, and Y. Zhang.** 2001. Methylation of histone H4 at arginine 3 facilitating transcriptional activation by nuclear hormone receptor. *Science* **293**:853-7.
 163. **Wang, L., L. Liu, and S. L. Berger.** 1998. Critical residues for histone acetylation by Gcn5, functioning in Ada and SAGA complexes, are also required for transcriptional function in vivo. *Genes Dev* **12**:640-53.
 164. **Wang, L., C. Mizzen, C. Ying, R. Candau, N. Barlev, J. Brownell, C. D. Allis, and S. L. Berger.** 1997. Histone acetyltransferase activity is conserved between yeast and human GCN5 and is required for complementation of growth and transcriptional activation. *Mol Cell Biol* **17**:519-27.

165. **Wang, Y., J. Wysocka, J. Sayegh, Y. H. Lee, J. R. Perlin, L. Leonelli, L. S. Sonbuchner, C. H. McDonald, R. G. Cook, Y. Dou, R. G. Roeder, S. Clarke, M. R. Stallcup, C. D. Allis, and S. A. Coonrod.** 2004. Human PAD4 regulates histone arginine methylation levels via demethylination. *Science* **306**:279-83.
166. **Wang, Y., W. Zhang, Y. Jin, J. Johansen, and K. M. Johansen.** 2001. The JIL-1 tandem kinase mediates histone H3 phosphorylation and is required for maintenance of chromatin structure in *Drosophila*. *Cell* **105**:433-43.
167. **Wang, Y. L., F. Faiola, M. Xu, S. Pan, and E. Martinez.** 2008. Human ATAC is a GCN5/PCAF-containing acetylase complex with a novel NC2-like histone fold module that interacts with the TATA-binding protein. *J Biol Chem*.
168. **Winer, J., C. K. Jung, I. Shackel, and P. M. Williams.** 1999. Development and validation of real-time quantitative reverse transcriptase-polymerase chain reaction for monitoring gene expression in cardiac myocytes in vitro. *Anal Biochem* **270**:41-9.
169. **Winston, F., and C. D. Allis.** 1999. The bromodomain: a chromatin-targeting module? *Nat Struct Biol* **6**:601-4.
170. **Wolf, E., A. Vassilev, Y. Makino, A. Sali, Y. Nakatani, and S. K. Burley.** 1998. Crystal structure of a GCN5-related N-acetyltransferase: *Serratia marcescens* aminoglycoside 3-N-acetyltransferase. *Cell* **94**:439-49.
171. **Workman, J. L., and R. E. Kingston.** 1998. Alteration of nucleosome structure as a mechanism of transcriptional regulation. *Annu Rev Biochem* **67**:545-79.
172. **Xiao, H., R. Sandaltzopoulos, H. M. Wang, A. Hamiche, R. Ranallo, K. M. Lee, D. Fu, and C. Wu.** 2001. Dual functions of largest NURF subunit NURF301 in nucleosome sliding and transcription factor interactions. *Mol Cell* **8**:531-43.
173. **Xu, W., D. G. Edmondson, and S. Y. Roth.** 1998. Mammalian GCN5 and P/CAF acetyltransferases have homologous amino-terminal domains important for recognition of nucleosomal substrates. *Mol Cell Biol* **18**:5659-69.
174. **Yamamoto, T., and M. Horikoshi.** 1997. Novel substrate specificity of the histone acetyltransferase activity of HIV-1-Tat interactive protein Tip60. *J Biol Chem* **272**:30595-8.
175. **Yang, X. J., V. V. Ogryzko, J. Nishikawa, B. H. Howard, and Y. Nakatani.** 1996. A p300/CBP-associated factor that competes with the adenoviral oncoprotein E1A. *Nature* **382**:319-24.
176. **Zhang, W., J. R. Bone, D. G. Edmondson, B. M. Turner, and S. Y. Roth.** 1998. Essential and redundant functions of histone acetylation revealed by mutation of target lysines and loss of the Gcn5p acetyltransferase. *Embo J* **17**:3155-67.
177. **Zhang, W., H. Deng, X. Bao, S. Lerach, J. Girton, J. Johansen, and K. M. Johansen.** 2006. The JIL-1 histone H3S10 kinase regulates dimethyl H3K9 modifications and heterochromatic spreading in *Drosophila*. *Development* **133**:229-35.
178. **Zhang, W., Y. Jin, Y. Ji, J. Girton, J. Johansen, and K. M. Johansen.** 2003. Genetic and phenotypic analysis of alleles of the *Drosophila* chromosomal JIL-1 kinase reveals a functional requirement at multiple developmental stages. *Genetics* **165**:1341-54.
179. **Zhang, Y., and D. Reinberg.** 2001. Transcription regulation by histone methylation: interplay between different covalent modifications of the core histone tails. *Genes Dev* **15**:2343-60.
180. **Zhao, T., T. Heyduk, and J. C. Eissenberg.** 2001. Phosphorylation site mutations in heterochromatin protein 1 (HP1) reduce or eliminate silencing activity. *J Biol Chem* **276**:9512-8.
181. **Zheng, J., M. Cho, A. D. Jones, and B. D. Hammock.** 1997. Evidence of quinone metabolites of naphthalene covalently bound to sulfur nucleophiles of proteins of murine Clara cells after exposure to naphthalene. *Chem Res Toxicol* **10**:1008-14.

